

THE ROLE OF TKS5 SH3 DOMAINS IN INVADOPODIA  
DEVELOPMENT AND ACTIVITY

A Thesis  
by  
CHRISTINA ADELE DALY

Submitted to the Graduate School  
at Appalachian State University  
in partial fulfillment of the requirements for the degree of  
MASTER OF SCIENCE

August 2016  
Department of Biology

THE ROLE OF TKS5 SH3 DOMAINS IN INVADOPODIA  
DEVELOPMENT AND ACTIVITY

A Thesis  
by  
CHRISTINA ADELE DALY  
August 2016

APPROVED BY:

---

Darren Seals, Ph.D.  
Chairperson, Thesis Committee

---

Maryam Ahmed, Ph.D.  
Member, Thesis Committee

---

Andrew Bellemer, Ph.D.  
Member, Thesis Committee

---

Zack Murrell, Ph.D.  
Chairperson, Department of Biology

---

Max C. Poole, Ph.D.  
Dean, Cratis D. Williams School of Graduate Studies

Copyright by Christina Adele Daly 2016  
All Rights Reserved

## **Abstract**

### **THE ROLE OF TKS5 SH3 DOMAINS IN INVADOPODIA DEVELOPMENT AND ACTIVITY**

Christina Adele Daly  
B.S., Appalachian State University  
M.S., Appalachian State University

Chairperson: Darren Seals, Ph.D.

One mechanism by which cancer cells metastasize is through the formation of actin-rich structures called invadopodia. Tks5 is a Src tyrosine kinase substrate and scaffolding protein necessary for invadopodia formation and associated extracellular matrix-remodeling activity. The purpose of this study is to appreciate how the five, protein binding SH3 domains of Tks5 impact its function. SH3 domains are commonly found in adaptor/scaffolding proteins where they mediate binding to poly-proline-containing amino acid sequences. Some binding partners for Tks5 have been previously identified, but the functional implications for these interactions are not well understood in the context of cancer. Here, Tks5 constructs harboring point mutations in a key tryptophan residue involved in SH3 domain binding activity were introduced into cancer cells to study invadopodia development and activity. In the LNCaP prostate cancer model system, mutant Tks5 constructs exert differential effects on extracellular matrix degradation based on a microscopic cell-based assay involving the proteolysis of gelatin. Specifically, mutations in the last two SH3 domains inhibit gelatin degradation relative to a wild-type Tks5 construct while mutations in

the first three SH3 domains accentuate this activity approximately 2.5 to 4.0 fold. In a related study, Myc epitope tagged, mutant Tks5 constructs were introduced into invadopodia-competent Src-transformed fibroblasts in order to observe their localization by fluorescence microscopy. Wild-type Tks5-Myc readily co-localizes with punctate and ring-shaped, F-actin-rich invadopodia structures in this cell line, as do Tks5-Myc constructs with mutations in either of the last two SH3 domains. In contrast, Tks5-Myc constructs with mutations in any of the first three SH3 domains collect in cytoplasmic aggregates and inhibit the ability of these cells to form invadopodia. Interestingly, while these mutations affect invadopodia formation, the ability to degrade extracellular matrix is maintained, albeit in a far less efficient and focalized manner than what is normally seen in this cell line. The aggregates were identified as being phosphoinositide-rich endosomes due to the co-localization of endosomal markers like EEA1. The loss of invadopodia formation was attributed to a retention of Src kinase in these perinuclear endosomes. Current experimentation is focused on elucidating the mechanisms behind the observed results with particular focus on the putative intra and intermolecular Tks5 interactions that would drive the invasive/metastatic behavior of cancer cells.

## **Acknowledgments**

This thesis would not have been possible without the guidance and support of those around me. I would first like to express my gratitude to Dr. Darren Seals who has been an incredible mentor throughout this experience and has truly fostered my love for scientific research and discovery. I would also like to thank Dr. Maryam Ahmed for her dedicated involvement in the production of this thesis. I am grateful for the assistance provided by Dr. Andrew Bellemer on this project. I appreciate the support of the graduate and undergraduate members of the Seals and Ahmed labs throughout my time in this program. I finally would like to express my love and gratitude to my family and friends for the love and support they have offered throughout this experience.

## **Dedication**

This thesis is dedicated in loving memory of Angelina Pistoressi Smith, whose hard work and passion for learning has inspired my own. Her sunny disposition, sense of humor, and unconditional love were comforting throughout my first year of the graduate program.

## Table of Contents

Abstract.....	iv
Acknowledgments.....	vi
Dedication.....	vii
Introduction.....	1
Methods and Materials.....	61
Results.....	71
Discussion.....	103
Future Directions.....	115
References.....	120
Supplemental Information.....	138
Biographical Sketch.....	146

## **Introduction**

### **Prologue**

It is not uncommon for cells to control their most important cellular processes via the formation and function of macromolecular assemblies—transcriptional and translational regulatory complexes come to mind as examples.

Podosomes/invadopodia are the macromolecular assemblies that govern the cellular process of motility and invasion. Cancer cells, in particular, invoke the formation of invadopodia to drive the deadliest aspect of cancer progression called metastasis. The purpose of this thesis project was to investigate the mechanism by which one of the most integral signal transduction pathways that govern invadopodia development functions. This pathway is controlled by Src tyrosine kinase and its substrate, the adaptor and scaffolding protein Tks5. A notorious feature of Tks5, but a feature of strikingly poor understanding, are its five SH3 domains, including the role they play in the assembly and function of invadopodial complexes in cancer cells. In this thesis project, the SH3 domains were individually mutated, and then analyzed for their impact on invadopodia development. This introduction seeks to better clarify the context of this objective by identifying the nature of metastasis, the signal transduction processes that regulate invadopodia development with emphasis on the roles of Src and Tks5, and the possible functions of Tks5 SH3 domains, including their potential as a therapeutic target for aggressive forms of cancer.

## **Src Signaling and Invadopodia Formation**

### *Src Signaling Mechanism*

The main cause of cancer patient morbidity and mortality is the spread of cancerous cells to distant sites in the body, a process known as metastasis. To metastasize, cancer cells must invade the surrounding tissue through increased motility and degradation of the extracellular matrix (ECM) (Chang and Werb, 2001; Friedl and Wolf, 2003). It is important to understand the invasive mechanisms responsible for metastasis in order to greatly improve cancer patient prognosis. In the 1980's, one such mechanism for metastasis was discovered. Fibroblasts transformed with Rous sarcoma virus (RSV) were shown to create actin-based protrusions with focalized protease activity towards the ECM (Chen et al., 1985; Chen, 1989; David-Pfeuty and Singer, 1980; Tarone et al., 1985). Later, the viral protein pp60<sup>src</sup> was identified as being responsible for these morphological and functional changes (Chen et al., 1985). This transforming protein had in fact been derived from a cellular homolog, referred to as Src, which functions as a tyrosine kinase (Spector et al., 1978; Takeya and Hanafusa, 1983).

The Src family kinases are prominent nonreceptor tyrosine kinases involved in signaling transduction pathways that control multiple cellular processes such as cell-cycle regulation, survival, and cytoskeletal remodeling. There are nine Src family kinases: Src, Fyn, and Yes, which are expressed in most tissues, and Blk, Yrk, Fgr, Hck, Lck, and Lyn, which exhibit more tissue-specific expression patterns. Src is primarily involved in the development of human cancers due to its activation of pathways involved in cell proliferation, survival, and motility/invasion. Activated Src can transform cells and induce

tumor formation, and Src expression and activity is often elevated in advanced stage carcinomas (Frame, 2002).

Without the presence of a signal, Src is held in an inactive, closed conformation mediated by the binding of a phosphotyrosine residue at position 527 to its own Src homology 2 (SH2) domain (Figure 1). Displacement of this intramolecular interaction can

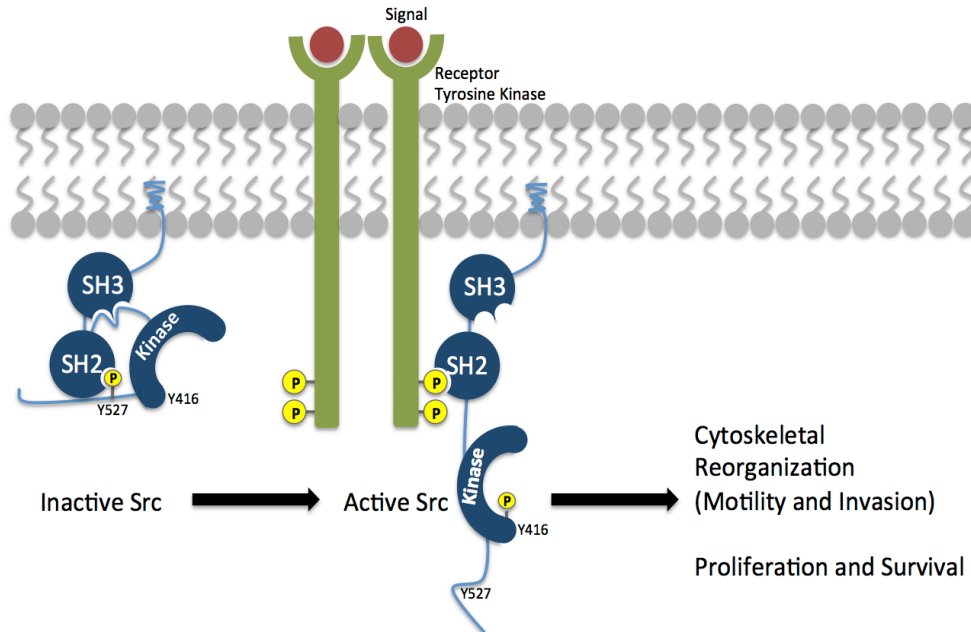


**Figure 1. Direct activation of Src by receptor tyrosine kinases.** An intramolecular interaction between the SH2 domain of Src and its phosphorylated Y527 residue holds it in an inactive, closed conformation. Receptor tyrosine kinases are activated when bound to an extracellular signal, leading to autophosphorylation of their kinase domains. The SH2 domain of Src preferentially binds these phosphorylated tyrosines on the receptor, disrupting the intramolecular binding of Src to create a catalytically active open conformation that enables Src autophosphorylation at Y416. Src signaling functions in processes related to cytoskeletal reorganization (motility and invasion) and cell proliferation and survival.

occur through higher affinity SH2 domain ligands, particularly the phosphotyrosines that are generated by activated receptor tyrosine kinases (Figure 1). Following the unfolding of Src, the catalytic Y416, located in the activation loop, becomes autophosphorylated and Src is fully activated. Due to this process, Src activity can be regulated by both phosphorylation

and protein-protein interactions. For example, Src signaling can be activated by the dephosphorylation of Y527 by tyrosine phosphatases, the deletion or mutation of Y527, or the phosphorylation of Y416 by other tyrosine kinases (Frame, 2002). Interestingly, phosphorylation of Y416 is not sufficient to fully activate kinase activity. Kinase activity is greatly increased when the Src Homology 3 (SH3) domain of Src has been displaced from an intramolecular interaction, possibly due to constraints this interaction may cause on the kinase domain (Moroco et al., 2014).

Once released, the SH3 domain of Src binds to some of its substrates such as AFAP1 and p130Cas, allowing for efficient substrate tyrosine phosphorylation and communication between the kinase and these two cytoskeletal regulatory proteins (Reynolds et al., 2014). The SH3 domain of Src is also important for its recruitment to cell-ECM bundling sites called focal adhesions via RhoA and Rho kinase. Additionally, Src is activated at sites of cellular adhesion through SH3 domain interactions with integrin receptors (Playford and Schaller, 2004). Through these mechanisms, Src is involved in activating pathways associated with cytoskeletal reorganization, which is necessary for increased motility and/or invasion.

### *Invadopodia*

The invasive structures formed by Src activity are called invadopodia, for their likeness to invasive feet (Chen, 1989). Invadopodia are dynamic, actin-rich cell surface protrusions with a diameter of 0.5 to 2  $\mu\text{m}$ , and which extend 1 to 7  $\mu\text{m}$  into the surrounding tissue (Chen, 1989; Schoumacher et al., 2010) (Figure 2). These structures provide sites of adhesion to the ECM, but unlike focal adhesions have the added capability of being able to

degrade the surrounding tissue through proteolytic activity (Chen et al., 1984; Nakahara et al., 1997; Seals et al., 2005). Following the discovery of invadopodia, four human melanoma cell lines were shown to both form invadopodia and invade through gelatin, fibronectin, and Matrigel, thus suggesting a hypothesis that invadopodia drive ECM degradation *in vivo* during cancer cell invasion and metastasis (Monsky et al., 1994).

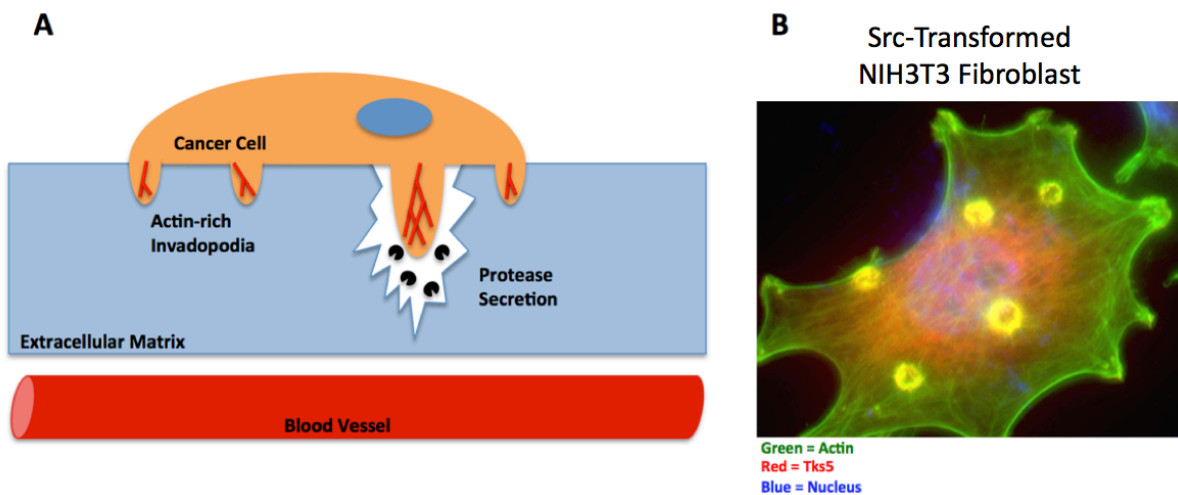


**Figure 2. Depiction of invadopodia formed by Src-transformed cells.** (A) Cartoon of a cancer cell forming invadopodia. Proteolytic activity allows for degradation of the ECM and access to the surrounding tissue and vasculature. (B) Src-transformed NIH3T3 fibroblast showing invadopodia formation through the co-localization (yellow) of the actin cytoskeleton (green) and the invadopodia marker protein Tks5 (red). Some invadopodia arrange into the rosette super structures shown in the image. Nuclei (blue).

### Src Signaling and Tks5

As Src-transformed cells were shown to form invadopodia and Src was shown to localize to sites of matrix degradation, the Src signaling pathway has long been studied for its role in invadopodia development (Chen et al., 1985). In 1998, a cDNA library was screened for novel Src substrates, revealing the tyrosine-phosphorylated protein FISH/Tks5 (Lock et al., 1998). Tks5 is approximately 150 kDa in size (comprised of 1124 amino acids) and

contains one amino-terminal phox homology (PX) domain followed by five SH3 domains (Figure 3). There are also two alternative splice sites that code for protein sequences lying on either side of the first SH3 domain of Tks5 leading to the expression of various Tks5 splice forms of unknown functional consequence. Tks5 contains three potential Src



**Figure 3. Modular structure of Tks5.** Tks5 has a lipid-binding phox homology (PX) domain, five Src homology 3 (SH3) domains, and numerous poly-proline motifs. The tyrosine (Y) residues represent candidate Src phosphorylation sites at positions Y552, Y557, and Y619. Tks5 also contains two alternative splice sites that code for protein sequences on either side of its first SH3 domain (orange).

phosphorylation sites at Y552, Y557, and Y619, based on homology to consensus Src phosphorylation sites (Figure 3). Tks5 tyrosine phosphorylation has been shown to be associated with cytoskeletal reorganization in Rat1 fibroblasts treated with platelet-derived growth factor (PDGF), the signaling molecule responsible for PDGF receptor tyrosine kinase as well as Src activation (Lock et al., 1998).

Further study of the effect of Tks5 on the actin cytoskeleton of Src-transformed NIH3T3 fibroblasts revealed that Tks5 localizes to invadopodia (Abram et al., 2003). Later, Tks5 was shown to be necessary for invadopodia formation and the associated ECM degradation carried out by Src-transformed fibroblasts, Bt549 breast cancer cells, and RPMI-7951 melanoma cells (Seals et al., 2005).

Src, as a tyrosine kinase, phosphorylates many invadopodia-associated substrates. Indeed, Src-dependent Tks5 phosphorylation at Y557 and Y619 has been shown to be important for invadopodia-associated matrix degradation, suggesting activation of Tks5

through Src signaling (Burger et al., 2014; Stylli et al., 2009). Additionally, tyrosine phosphorylation of Tks5 renders it accessible to binding by phosphotyrosine binding domains on other proteins. One example of these interactions involves Nck adaptor proteins. Immunoprecipitation techniques were used to show that the SH2 domain of Nck mediated an association with Tks5 in a Src-inducible manner. A Y557F mutation in Tks5 prevented tyrosine phosphorylation and abolished the interaction with Nck and invadopodia (Stylli et al., 2009). Together, these data point to an important Src-Tks5 signaling circuit in the regulation of invadopodia development in cancer cells.

## **Tks5 Function and Invadopodia Assembly**

### *Stages of Invadopodia Assembly*

Invadopodia formation occurs in stages, beginning with the initiation of signal transduction pathways responsible for assembling and activating invadopodia components. Shortly after these pathways are activated, cells develop invadopodia precursor structures that contain invadopodia-associated complexes, but which do not degrade ECM. These protein complexes are responsible for stabilization of invadopodia and initiation of actin polymerization. Invadopodia maturation occurs through sustained actin polymerization leading to protrusion of the cell membrane and focalized matrix degradation. Finally, invadopodia are disassembled, thus allowing for continued invadopodia reassembly at the leading edge of cells. The dynamic nature of invadopodia and their regulated turnover allow for efficient invadopodia function in the context of motility and invasion (Beatty et al., 2014).

### *Extracellular Stimuli Responsible for Invadopodia Development*

Extracellular stimuli activate invadopodia-formation pathways. Stimuli involved in invadopodia formation include growth factors, phorbol esters (*e.g.* PMA), reactive oxygen species, or activation of Notch signaling in hypoxic environments (Figure 4) (Diaz et al., 2013; Hoshino et al., 2013).

Transforming growth factor beta (TGF- $\beta$ ) binds to receptor serine/threonine kinases, which can either phosphorylate Ras/Raf kinase signaling pathway intermediates or can phosphorylate transcription factors known as Smads (Figure 4) (Lee et al., 2007). Once phosphorylated, the Smads can partner with co-regulators to promote or repress transcription of specific genes (Varon et al., 2006). In the case of cancer cell invasion, Smads have been shown to couple with the transcription factor Twist1 in order to upregulate PDGF receptor (PDGFR) expression. This leads to an increase in invadopodia formation and invasion through stimulation with PDGF (Eckert et al., 2011). Smads have also been shown to increase expression of Hic-5, a protein that is linked with the activation of the small GTP-binding proteins RhoC and Rac1, along with Src (Pignatelli et al., 2012). TGF- $\beta$  treatment of aortic endothelial cells has also been linked to an increase in expression of the Rho GTPase Cdc42, leading to actin polymerization, and of the matrix metalloproteinases MT1-MMP and MMP9, leading to ECM degradation, both of which are important characteristics of invadopodia (Varon et al., 2006).

Both PDGF and the epidermal growth factor EGF bind to their respective receptor tyrosine kinases to activate the Ras/Raf kinase pathway, Src, and/or the Abl kinases Abl/Arg through direct phosphorylation (Figure 4). The downstream substrates of these kinases are

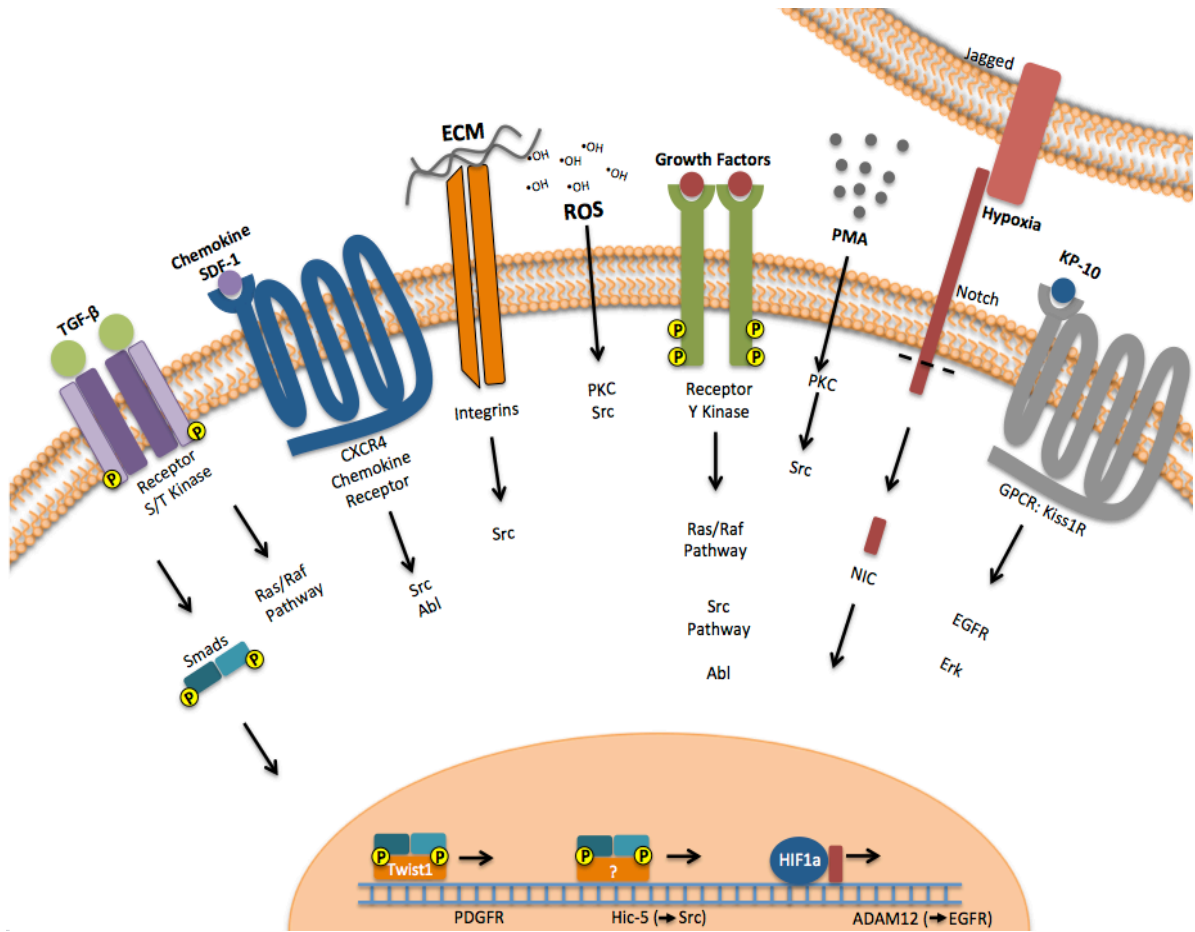


**Figure 4. Extracellular stimuli leading to invadopodia formation.**

Signaling pathways are activated by extracellular stimuli in order to initiate invadopodia formation. The stimuli depicted here include transforming growth factor  $\beta$  (TGF- $\beta$ ), stromal cell-derived factor 1 (SDF-1), ECM proteins, reactive oxygen species (ROS), other generalized growth factors (*e.g.* PDGF, EGF), phorbol esters (*e.g.* PMA), Notch, and G-protein coupled receptor (GPCR) activation by kisspeptins like KP-10.

then involved in invadopodia formation and activity (see below) (Murphy and Courtneidge, 2011).

Invadopodia formation can also be activated by stimuli other than growth factors. For example, application of the phorbol ester PMA (phorbol-12-myristate-13-acetate) activates protein kinase C (PKC) to induce invadopodia formation through its kinase activity (Figure

4) (Crimaldi et al., 2009). Chemokines have also been shown to signal invadopodia formation. The chemokine receptor CXCR4 is activated by stromal cell-derived factor 1 (SDF-1) and functions to activate Abl/Arg (Smith-Pearson et al., 2010).

The presence of reactive oxygen species (ROS), such as the superoxide produced by NADPH oxidases, was recently shown to promote invadopodia formation in Src-transformed fibroblasts, SCC61 squamous carcinoma cells from a head and neck cancer, C8161.9 melanoma cells, Bt549 breast cancer cells, and RPMI-7951 melanoma cells (Figure 4). It is thought that ROS are able to activate invadopodia formation through oxidation of the regulatory regions of PKC and Src, resulting in open and catalytically active enzymes. ROS can also transiently inhibit the catalytic activity of some tyrosine phosphatases, a family of enzymes that remove phosphate groups from tyrosine residues. Src-transformed fibroblasts treated with ROS inhibitors showed a reduction in Tks5 phosphorylation. For this reason, ROS may act locally to promote invadopodia formation by inhibiting phosphatase activity in a positive feedback loop and keeping Src and its substrates phosphorylated and activated for longer periods of time (Diaz et al., 2009).

Activation of the Notch signaling pathway in hypoxic environments has also been shown to induce invadopodia formation (Figure 4). The Notch signaling pathway allows for cell-cell signaling through receptor interactions on neighboring cells. For example, hypoxic environments can activate Notch signaling through an increase in its ligand Jagged-2. When an interaction occurs, two cleavages occur in the Notch receptor, one of which releases an intracellular functioning transcriptional regulator called Notch intracellular fragment (NIC). NIC partners with hypoxia-inducible factor 1 alpha (HIF1 $\alpha$ ) to upregulate the expression of genes associated with the hypoxia response. One of the upregulated genes, ADAM12, is a

transmembrane protease, which functions to activate latent growth factors and induce invadopodia formation through EGFR signaling (Diaz et al., 2013).

Matrix proteins can also stimulate invadopodia formation through activation of ECM receptors known as integrins (Figure 4). When bound to ECM proteins, integrins signal to Src-FAK (focal adhesion kinase) complexes at focal adhesions. Invadopodia are rich in integrins, therefore integrins are thought to play a similar role in activation of invadopodia formation through Src signaling (Playford and Schaller, 2004).

Finally, G-protein coupled receptor signaling has recently been associated with invadopodia formation. Kisspeptins are peptide products that activate the G-protein coupled receptor KISS1R (Figure 4). KISS1R can then directly bind to the EGFR to activate its signaling pathway. Alternatively, KISS1R can bind to the adaptor protein  $\beta$ -arrestin2, which in turn activates EGFR and Erk1/2 resulting in formation of invadopodia (Goertzen et al., 2015; Zajac et al., 2011).

#### *Invadopodia-Associated Intracellular Signaling Pathway Components*

Extracellular stimuli generally activate a host of intracellular second messengers, which carry out functions leading to cellular responses. The pathways turned on through the aforementioned signaling events are regulated by the Ras pathway, Src kinases, and Arg/Abl kinases (Figure 5). Receptor tyrosine kinases (*e.g.*, PDGFR, EGFR) can phosphorylate and activate the adaptor protein Shc, which relays the signal through the adaptor protein Grb2 to Sos (Lee et al., 2007). Sos, a Ras guanine nucleotide exchange factor, is then able stimulate the exchange of the GDP bound to Ras for a GTP molecule. When bound to GTP, Ras is activated. Thus, Ras binds to and activates Raf, Raf phosphorylates MEK, and MEK

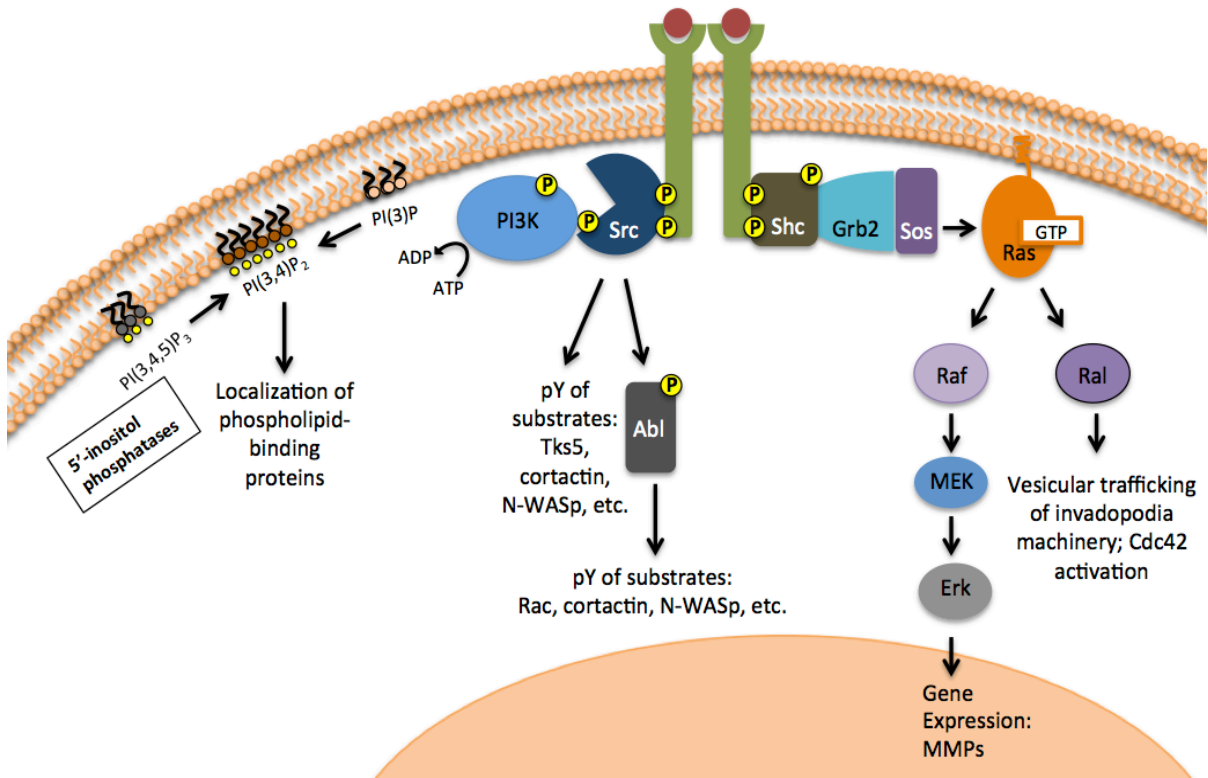


**Figure 5. Intracellular signaling leading to invadopodia formation.**

Intracellular second messengers involved in activating invadopodia formation and activity through kinase function.

phosphorylates Erk. Erk is then implicated in activation of MMP expression (see below) (Moon et al., 2004). Ras is also able to bind to and activate Ral effectors, resulting in implementation of exocyst-mediated vesicle trafficking, and Cdc42, both of which are involved in invadopodia maturation (Neel et al., 2012).

Src tyrosine kinase has been extensively studied for its role in cancer cell invasion. It plays an integral role in the regulation of each stage of invadopodia development, including disassembly (Boateng and Huttenlocher, 2012). Cell surface Src is internalized at the plasma membrane and, upon growth factor stimulation, is recruited to sites of receptor tyrosine kinases through endosomal trafficking. Once at these sites, Src interacts with and becomes

activated by receptor tyrosine kinases. Disruption of endosomal recycling machinery results in retention of inactive Src in the perinuclear region (Sandilands and Frame, 2008). Protein kinase C (PKC) activity can also activate Src through direct phosphorylation of S12 and S48 or by relaying phosphorylation signals through the adaptor protein AFAP-110. Briefly, PKC phosphorylates AFAP-110, inducing a conformational change that renders AFAP-110 open and able to bind the SH3 domain of Src (Figure 6). When AFAP-110 is bound to Src's SH3 domain, the structure of Src becomes open and active (Gatesman et al., 2004). Additionally, Src can be activated by phosphatases such as PTP1B, which cleaves the inhibitory phosphate from Y527 of Src. When dephosphorylated at this site, Src becomes active, phosphorylating numerous substrates involved in invadopodia formation, such as cortactin, dynamin, N-WASp, Tks4, and Tks5 (Cortesio et al., 2008). Cellular transformation by activated Src is sufficient to instigate invadopodia formation (Tarone et al., 1985).

Src activity also leads to phosphoinositide-3 kinase (PI3K) activation (Figure 6). Upon activation, Src's SH3 domain becomes available for interaction with the p85 subunit of PI3K. Src is then able to phosphorylate PI3K on Y688 in order to render it available for activation by small GTPases (Figure 6) (Sun et al., 2003). Cells can also be stimulated with PMA in order to activate PKC and PI3K. Active PI3K hydrolyzes ATP in order to phosphorylate phosphatidylinositols. Among the products of PI3K activity is PI(3,4)P<sub>2</sub>, whose enrichment at the cell membrane in areas with active Src and PI3K allows for recruitment of invadopodia early precursor proteins with phospholipid binding domains. This step in the process is likely an initial trigger for invadopodia formation (Oikawa et al., 2008).

## Tks5 Localization

The amino terminal PX domain of Tks5 has been shown to bind tightly to PI(3)P and PI(3,4)P<sub>2</sub> in order to enable plasma membrane localization (Figure 6) (Abram et al., 2003).

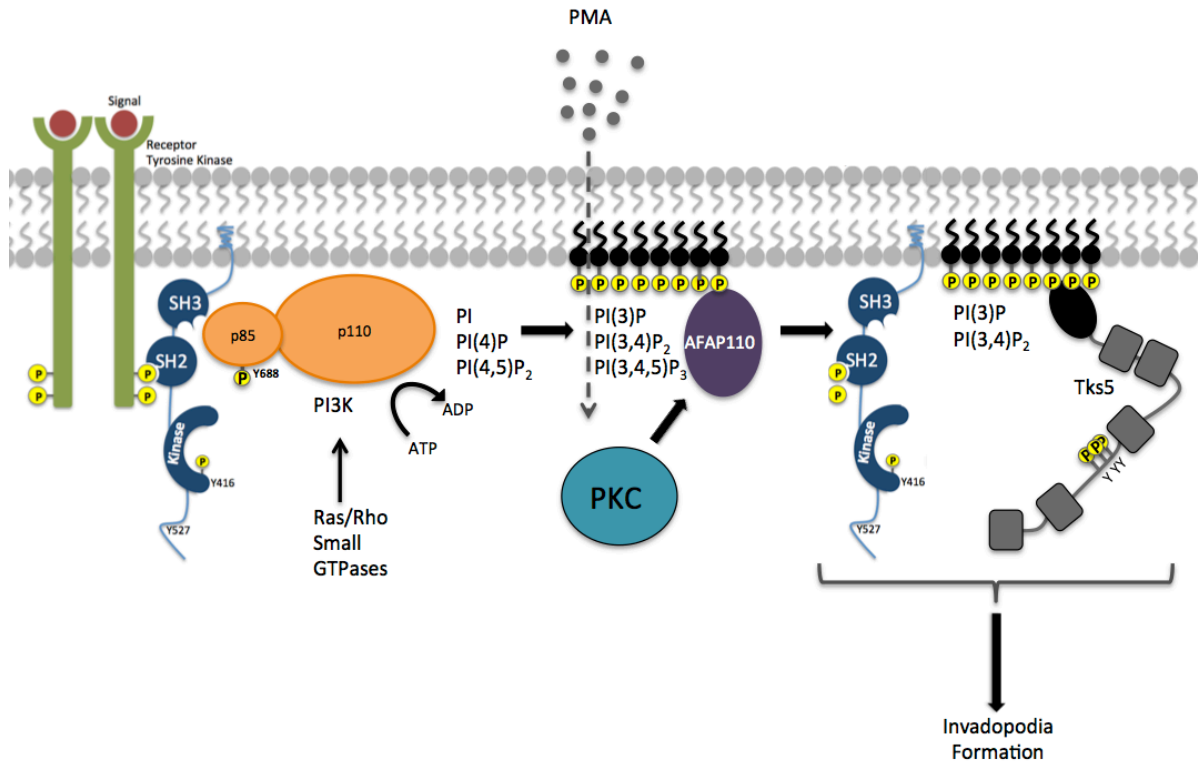


**Figure 6. PI3K activation and Tks5 localization.** Src activation by receptor tyrosine kinases allows for an open conformation, rendering its SH3 domain available for binding to the p85 subunit of PI3K. Src then phosphorylates Y688 of PI3K, relieving it of its inhibitory function and allowing for activation by small GTPases. Once active, PI3K transfers a phosphate group from ATP to the 3' position of a phosphatidylinositol, creating PI(3)P, PI(3,4)P<sub>2</sub>, and PI(3,4,5)P<sub>3</sub>. This enrichment of phosphatidylinositol phosphates at the membrane allows for localization of proteins with lipid binding domains. For example, AFAP110 can be recruited to close proximity of inactive Src through its PH domain. AFAP110 can then transmit activation signals from PKC (activated by PMA) to Src. Additionally, while Tks5 gets activated by direct Src phosphorylation, PI3K supports the relocalization of Tks5 to the membrane surface via its lipid-binding PX domain where invadopodia formation occurs.

Mutations of R42 and R93 in the PX domain of Tks5 have been shown to disrupt its lipid binding capabilities (Abram et al., 2003). Additionally, interference with the binding of endogenous Tks5 to lipids through overexpression of an isolated PX domain suppresses

invadopodia formation in Src-transformed fibroblasts (Abram et al., 2003; Oikawa et al., 2008).

In order to better understand the significance of the lipid binding properties of Tks5, further studies focused on the localization of its isolated PX domain. In normal fibroblasts, the isolated PX domain has a punctate distribution, similar to that seen by an isolated FYVE domain of Hrs, which is known to bind to PI(3)P in early endosomes. In contrast, full length Tks5 shows a more uniform cytoplasmic distribution, suggesting the existence of a mechanism for regulating the lipid-binding properties of Tks5 (Abram et al., 2003).

Expression of a form of Tks5 lacking the PX domain (Tks5 $\Delta$ PX) in RAW264.7 macrophages results in large dot-shaped actin aggregates, possibly due to the inability of Tks5 $\Delta$ PX to properly bind to PI(3,4)P<sub>2</sub> at the plasma membrane (Oikawa et al., 2012). This may also lead to cytoplasmic mis-localization of actin-associated Tks5 binding partners. This is different from full length Tks5, which is tightly regulated spatiotemporally. Thus, it is likely that Tks5 exists in a conformation allowing for the masking of its PX domain prior to Src phosphorylation in order to activate the lipid-binding properties of Tks5 only upon localization to sites of activated Src (Oikawa et al., 2012). In keeping with this hypothesis, Tks5 phosphorylation defective mutants, acting independently of Src, have been shown to localize to invadopodia-related structures called podosomes in osteoclasts, if there is displacement of Tks5's closed conformation via the binding of its PX domain to PI(3)P and PI(3,4)P<sub>2</sub> (Oikawa et al., 2012).

Another study was done using MTLn3 rat mammary adenocarcinoma cells to assess invadopodia precursor development (Sharma et al., 2013). The authors found that there is weak binding of Tks5 to the membrane due to basal levels of PI(3,4)P<sub>2</sub> in invadopodia

precursors. Recruitment of SHIP2, a 5'-inositol phosphatase, to invadopodia allows for further generation of PI(3,4)P<sub>2</sub> through dephosphorylation of PI(3,4,5)P<sub>3</sub> (Figure 5). This added enrichment of PI(3,4)P<sub>2</sub> allows for Tks5 binding stabilization leading to invadopodia maturation and ECM degradation. Invadopodia are highly dynamic structures, and the reversible nature of Tks5/PI(3,4)P<sub>2</sub> binding may contribute to this. Reversing this binding destabilizes the precursor and allows for environmental influence on invadopodia through fluctuations in Src and PI3K activation.

#### *Formation of Early Precursor Invadopodia*

Another early invadopodia precursor protein, the small GTPase Cdc42, is also activated through phosphorylation by Src. Cdc42 then binds to and activates the actin-related protein N-WASp by displacing an inhibitory intramolecular interaction (Figure 7) (Rohatgi et al., 2000). Once active, N-WASp binds cortactin, which acts as a scaffold to bring the actin-severing protein cofilin, N-WASp, and actin together at the plasma membrane. N-WASp also binds to the actin-nucleating Arp2/3 complex in order to stimulate actin polymerization.

N-WASp has also been shown to interact with Tks5 (Oikawa et al., 2008). Similar to the lipid-binding PX domain of Tks5, N-WASp contains a WASp homology 1 (WH1) domain which is not only able to bind actin but can also interact with PI(4,5)P<sub>2</sub>. It has been suggested that the interactions between N-WASp and PI(4,5)P<sub>2</sub> help promote N-WASp activation at the plasma membrane (Rohatgi et al., 2000). As lipid-binding Src substrates, both Tks5 and N-WASp have the potential to recruit one another to sites of invadopodia formation. A study investigating invadopodia maturation in adenocarcinoma cells observed N-WASp localization to invadopodia prior to Tks5 localization (Sharma et al., 2013).

However, an earlier study carried out in Src-transformed fibroblasts suggested that Tks5 is instrumental in recruiting large quantities of N-WASp to sites of invadopodia formation (Oikawa et al., 2008). Therefore, there is contradictory evidence as to whether N-WASp recruits Tks5 or vice versa.

Src can also activate another tyrosine kinase called Arg. Arg phosphorylates cortactin at Y421 (Figure 7). The adaptor protein Nck is then recruited to sites of cortactin phosphorylation and has the ability to bind to cortactin, N-WASp, and Tks5 (Beatty et al., 2013; Stylli et al., 2009). Nck is able to induce N-WASp and Arp2/3-mediated actin polymerization, although the mechanism behind this is not well understood (Bravo-Cordero et al., 2011).

Talin, a focal adhesion adaptor protein, has been shown to localize to early precursors by binding to actin and assists with the process of invadopodia maturation (Figure 7). Once at precursors, talin binds to  $\beta 1$  integrins, then to moesin, a membrane-organizing protein. Moesin arrives to early invadopodia precursors bound to sodium-hydrogen exchanger 1 (NHE1), which functions to increase the intracellular pH. This change in the intracellular environment leads to cofilin release from cortactin, thus allowing for cofilin activation on site (Beatty et al., 2013). Upon its release, cofilin is able to carry out its actin-severing abilities,

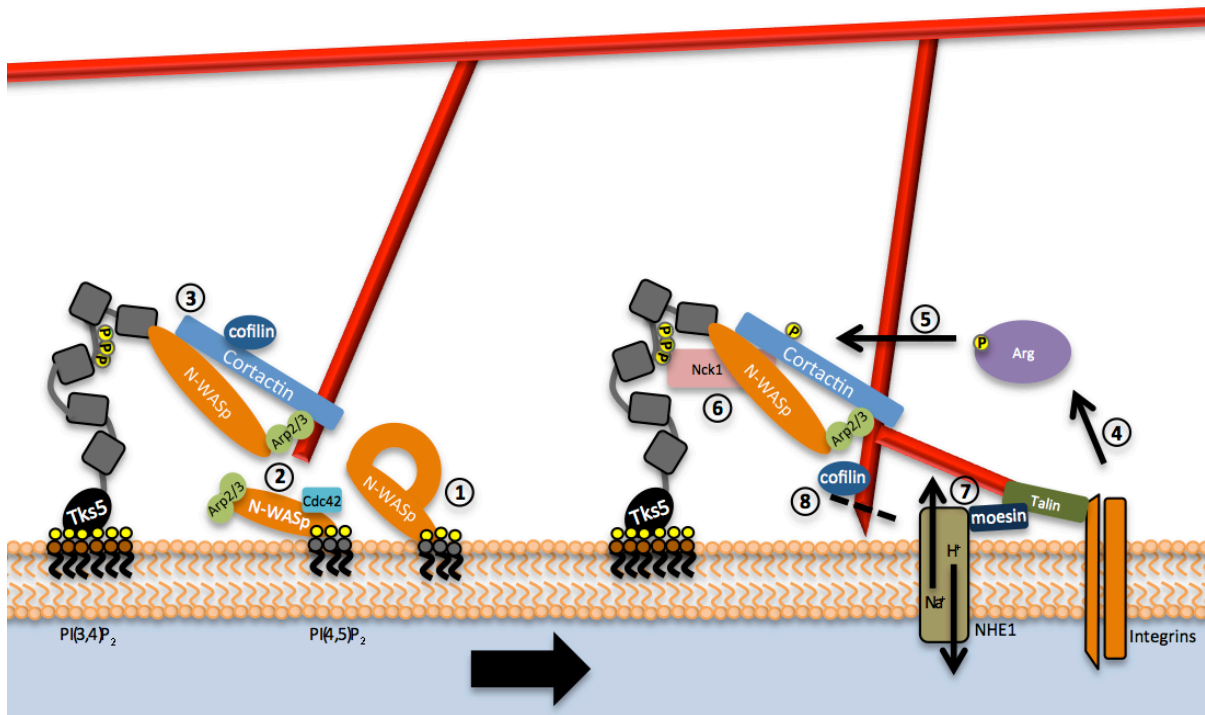


**Figure 7. Formation of invadopodia early precursors.** Proteins involved in the formation of early invadopodia precursors are responsible for initiating polymerization of actin (red) at the site. The numbering and black arrow show the progression of protein recruitment to the site as described in the text.

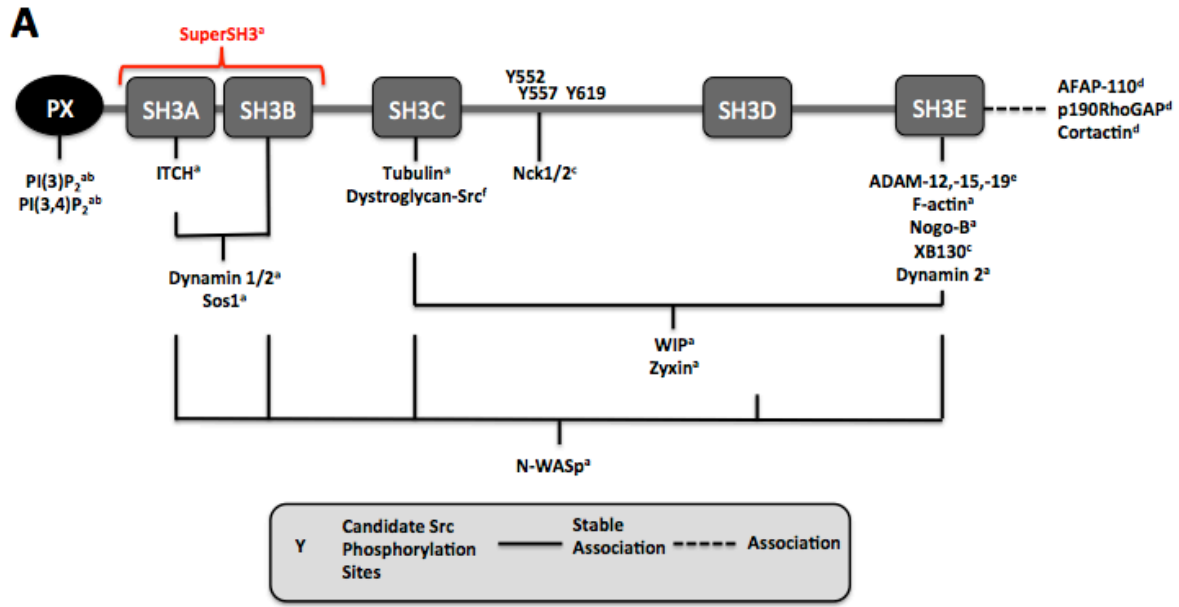
generating free actin barbed ends and allowing for branched actin polymerization by Arp2/3 (Figure 7) (Bravo-Cordero et al., 2011).

### *Tks5 Adaptor and Scaffolding Functions*

Following the formation of the early precursor invadopodia and initial actin polymerization, a large number of proteins are recruited to the site in which mature invadopodia will develop. The proteins found at these sites exist at the centers, or cores, of invadopodia. The early precursor proteins Tks5, Nck, and cortactin function as adaptor proteins to bring complexes together at these sites.

Tks5 clusters the structural and enzymatic components of invadopodia, most likely through its SH3 domain-associated, protein-binding properties (Eckert et al., 2011). The five SH3 domains of Tks5 are known to mediate interactions with poly-proline motifs on other proteins (Figure 8A). In addition, Tks5 has three poly-proline motifs located between these domains, which can bind to SH3 domains on other proteins (or to one of its own SH3 domains) (Figure 3) (Crimaldi et al., 2009). Tks5 also has a poly-proline motif located within its PX domain (Figure 3) (Lock et al., 1998).

GST-SH3 domain pull down assays suggest that the 3<sup>rd</sup> and 5<sup>th</sup> SH3 domains of Tks5 have the largest number of binding partners (Abram et al., 2003). These GST pull down experiments along with co-immunoprecipitation assays have helped identify some of these binding partners. In Src-transformed fibroblasts, the microtubule-associated protein dynamin2 can bind the 1<sup>st</sup> and 5<sup>th</sup> SH3 domains (Figure 8A), tubulin can bind the 3<sup>rd</sup> SH3 domain, and zyxin, an actin-associated zinc binding protein, can bind the 3<sup>rd</sup> and 5<sup>th</sup> SH3 domains of Tks5 (Oikawa et al., 2008). Nogo-B, an endoplasmic reticulum protein recently associated with the cytoskeleton, can also bind the 5<sup>th</sup> SH3 domain of Tks5 (Oikawa et al., 2008; Schanda et al., 2011). And finally there is evidence that F-actin itself can bind the 5<sup>th</sup> SH3 domain of Tks5 as well (Oikawa et al., 2008). N-WASp is capable of binding to all five SH3 domains of Tks5. In this case, full length Tks5 is able to more efficiently bind N-WASp than the isolated SH3 domains. The binding between Tks5 and N-WASp may also be constitutive, occurring with or without activation by Src (Oikawa et al., 2008), though this does not explain the ability of these proteins to recruit the other during invadopodia formation. WASp-interacting protein (WIP), a protein involved in stabilizing N-WASp, can bind the 3<sup>rd</sup> and 5<sup>th</sup> SH3 domains of Tks5 (Figure 8A) (Oikawa et al., 2008).



**B**

	Binding Partner	References
Polyproline motif of Tks5	• Grb2 <sup>cd</sup>	Oikawa et al., 2008
Full length Tks5 <sup>e</sup>	<ul style="list-style-type: none"> <li>• DBNL</li> <li>• Tropomyosin1</li> <li>• WIRE</li> <li>• Arp2/3</li> <li>• Drebrin</li> <li>• F-actin capping protein</li> <li>• <math>\beta</math>-actin</li> <li>• G-actin</li> <li>• Eg5</li> <li>• Myosin light polypeptide 6</li> <li>• Myosin regulatory light chain 2</li> <li>• Vimentin</li> <li>• Pontin</li> <li>• Reptin</li> <li>• NDR1</li> <li>• Protein phosphatase 2C</li> <li>• 14-3-3 <math>\beta</math>, <math>\gamma</math>, <math>\theta</math>, <math>\xi</math></li> <li>• Myosin2</li> <li>• CrkL</li> <li>• 5'AMP activated protein kinase</li> <li>• Creatine kinase B type</li> <li>• D-3-phosphoglycerate dehydrogenase</li> <li>• Tks5</li> <li>• peroxiredoxin1</li> </ul>	Stylli et al., 2011
Full length Tks5 in osteoclasts <sup>f</sup>	<ul style="list-style-type: none"> <li>• Gelsolin precursor</li> <li>• Filamin-A</li> <li>• Flightless 1 homolog</li> <li>• Tropomodulin3</li> <li>• Moesin</li> <li>• Cofilin</li> </ul>	Oikawa et al., 2012
PX Tks5 in osteoclasts <sup>f</sup>	<ul style="list-style-type: none"> <li>• Radixin isoform a</li> <li>• Abi1</li> <li>• WAVE2</li> <li>• Filamin-B</li> </ul>	Oikawa et al., 2012
Truncated Tks5: PX-SH3A-SH3B <sup>e</sup>	• p22-phox	Diaz et al., 2009 Rufer et al., 2009

<sup>a</sup>GST pull down with isolated Tks5 domain

<sup>b</sup>PIP Assay

<sup>c</sup>Coimmunoprecipitation

<sup>d</sup>Colocalization

<sup>e</sup>Phage Display

<sup>f</sup>Phage display, coimmunoprecipitation, and colocalization in myoblasts

**Figure 8. Binding Partners of Tks5.** (A) Diagram of Tks5 with binding partners according to binding site. (B) Chart of Tks5 binding partners without an identified site of binding.

Using a phage display screen in Src-transformed fibroblasts, ADAMs family matrix metalloproteases, specifically ADAMs 12, 15, and 19, were shown to bind to the 5<sup>th</sup> SH3 domain of Tks5 via poly-proline motifs in their cytoplasmic tails (Figure 8A). This interaction was confirmed by a co-immunoprecipitation assay (Abram et al., 2003). The ADAMs (a disintegrin and metalloprotease) family proteases act as membrane-bound sheddases to modify cell-cell interactions and to release active signaling molecules such as growth factors and cytokines from the cell surface or the ECM (Seals and Courtneidge, 2003). It has been suggested that the association between Tks5 and ADAMs may contribute to the regulation of ADAMs enzymatic activity (Abram et al., 2003; Rufer et al., 2009).

The tandem 1<sup>st</sup> and 2<sup>nd</sup> SH3 domains of the short form of Tks5 (lacking both of the alternatively spliced exons; see Figure 3) have a very high similarity to the two SH3 domains of p47-phox, a component of the NADPH oxidase. The SH3 domains of p47-phox are known to function as a superSH3 domain, a continuous binding surface with a very high affinity for a single ligand. There is evidence in Src-transformed fibroblasts that the first two SH3 domains of Tks5 similarly function as a superSH3 domain to bind Sos1, an activator of Ras and Rac GTPase activity, as well as to dynamins 1 and 2 (Figure 8A) (Rufer et al., 2009).

Additionally, the 5<sup>th</sup> SH3 domain of Tks5 is known to recruit AFAP-110, cortactin, and p190RhoGAP to podosomes formed by A7r5 rat smooth muscle cells (Figure 8A). Cortactin promotes actin polymerization, while p190RhoGAP downregulates RhoA activity and inhibits stress fiber and focal adhesion formation, thus enabling new invadopodia development. However, Tks5 failed to co-immunoprecipitate with any of these three

proteins suggesting a possible indirect interaction mediated through additional proteins (Crimaldi et al., 2009).

A comprehensive study of SH3 domains using HEK293 human embryonic kidney cells found an interaction between the transiently expressed GST-SH3A of Tks5 and ITCH. ITCH is an E3 ubiquitin ligase that has been shown to be involved in an epithelial to mesenchymal transition (EMT), a developmental program associated with an invasive phenotype that is often reactivated in cancer cells (Figure 8A). This interaction remains to be fully investigated (Carducci et al., 2012; Salah et al., 2014).

Perhaps the most comprehensive study of Tks5 binding partners involved a co-immunoprecipitation assay in HEK293T cells transiently expressing a full-length Tks5 construct. This experiment was able to identify a large number of potential binding partners, most of which have not been investigated any further (Figure 8B) (Supplemental Table SI) (Stylli et al., 2009). Interestingly, another study involving co-immunoprecipitation in osteoclasts found that Tks5 $\Delta$ PX was able to bind to more proteins than full length Tks5. This suggests that the PX domain somehow interferes with the binding capabilities of Tks5, possibly by sequestering Tks5 in a closed and inactive conformation as discussed previously (Oikawa et al., 2012).

A study using Src-transformed fibroblasts demonstrated that the adaptor protein Grb2 precedes Tks5 at areas of invadopodia formation (Figure 9A) (Oikawa et al., 2008). The N-terminal SH3 domain of Grb2 has been shown to bind to a poly-proline motif of Tks5, and this complex is formed at invadopodial structures. For this reason, Grb2 may assist in targeting Tks5 to invadopodia. Tks5 is also known to recruit Nck adaptor proteins to invadopodia. N-WASp and dynamin2 follow shortly after, thus allowing for actin

polymerization and invadopodia maturation (Oikawa et al., 2008). In a separate study involving MTLn3 rat mammary adenocarcinoma cells, cortactin, N-WASp, the actin-severing protein cofilin, and F-actin were shown to localize before Tks5 recruitment to invadopodia (Figure 9B). In this case, the cortactin-actin complex is thought to function in the recruitment of N-WASp and cofilin. N-WASp may then assist in the subsequent localization of Tks5. Binding of Tks5 to PI(3,4)P<sub>2</sub> at the plasma membrane

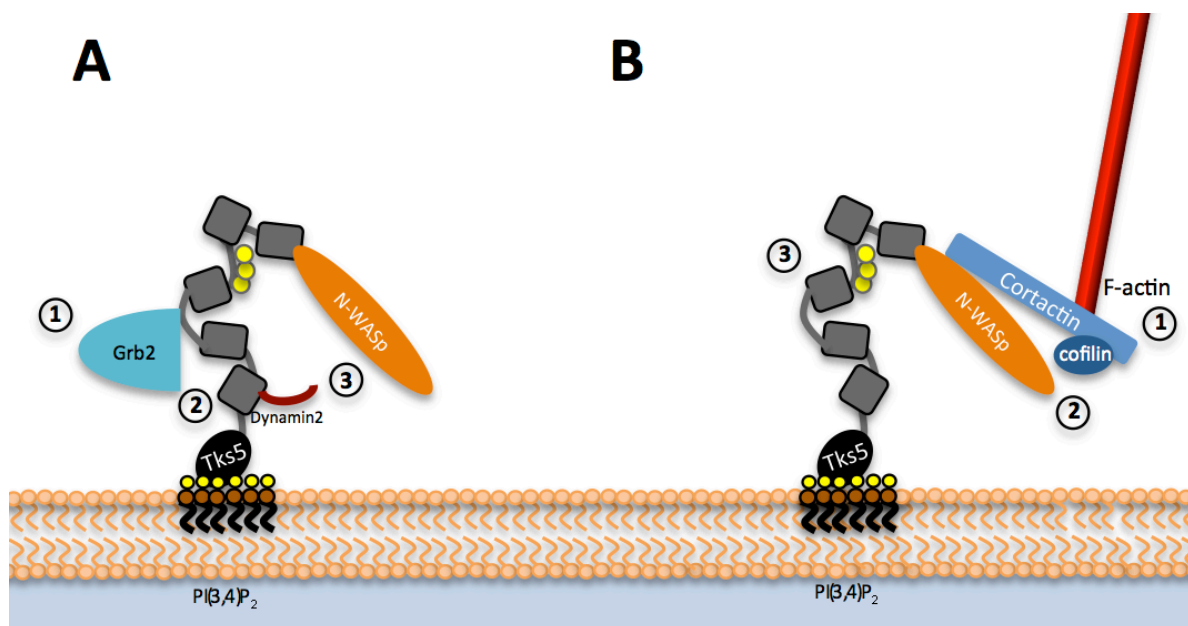


**Figure 9. Roles for Tks5 in early invadopodia precursor formation.** (A) In Src-transformed fibroblasts, Grb2 precedes Tks5 at invadopodia and may assist in targeting Tks5 to the membrane. Tks5, in turn, recruits N-WASp and dynamin2 to the early precursor for subsequent actin polymerization (Oikawa et al., 2008). (B) In MTLN3 cells, cortactin and F-actin localize first and recruit N-WASp and cofilin for actin polymerization. Tks5 localizes next to stabilize the structure through interactions with the plasma membrane (Sharma et al., 2013).

would then stabilize these invadopodia precursors (Sharma et al., 2013). Thus, it is possible that the nature of Tks5 binding may differ based on cell type and mode of activation.

Taken together, invadopodia formation is triggered by extracellular signaling allowing for activation of several second messengers. Included among these is Src tyrosine

kinase at the plasma membrane. Here, Src phosphorylates Tks5 on Y557 and Y619 in order to promote accessibility of its PX domain. The PX domain of Tks5 is then free to bind PI(3,4)P<sub>2</sub> generated at the plasma membrane by PI3K and SHIP2. Then, Tks5 is able to bind other proteins through its SH3 domains, phosphotyrosines, and poly-proline motifs. The ability to bind other proteins gives Tks5 its scaffolding function, allowing it to bring protein complexes together at sites of activated Src in order to potentiate invadopodia development.

#### *Tks4*

There is a protein known as Tks4, which is similar in domain structure to Tks5, but with a lipid-binding PX domain followed by four SH3 domains (Buschman et al., 2009). Tks4 is also found to localize at invadopodia through interactions with PI(3,4)P<sub>2</sub> and has been shown to be necessary for complete formation of these structures. Knockdown of Tks4 results in accumulation of Tks5 and other invadopodia-related proteins at the plasma membrane, but actin polymerization does not take place. However, this loss of invadopodia due to Tks4 depletion can be rescued by Tks5 overexpression, thus suggesting that these related proteins may have some overlapping roles in recruiting proteins to sites of invadopodia formation for actin polymerization (Buschman et al., 2009).

#### *Formation of Late Precursor Invadopodia*

N-WASp, Arp2/3, and cofilin function to polymerize actin at the site of invadopodia, allowing for protrusion of the cell membrane (Figure 10). Another actin adaptor protein,  $\alpha$ -actinin, bundles actin microfilaments together and links actin to integrin receptors (Sjoblon et

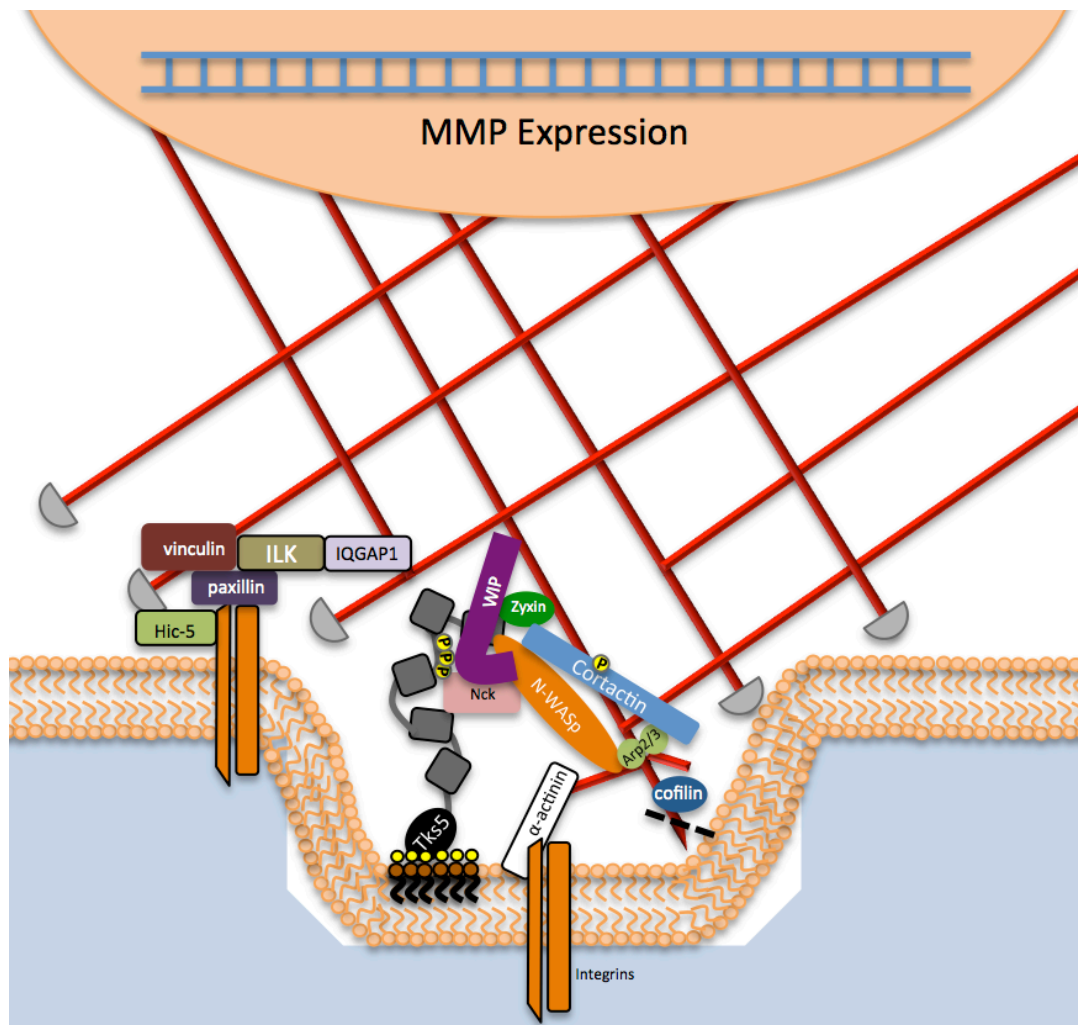


**Figure 10. Formation of late precursor invadopodia.** Scaffolding proteins are responsible for recruiting more actin-associated proteins, and a vesicle targeting system is established for further recruitment of components.

al., 2008).  $\alpha$ -actinin is found at invadopodia bound to the Tks5 and WIP binding partner Zyxin (Oikawa et al., 2008; Sjoblon et al., 2008).

$\beta$ 1 integrin binding to ECM ligands stabilizes developing invadopodia structures and triggers their maturation (Figure 10). Focal adhesion adaptor proteins such as Hic-5, paxillin, vinculin, and the aforementioned integrin receptors are found in an adhesion ring surrounding the invadopodia core where they further stabilize the structure for invadopodia

maturation (Figure 10) (Pignatelli et al., 2012). The integrins in the surrounding adhesion rings have been shown to bind to paxillin, which in turn binds to integrin-linked kinase (ILK). ILK is then able to recruit its binding partner IQGAP1, a polarizing protein involved in vesicle trafficking. This is thought to prepare the precursor site for focalized delivery of invadopodia components for efficient matrix degradation (Branch et al., 2012).

## **Invadopodia Maturation and Disassembly**

### *Invadopodia Maturation Through Elongation*

In order to elongate invadopodia protrusions during maturation, it is necessary for the cell to generate both branched and unbranched actin microfilaments. The branched actin is maintained at the base of invadopodia by the proteins responsible for the initiation of actin polymerization, such as N-WASp, cortactin, cofilin, and Arp2/3 (Figure 11). The unbranched actin is created by the formin mDia2, which prevents capping of actin microfilaments while simultaneously nucleating new actin polymerization. VASP proteins such as Mena<sup>INV</sup> are also responsible for protection from capping and they function to bundle actin filaments at the growing ends. Cross-linker fascin are also present, being responsible for the bundling of unbranched actin filaments and promoting their stability within maturing invadopodia (Figure 11) (Schoumacher et al., 2010).

Cofilin remains active within mature invadopodia as it is responsible for regenerating barbed ends for continued actin polymerization. RhoGTPases are also present in invadopodia. Indeed, the entire Rho family, though particularly RhoC, is able to activate the Rho kinase ROCK. Once active, ROCK phosphorylates and activates LIM kinase (LIMK),

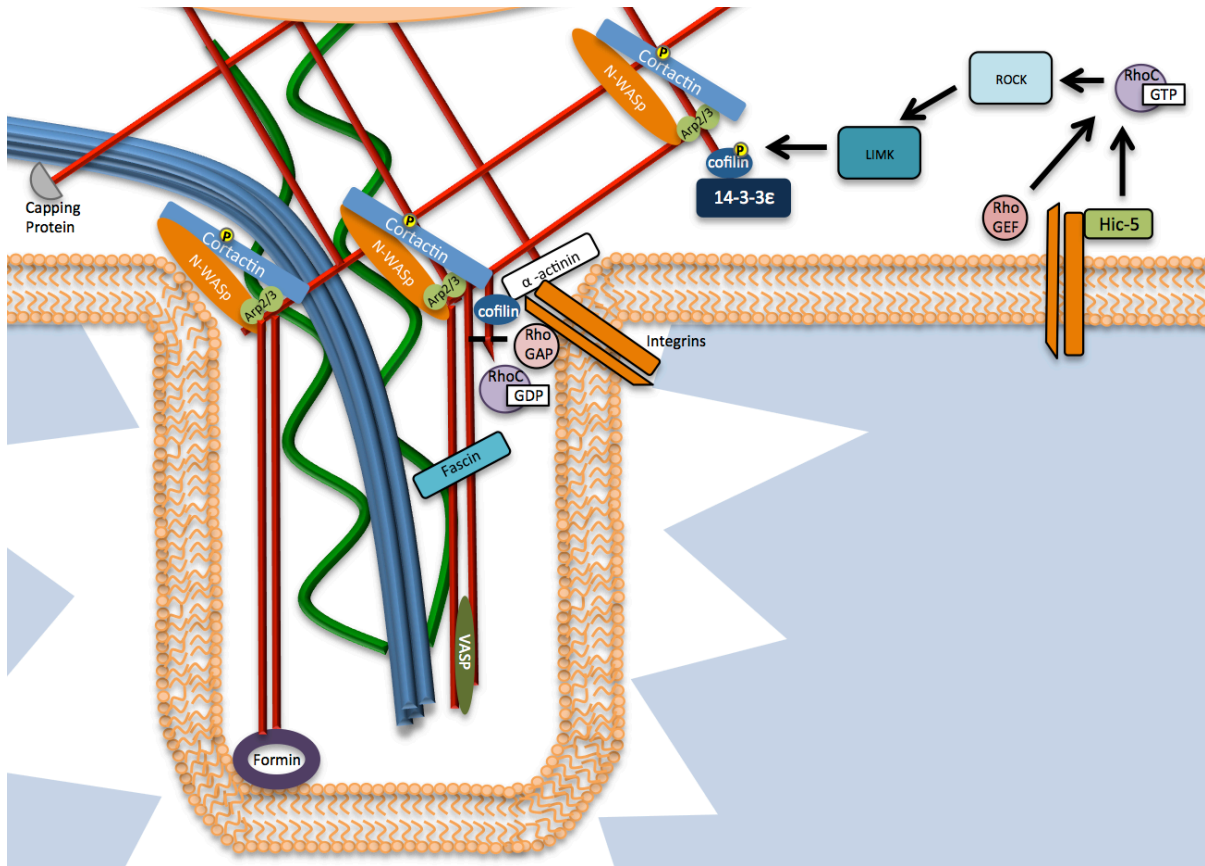


**Figure 11. Elongation of mature invadopodia.** Elongation of invadopodia involves branched and unbranched actin (red), intermediate filaments (green), and microtubules (blue). Actin polymerization surrounding invadopodia is regulated, allowing for focalized invadopodia development.

which in turn phosphorylates cofilin on S3 to prevent its actin-severing activity. 14-3-3 $\epsilon$  can bind this phosphorylated S3 on cofilin to prevent its dephosphorylation and lock it in an inactive state (Figure 11) (Bravo-Cordero et al., 2011). Because RhoC activity leads to a loss in cofilin activity, p190RhoGAP, the protein responsible for RhoC inactivation, is recruited to invadopodia cores and activated by  $\beta$ 1 integrin (Beatty et al., 2013; Bravo-Cordero et al., 2011). Alternatively, p190RhoGEF is present in the rings surrounding invadopodia where it can activate RhoC to its GTP bound state, leading to the phosphorylation-dependent loss of cofilin activity. This allows for actin polymerization to be focalized at invadopodia, while promoting elongation at the site at the same time (Figure 11) (Bravo-Cordero et al., 2011).

p190RhoGAP also leads to a decrease in RhoA activity at invadopodia cores, allowing for disassembly of stress fibers and focal adhesions. This prevents any actin-associated machinery from being retained in actin-related structures other than invadopodia, *i.e.* focal adhesions (Crimaldi et al., 2009).

Microtubules along with vimentin and keratin intermediate filaments are also present at invadopodia. They stabilize these invadopodia structures and support the movement of cells through the degraded extracellular space (Figure 11). Microtubules and vimentin intermediate filaments are only found in mature invadopodia and are required for the maturation process (Schoumacher et al., 2010).

#### *Matrix Degradation by Mature Invadopodia*

Invadopodia-associated ECM degradation is linked to proteolytic activity, specifically by the transmembrane proteases MT1-MMP, seprase, and ADAMs family proteases as well as by secreted MMPs like MMP2 and MMP9 (Figure 12). These proteases digest ECM components like collagen, fibronectin, and laminins (Weaver, 2006).

Protease expression is regulated by NF- $\kappa$ B and AP-1 transcription factor activation downstream of Erk1/2 signaling (Figures 5 and 12) (Moon et al., 2004). Once proteases are synthesized, they are packaged for vesicle trafficking to sites of invadopodia formation (Hu et al., 2011). Endophilin A2 generates membrane curvature for vesicle formation, and dynamin2 functions as a pinchase to dissociate vesicles from the trans-Golgi network (Figure 12) (Krutchen and McNiven, 2006). Rab proteins, particularly Rab8 and Rab40b, have been found to be associated with protease trafficking to invadopodia (Jacob et al., 2013; Poincloux et al., 2009). Rabs are GTPases involved in the compartmentalization of vesicle contents,

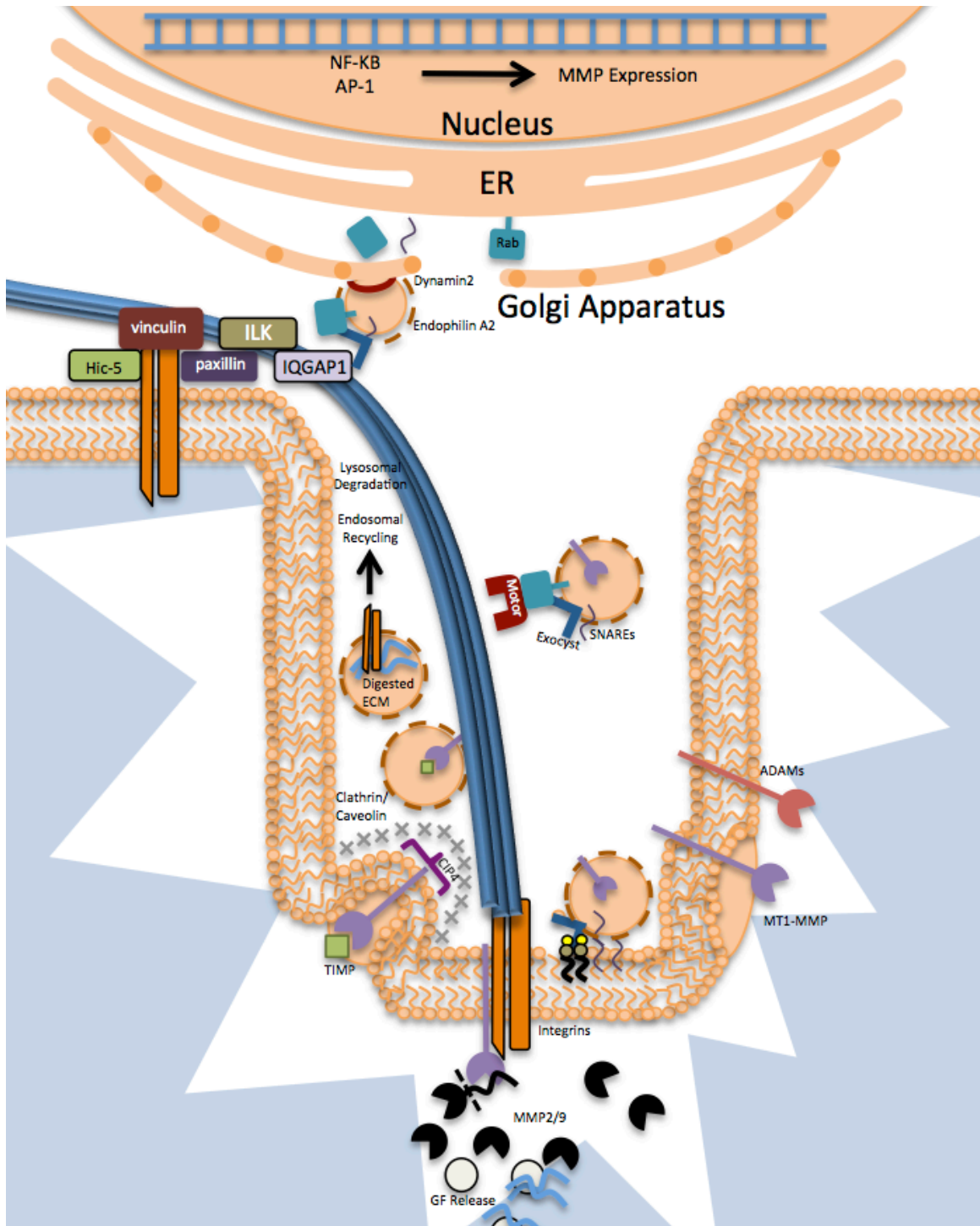


**Figure 12. Degradation by mature invadopodia.** Microtubules (blue) allow for vesicular delivery of MMPs and other proteases to invadopodia to allow for degradation of the surrounding matrix.

and the tethering and targeting of vesicles to organelles. Cytosolic inactive Rabs bound to a GDP molecule interact with REPs (Rab escort proteins), which help target Rabs to organelle membranes. Once at their target membranes, inactive Rabs are subject to activation by RabGEFs. Once bound to GTP, Rabs are incorporated into vesicles where they can interact with effectors such as motor proteins and tethering complexes to ensure that vesicles are delivered to the proper location in the cell (Figure 12) (Sandoval and Simmen, 2012).

Motor proteins such as kinesins and myosins have been associated with trafficking of proteins to invadopodia, and it is thought that they use microtubules to deliver proteins to the invadopodia core. IQGAP1 has been thought to play a role in anchoring microtubules at sites of invadopodia to allow for directed trafficking of components like MT1-MMP (Figure 12) (Poincloux et al., 2009). Once at invadopodia, vesicles are brought closer to the membrane through the exocyst, a complex comprised of eight subunits that can interact with microtubules and motor proteins and, once in close proximity to the plasma membrane, PI(4,5)P<sub>2</sub>. The exocyst allows for SNARE proteins (*e.g.*, Ti-VAMP) located both in the vesicle and at target membranes to associate and drive membrane fusion (Figure 12) (Synek et al., 2014). IQGAP1 has also been shown to bind to the exocyst through interactions with RhoA and Cdc42, thus allowing for targeted delivery of MT1-MMP at the plasma membrane. Fusion of the vesicle with the plasma membrane allows for proper placement of transmembrane proteases or secretion of pro-MMPs at ECM contact sites (Poincloux et al., 2009).

MT1-MMP is activated on its way from the Golgi apparatus by furin-like convertases, which cleave off the pro-peptide (Osenkowski et al., 2004). Once embedded in the plasma membrane, MT1-MMP activates secreted MMP2 and MMP9 through cleavage of

their pro-peptide domains (Figure 12). This activation is facilitated by MT1-MMP binding to integrins like  $\alpha\text{v}\beta\text{3}$ . These MMPs then collectively function to digest the ECM, and release sequestered growth factors in the process (Clark et al., 2007). MT1-MMP has also been shown to activate latent growth factors and cellular receptors such as those involved in Notch signaling through its sheddase activity (Osenkowski et al., 2004).

Interestingly, depletion of the adaptor protein Tks4 results in a loss of accumulation of MT1-MMP at invadopodia and an inability to degrade ECM (Buschman et al., 2009). It has been suggested that Tks4 holds a significant role in MT1-MMP localization, although the precise role it plays has not been elucidated. Since Tks4 and Tks5 appear to have some overlapping roles in terms of actin polymerization, Tks5 was overexpressed in Tks4-depleted cells to identify any redundant roles in MT1-MMP localization. However, ECM degradation was unable to be rescued, suggesting that this specific function is unique to Tks4 (Buschman et al., 2009).

The ADAMs family of metalloproteinases function as sheddases to modulate integrin function, mediate cell-matrix interactions, and activate latent transmembrane growth factors (Figure 12) (Stautz et al., 2010). In addition, ADAMs family members have been shown to degrade matrix proteins like collagen and fibronectin (Roy et al., 2004). Tks4 and Tks5 have both been shown to associate with ADAMs family proteases, however the functional implications behind these interactions have yet to be discovered (Courtneidge, 2012).

$\beta\text{1}$  integrin recruits seprase, a membrane-bound gelatinase, to invadopodia cores (Beatty et al., 2013).  $\beta\text{3}$  integrins recruit MMP2 to the cell surface as well. This suggests that integrins may play a general role in targeting proteolytic activity at invadopodia, possibly due

to the need for coordination between matrix-targeting proteolysis with sites of ECM contact (Mueller et al., 1999).

Tissue inhibitors of metalloproteinases (*e.g.*, TIMP1 and TIMP3), as the name implies, inhibit MT1-MMP by directly binding to the enzyme's active site (Figure 12). Interestingly, however, MT1-MMP bound to TIMP2 still maintains the ability to activate MMP2. In addition, low concentrations of TIMP2 are essential for the efficient activation of MMP2, allowing for recruitment of MMP2 to active MT1-MMP molecules. This suggests that TIMP2 functions to promote MMP2 activation (Lu et al., 2004; Murphy and Courtneidge, 2011). Proteolytically inactive MT1-MMP is internalized through caveolar- or clathrin-mediated endocytosis (Poincloux et al., 2009). The Cdc42-interacting protein CIP4 assists in this process, instigating membrane invagination at these sites (Figure 12). When CIP4 is phosphorylated by Src on Y471, its activity is inhibited, thus allowing for the accumulation of MT1-MMP at invadopodia (Hu et al., 2011).  $\beta$ 1 integrin interaction with MT1-MMP has also been shown to inhibit MT1-MMP endocytosis, further supporting the function of integrins in proteolytic activity. However, once internalized, MT1-MMP is transported to the lysosome for degradation, though a fraction of internalized MT1-MMP is recycled through the trans-Golgi network for regeneration of active enzyme at the cell surface (Figure 12) (Poincloux et al., 2009).

While endocytosis is used as a means of clearing inactive enzyme from the cell surface, it is also used to clear cleaved ECM from the extracellular space. Integrin-mediated ECM endocytosis has been proposed as a mechanism of internalizing cleaved matrix proteins for lysosomal degradation (Shi and Sottile, 2011). This process allows for removal of ECM from the surrounding space in order to provide room for the cell to move through.

### *Invadopodia Disassembly*

Invadopodia turnover is equally important for efficient invasion because it refocuses ECM degradation to sites where it is needed. Additionally, invasion pathways can be switched to motility pathways, allowing for movement through the newly degraded tissue (Poincloux et al., 2009). Optimally concerted proteolytic activity and motility must be achieved for maximum invasive potential (Moshfegh et al., 2014).

In order for invadopodia to disassemble, the activity of the main components of invadopodia must be inhibited. The actin-binding protein caldesmon (CaD), a p53 transcriptional target, downregulates invadopodia formation by competing with Arp2/3 (Figure 13) (Mukhopadhyay et al., 2009; Yoshio et al., 2007). Expression of CaD decreases invadopodia formation and increases the incidence of stress fibers by preventing actin polymerization (Yoshio et al., 2007).

As previously discussed, CIP4 is involved in instigating MT1-MMP endocytosis and has been associated with inhibition of degradation by invadopodia. In this way, CIP4 activity could also play a role in invadopodia disassembly (Figure 13) (Hu et al., 2011).

Trio, a guanine exchange factor, has been shown to be involved in invadopodia disassembly by activating Rac1. Rac1, in its active GTP-bound state, is able to bind to numerous downstream effectors to trigger responses. One of the effectors activated by Rac1 is Pak1, or p21-activated protein kinase 1. Pak1 is a serine/threonine kinase, which phosphorylates cortactin on S113 to destabilize cortactin-actin interactions and inhibit actin polymerization (Figure 13) (Moshfegh et al., 2014).

The tyrosine phosphatase PTP-PEST localizes to invadopodia and induces invadopodia disassembly through dephosphorylation of Src substrates involved in invadopodia formation and activity. Conversely, it has been suggested that the presence of

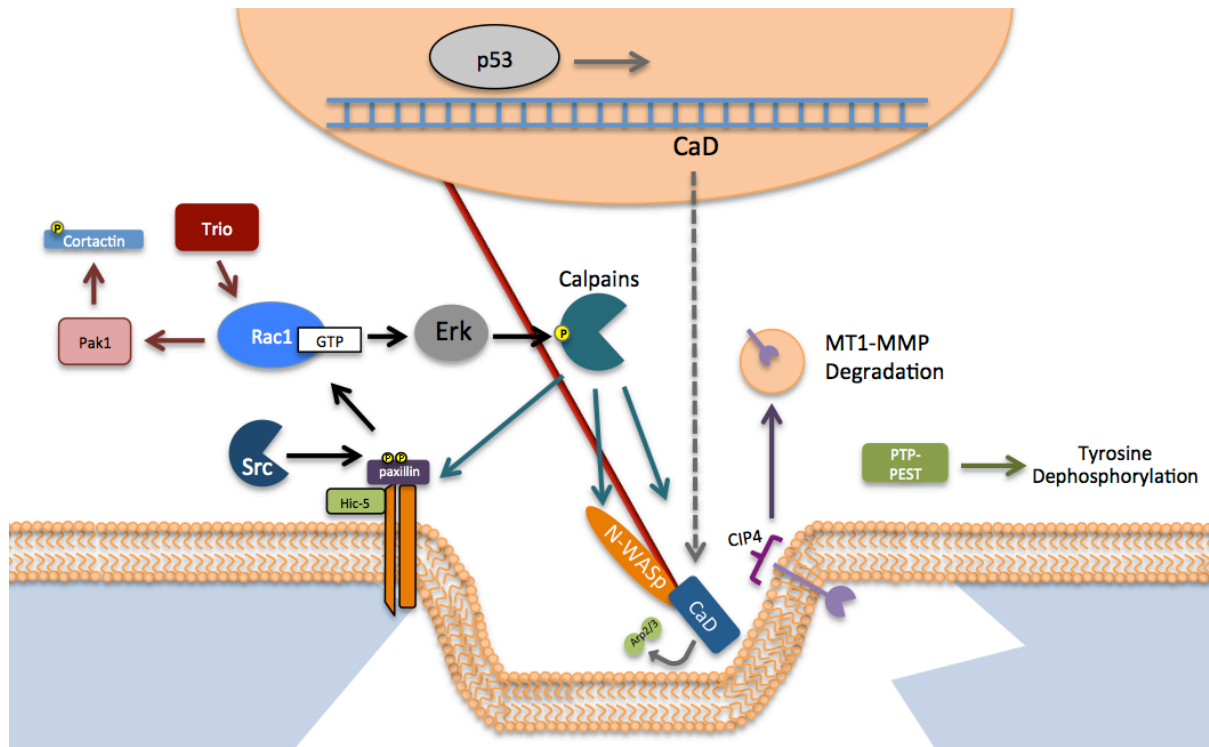


**Figure 13. Disassembly of invadopodia.** The tightly regulated disassembly of invadopodia occurs through deactivation of the components allowing for rapid turnover and more effective degradation.

PTP-PEST and other tyrosine phosphatases may allow for rapid turnover of protein complexes leading to more efficient invasion (Figure 13) (Diaz et al., 2009).

Src phosphorylates paxillin Y31 and Y118, leading to activation of Rac1, possibly through the adaptor protein Crk. The activation of Rac1 results in Erk activity. Erk in turn activates calpains by phosphorylation on S50 (Badowski et al., 2008; Franco and Huttenlocher, 2005). Calpains are intracellular  $\text{Ca}^{2+}$ -dependent thiol proteases that have been

shown to regulate disassembly of podosomes. Moderate calpain2 expression is associated with increased degradation and invasion, due to the importance of efficient invadopodia turnover. It functions to cleave proteins such as paxillin, cortactin, N-WASp, and PTP1B (Figure 13). Once cleaved, PTP1B is activated and is able to cleave the inhibitory phosphate of Src leading to its activation. This may provide a pathway for subsequent invadopodia formation allowing for rapid turnover of protein complexes and efficient invasion (Cortesio et al., 2008).

### **Regulation of Tks5 Gene and mRNA Expression**

#### *SH3PXD2A*

Since Tks5 is required for invadopodia formation and stability through recruitment of accessory proteins, it is prudent to consider how Tks5 is regulated in cells. Human Tks5 is encoded by the gene *SH3PXD2A* (sometimes referred to as *SH3MD1*), a 267 kb gene containing 15 exons located on chromosome 10 (Figure 14). The closest homolog to *SH3PXD2A*, with 47% homology, is *SH3PXD2B*, the gene encoding Tks4 (Cejudo-Martin et al., 2014). Interestingly, simpler organisms such as the tunicate *Ciona intestinalis* and the sea urchin *Strongylocentrotus purpuratus* each contain one gene encoding for a Tks protein containing a PX domain followed by three or four SH3 domains, respectively. This suggests that both *SH3PXD2A* and *SH3PXD2B* may have evolutionarily arisen from a single common gene (Buschman et al., 2009).

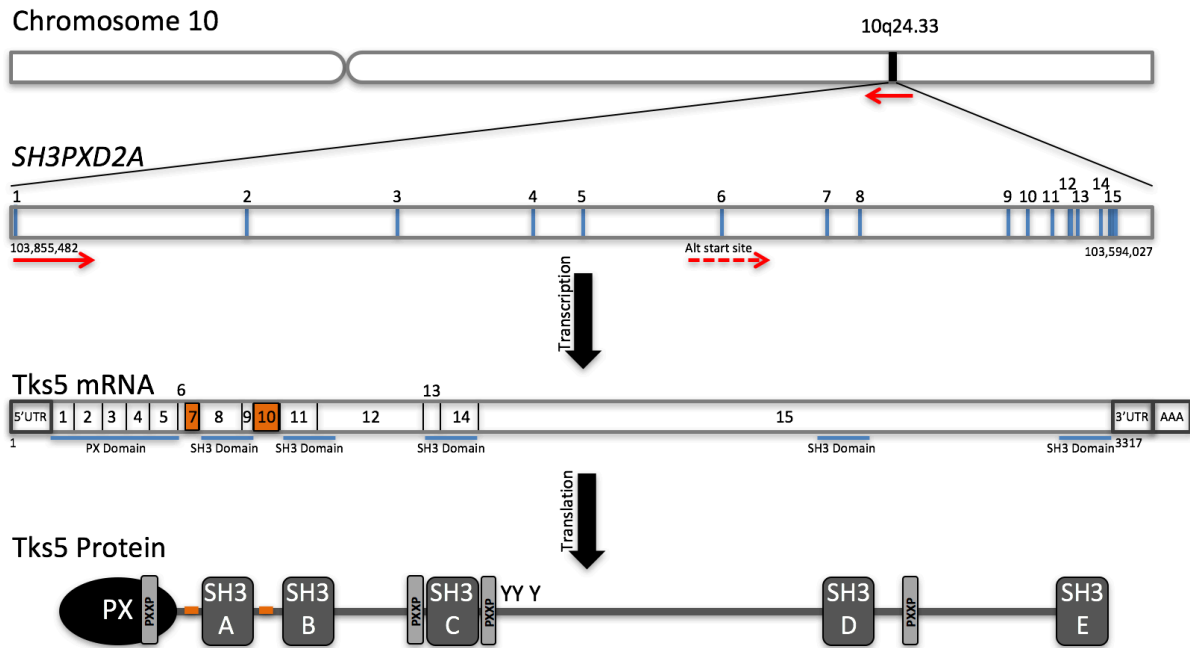


**Figure 14. *SH3PXD2A*, Tks5 mRNA, and Tks5 protein domain structure.** The gene for Tks5, *SH3PXD2A* or *SH3MD1*, is located on chromosome 10 at 10q24.33 (Gene Cards human gene database). *SH3PXD2A* contains 15 exons (blue), with a possible alternative transcriptional start site located at exon 6 (dashed red), resulting in a Tks5 isoform lacking the PX domain (Cejudo-Martin et al., 2014; NCBI Gene; UCSC Genome Browser). The mRNA of Tks5 contains two alternatively spliced exons (orange) conforming to exons 7 and 10 (Cejudo-Martin, 2014; NCBI Nucleotide). Tks5 protein contains one amino terminal PX domain followed by five SH3 domains. Polyproline motifs (PXXP; light grey), and candidate Src phosphorylation sites (Y) are noted (NCBI Conserved Domain Database).

There are recognition sites for a wide variety of transcription factors in close proximity to the *SH3PXD2A* gene according to a SABiosciences' DECODE database search, however not much is known about the factors regulating Tks5 expression at the gene level (Figure 15). The DECODE database identified the ten most relevant transcription factors with potential regulation of *SH3PXD2A* gene expression through automated text-mining of published papers and use of the UCSC genome browser, a collection of annotated genomes. These transcription factors include AML1a, a transcription factor associated with proliferation of acute myeloid leukemic cells (Liu et al., 2009), c-Myc, a very common

oncogene that promotes cell proliferation (Lin et al., 2012), and the glucocorticoid receptors, which have been shown in the past to initiate anti-apoptotic signaling in breast epithelial cells

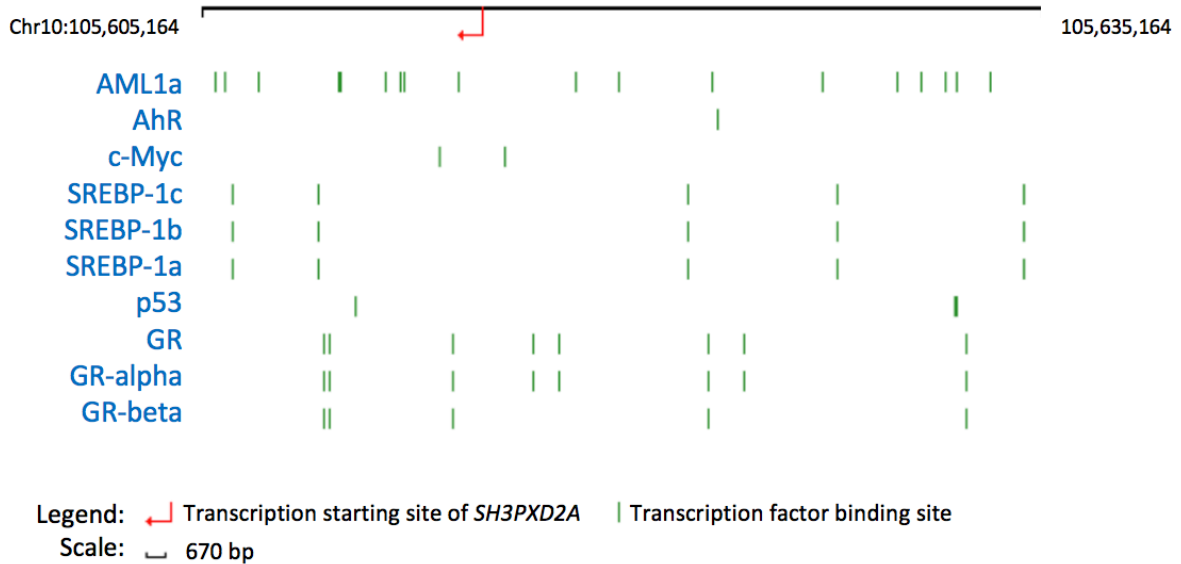


**Figure 15. Transcription factors with binding sites in close proximity to the *SH3PXD2A* gene.** Ten most relevant transcription factors that bind from 20kb upstream to 10kb downstream of the Tks5 transcriptional start site (red arrow; 105,605,164 to 105,635,164 of chromosome 10). Adapted from SABiosciences' DECODE database. Transcription factors include acute myeloid leukemia protein 1 (AML1a), aryl hydrocarbon receptor (AhR), oncogenic c-Myc, the sterol regulatory element-binding proteins (SREBP), the tumor suppressor p53, and the glucocorticoid receptors (GR).

but operate in a cell-type specific manner (Skor et al., 2013). Other transcription factors include AhR, a ligand-activated transcription factor that regulates differentiation of certain immune cells (Hughes et al., 2014), the SREBPs, which are sterol regulatory element-binding proteins involved in lipogenesis (Shao and Espenshade, 2012), and p53, the tumor suppressor that serves as a regulator of cell-cycle arrest and apoptosis (Wei et al., 2006).

It has been noted in the literature that there is an NFATc1 recognition site located upstream of the *SH3PXD2A* gene (Oikawa et al., 2012). NFATc1 is a transcription factor found in activated T cells, however it has been suggested that tumor cells may fuse with

immune cells located in the tumor microenvironment to acquire the protein (Oikawa et al., 2013). Cell-cell fusion between immune cells and cancer cells has been shown to occur *in vivo*, so immunological regulation of Tks5 expression is possible (Oikawa et al., 2012). Acquired NFATc1 expression in tumor cells has also been linked to the induction of Snail and Zeb1, two transcription factors that activate EMT programming (Oikawa et al., 2013).

Tks5 mRNA and protein levels have been elevated in RAW264.7 macrophages treated with receptor activator of NF- $\kappa$ B ligand (RANKL), a factor involved in bone metastasis (Oikawa et al., 2012). Tks5 mRNA and protein levels were also elevated in A549 human pulmonary carcinoma cells treated with transforming growth factor beta (TGF- $\beta$ ), another EMT activator. NFATc1 is known to be activated downstream of RANKL stimulation, however the mechanism behind TGF- $\beta$ -induced Tks5 expression is largely unknown. Further understanding of the naturally available transcription factors responsible for Tks5 expression could elucidate these pathways.

There is an alternative promoter found within the fifth intron of *SH3PXD2A* that promotes transcription at exon 6 and generates a Tks5 isoform lacking the PX domain (Figure 14). This isoform is targeted for proteasomal degradation in Src-transformed fibroblasts, as it accumulates upon treatment with various proteasome inhibitors (Cejudo-Martin et al., 2014). Additionally, while a Tks5 mRNA ratio favoring the full length Tks5 is associated with metastatic lung adenocarcinoma, an mRNA ratio favoring the isoform lacking the PX domain is associated with nonmetastatic primary tumors (Li et al., 2013). This not only suggests isoform switching in the context of lung tumor progression, but also confirms that the functionality of Tks5 is highly regulated by its PX domain.

Upstream of *SH3PXD2A* there are at least three cytosine- and guanine-rich (CG-rich) islands (CGIs). CGIs, when methylated, silence gene transcription. These particular CGIs have been shown to be hypermethylated in the placentas of women with pregnancy-associated high blood pressure, or preeclampsia. It has been suggested that the downregulation of *Tks5* expression through promoter methylation could in turn downregulate the invasion of trophoblast cells, thus allowing for preeclampsia development (Xiang et al., 2013). The invasion of trophoblast cells into the myometrium is necessary for successful pregnancy and requires similar invasion machinery to tumor cells. Insufficient invasion leads to a reduction in blood flow to the fetus and fetal hypoxia, features seen in preeclampsia (Zhu et al., 2012). Although this is the only known epigenetic regulation of *SH3PXD2A* that has been studied, it does bring up the possibility of epigenetic control of *Tks5* expression in cancer cell invasion as well.

#### *Tks5 mRNA*

As previously mentioned, *SH3PXD2A* contains two alternative splice sites at exons 7 and 10 (Figure 14). These splice sites suggest at least four possible alternative splice forms (short, AS1, AS2, long), but it is speculated that a total of at least 12 different *Tks5* mRNA transcripts could be expressed based on the presence of undiscovered alternative promoters in *SH3PXD2A* introns. It is further possible that all of these *Tks5* isoforms potentially could hold differential roles in tumor progression (Cejudo-Martin et al., 2014).

Some cell lines, such as MCF7 breast cancer cells, have *Tks5* mRNA transcripts but little, if any, protein, suggesting methods of regulating gene expression at the mRNA level (Seals et al., 2005). One of these mechanisms may be through microRNA expression.

MicroRNAs have the ability to target and block translation of specific mRNAs. Tks5 mRNAs have been shown to be a target of miR-200c, an established EMT suppressor. Upon transient overexpression of miR-200c in MDA-MB-231 breast cancer cells, there was a reduction in Tks5 mRNA and protein, and these normally invasive cells acquired an epithelial phenotype with diminished invasive capacity. Interestingly, when miR-200s were inhibited in MCF7 cells, Tks5 mRNA levels increased, though Tks5 protein levels remained unchanged. This indicates that Tks5 is not only subject to microRNA regulation, but that there are also currently unidentified mechanisms of Tks5 regulation at the mRNA and/or protein level in order to explain the lack of Tks5 in the MCF7 cell line (Sundararajan et al., 2015).

### **Targeting Tks5 SH3 Domains as a Cancer Metastasis Therapeutic**

#### *SH3 Domains*

With further understanding of the roles that the individual SH3 domains of Tks5 play in invadopodia formation and cell invasion, specific interactions can be identified as potential targets for metastasis. SH3 domains were first discovered when a region of Crk was characterized. This region was identified as a Src homology 3 domain based on its homology to the third modular region of Src tyrosine kinase (Mayer et al., 1988). Several years later, the isolated SH3 domain of Abl tyrosine kinase was used to identify the regions within two of its binding proteins, 3BP1 and 3BP2, which interact with the kinase. Both binding motifs were identified as proline-rich regions, allowing for categorization of SH3 domains as proline-recognition domains (Ren et al., 1993). The SH3 domain is just one member of a larger proline-recognition domain superfamily. This superfamily is also comprised of the

WW (named for two conserved tryptophans), EVH1 (Ena/VASP homology domain 1), GYF (glycine-tyrosine-phenylalanine), profilin, and UEV (ubiquitin E2 variant) subfamilies (Carducci et al., 2012). It is unlikely that proline-recognition domains have a common ancestor as they differ drastically in sequence and three-dimensional structure (Li, 2005).

### *SH3 Domain Diversity*

SH3 domains are the most widespread proline-recognition domains in vertebrates with over 400 copies present in the human proteome. This abundance is due to the wide variety of functions associated with SH3 domains (Li, 2005). Human SH3 domain-containing proteins are involved in processes surrounding actin cytoskeleton reorganization, endocytosis, signal transduction, and the regulation of apoptosis (Carducci et al., 2012). A large number of SH3 domain-containing proteins fall into the category of adaptor/scaffolding proteins, which have a modular structure but no enzymatic activity. They consist of multiple protein-protein and/or protein-lipid interacting domains, allowing for binding to other proteins, the plasma membrane, or intracellular organelles (Csiszar, 2006)

### *SH3 Domain Structure*

SH3 domains are approximately 60 amino acids in length. One study compared the sequence homology of 266 non-redundant SH3 domain sequences and found that any two sequences shared an average of 27% identity (Larson and Davidson, 2000). This study also calculated the positional entropy for each of the 60 amino acid positions by identifying the frequency at which a specific amino acid was found at a site. The study identified and ranked the 24 most conserved residues, each with a positional frequency of greater than 14%

(Figure 16). The conserved residues of SH3 domains are known to be involved in maintaining the general structure of the domain and for binding its ligand (Larson and Davidson, 2000).

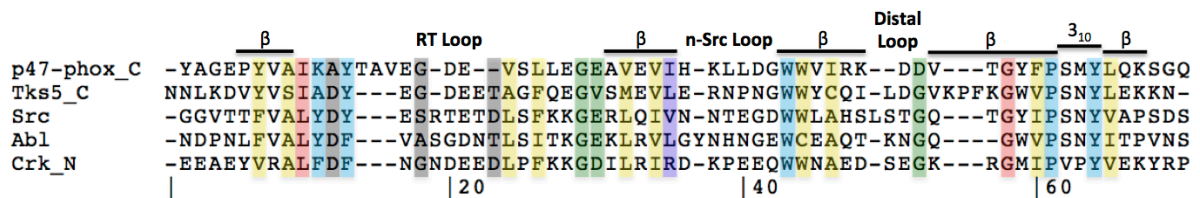


**Figure 16. SH3 Domain Sequence Homology.** The structural features of SH3 domains are noted above the amino acid sequences for the following proteins: p47-phox (C-terminal SH3), Tks5 (C-terminal SH3 #5), Src, Abl, and Crk (N-terminal SH3). Twenty-four of the most conserved residues are highlighted according to their functions: ligand binding (light blue), hydrophobic core (yellow), structural (red), RT loop (grey),  $\beta$ -turn (green),  $\beta$ -sheet bend (purple). The multiple sequence alignment was constructed using WebPRANK.

SH3 domain structure consists of approximately 5  $\beta$ -strands that are arranged in an anti-parallel formation to create two  $\beta$ -sheets. The first sheet is comprised of  $\beta$ -strands 1, 2, and 5, while the second is made from  $\beta$ -strands 3 and 4. This can be seen in a three-dimensional model of the 5<sup>th</sup> SH3 domain of Tks5 (Figure 17). The  $\beta$ -sheets are arranged at an approximate right angle to create a conserved  $\beta$ -barrel fold. The  $\beta$ -strands are connected by three variable loops: the RT-loop, the n-Src loop, and the distal loop. (Carducci et al., 2012). A short  $3_{10}$  helix is located between  $\beta$ -strands 4 and 5. The amino- and carboxy-termini of the SH3 domain of Src are located in close proximity, which suggests that the domain could extend from the protein surface without disrupting the overall protein structure. This may also be true of other SH3 domain-containing proteins as modeled for Tks5 (Figure 17) (Smithgall, 1995).

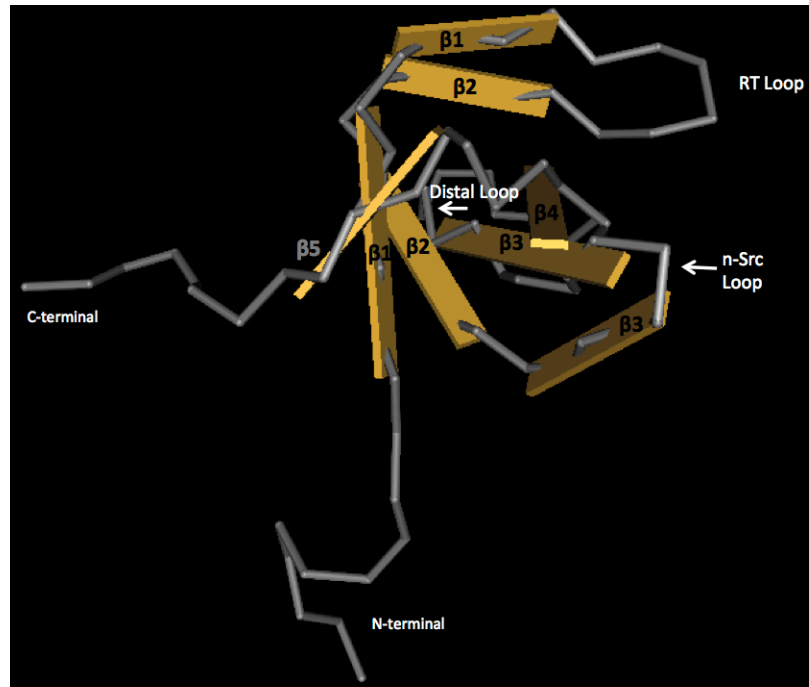


**Figure 17. SH3 Domain Structure.** Structure of the 5<sup>th</sup> SH3 domain of Tks5 adapted from NCBI Conserved Domain Database using Cn3D software.

The dissociation constants of SH3 domains are generally weak (1-200  $\mu\text{M}$ ), and thus SH3 domains are less selective than some of the other proline-recognition subfamilies, which tend to have dissociation constants ranging from the high nM to low  $\mu\text{M}$  range (Li, 2005; Nguyen et al., 1998; Zarrinpar et al., 2003). This low affinity can, on occasion, be advantageous to the cell as it allows for rapid turnover of signaling complexes. One example of this is seen in focal adhesions during integrin signaling in which SH3 domain-containing protein complexes are formed transiently, thus allowing for the brief interactions with the ECM conducive for cell motility.

As the low binding affinity allows for versatility in SH3 domain binding partners, it is difficult to predict specific interactions based on sequences alone. A given SH3 domain could interact with multiple different ligands, though only a fraction of these might take

place *in vivo* (Li, 2005). One of the ways by which cells increase SH3 domain specificity is through compartmentalization of binding. One example of this is CD2, a surface antigen that is expressed on all peripheral blood T cells. The GYF domain of CD2BP2 (CD2 binding partner 2) binds to CD2 in the detergent soluble membrane fraction whereas the SH3 domain of Fyn tyrosine kinase binds CD2 in the same cells, but in lipid rafts (Li, 2005).

Identification of the location of SH3 domain-containing proteins within a cell could thus help elucidate binding partners. Specificity can also be achieved through multiple potential binding sites and/or multiple SH3 domains. Although SH3 domain binding is weak, multiple contacts are made in the context of a folded protein. These contacts mediate further interactions, thus enabling tighter binding to ligands. Both the localization of SH3 domain containing proteins and their multiple sites of interaction make it less likely for the protein to diffuse away without rebinding at functional sites within the cell (Mayer and Eck, 1995).

### *SH3 Domain Interactions*

An SH3 domain is able to bind to proline-rich sequences in other proteins due to two main grooves and a pocket located in succession on the domain surface formed by large, hydrophobic amino acids (Figure 18). The two grooves have the ability to create hydrogen bonds and van der Waals interactions with the backbone of a left-handed helical structure formed by proline-rich peptides. The pocket, referred to as the specificity pocket, binds to an arginine or lysine residue located adjacent to the proline-rich sequence to confer specificity and stronger binding.

In a study of the ability of SH3 domains to bind various ligands, the majority of them appeared to recognize specific sequences dubbed class I and class II poly-proline motifs.

Class I ligands are characterized by the sequence (R/K)XΦPXΦP while class II ligands carry the sequence ΦPXΦPX(R/K) with ‘Φ’ representing any hydrophobic residue and ‘X’ representing any amino acid (Carducci et al., 2012). The proline-rich motif is able to bind in

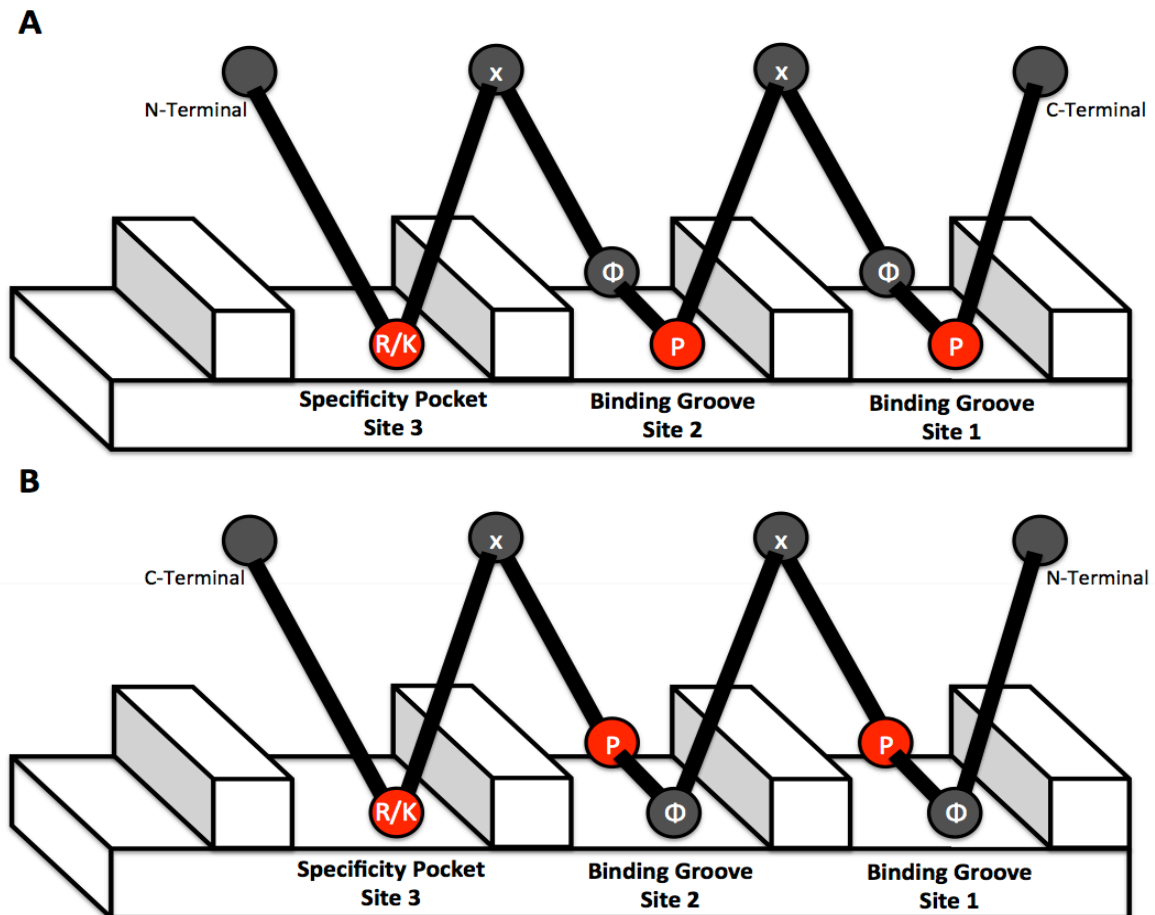


**Figure 18. SH3 Domain Binding to Class I and Class II Poly-proline Motifs.** (A) Class I, (R/K)XΦPXΦP, and (B) class II ΦPXΦPX(R/K) poly-proline motifs bind in opposite orientations due to orientation of the arginine or lysine residue. Φ represents any hydrophobic residue and X represents any amino acid.

two orientations (Li, 2005). Class I ligands have the upstream arginine or lysine in the specificity pocket, while class II ligands have the downstream arginine or lysine in this site (Mayer and Eck, 1995) (Figure 18). The majority of the SH3 domains that have been studied bind to class I and class II ligands with equal preference while some SH3 domains

preferentially bind to one class over the other, although the reasoning behind preference has not yet been made clear (Carducci et al., 2012).

In order for protein-protein binding to be possible, the interacting peptide sequence must be exposed to the solvent and be accessible to the binding partner. Proline is the best amino acid for this function as these sequences are found at the surface of proteins. Proline-rich sequences are widely distributed in the proteome, including 25% of all proteins in humans (Carducci et al., 2012). As proline-rich regions are common, it is important to establish rules regarding the binding of SH3 domains. The five member ring of proline restricts the  $\Phi$  torsional angle of the amino acid at approximately minus  $60^\circ$  thereby restricting the sequences containing prolines to a few specific conformations (Li, 2005) (Figure 19A).

The class I and class II binding partners of SH3 domains adopt a structural feature called a left-handed poly-proline-II (PPII) helix. This structure has average torsional angles of  $\Phi = -75^\circ$  and  $\Psi = +145^\circ$  (Chebrek et al., 2014) (Figure 19B). PPII helices contain a PXXP core comprised of two prolines on the same face of the helix separated by any two amino acids, with three residues per turn (Mayer and Eck, 1995). The overall sequence is roughly triangular in cross section (Cohen et al., 1995; Mayer and Eck, 1995) (Figure 19B). Side chains and backbone carbonyls are projected outward, available for interaction. It is not uncommon for 'X' to be additional prolines as it increases stabilization, however, the PPII helix is relatively stable and can resist several amino acid substitutions without changing the overall shape of the backbone (Li, 2005).

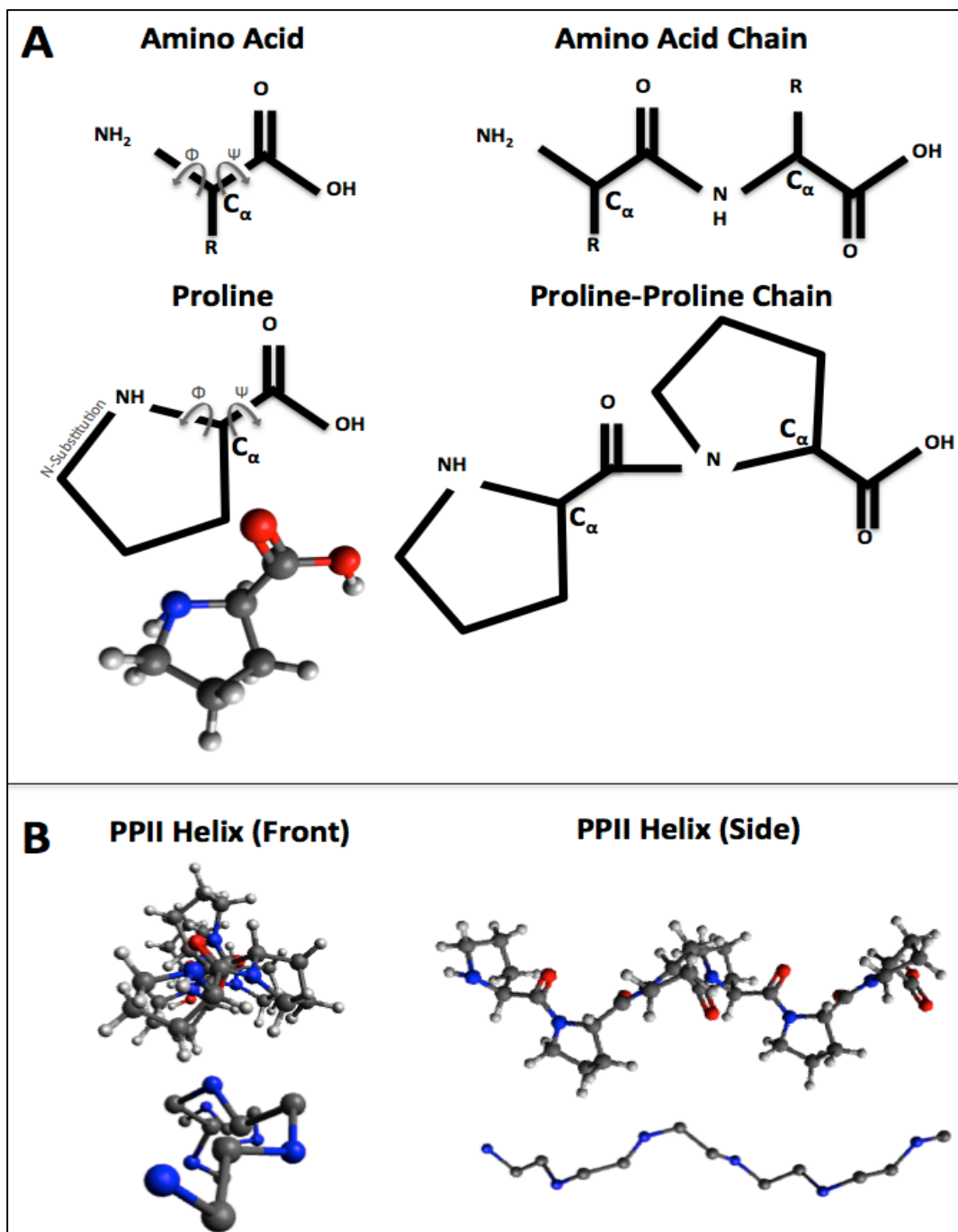


**Figure 19. Structure of a Poly-Proline-II (PPII) Helix.** (A) Comparison of a generalized amino acid structure to the N-substituted proline structure. Location of torsional angles and the bond conferring N-substitution are noted in grey. (B) PPII helix structure, front and side views. Constructed using six consecutive prolines and torsional angles of  $\Phi = -75^\circ$  and  $\Psi = +145^\circ$  with Avogadro software. Bottom images show the backbone structures.

The feature of PPII helices that is recognized by SH3 domains is the irregular backbone substitution pattern. The proline residues are N-substituted, meaning the nitrogen is bound to an atom besides the hydrogen and the C $\alpha$  carbon found in the middle of an amino acid (Figure 19A). These prolines are placed at key positions along the otherwise normal C $\alpha$ -substituted peptide scaffold. The C $\alpha$ - and N-substituted residues are separated by one backbone carbon, allowing for them to fit into the SH3 domain's binding grooves (Nguyen et al., 1998). Prolines are required at these sites because they are the only naturally available N-substituted amino acids. The requirement for N-substituted residues has been shown through replacement of proline with sarcosine, a non-natural N-substituted amino acid. These replacements are tolerated and still allow binding to SH3 domains because the N-substitution is maintained (Nguyen et al., 1998).

SH3 domain and ligand complexes have been studied using X-ray crystallography. The two main binding grooves are hydrophobic and are lined mainly by aromatic residues such as tryptophans, phenylalanines, and tyrosines. These residues are characterized as having bulky side chains with planar, near-parallel structures that accommodate the PPII helix (Li, 2005). Each groove has the potential to accommodate two residues, specifically the 'ΦP' dipeptide units at the base of the triangle (Li, 2005; Mayer and Eck, 1995) (Figure 18; Figure 20).

While the PXXP core is recognized by proline-recognition domains, this small area of interface creates a weak overall interaction (Li, 2005), and it does not explain the selectivity of SH3 domains for these ligands (Mayer and Eck, 1995). The selectivity of SH3 domains must be mediated, in part, through the SH3 domain residues flanking the proline-rich regions as well as a third site, the negatively charged specificity pocket found in SH3 domains

(Mayer and Eck, 1995). This pocket is located around the third and fourth  $\beta$  strands and is flanked by the far end of the second  $\beta$  strand, the n-Src loop, and the tip of the RT loop (Figure 20A). This surface often contains more than one subpocket and therefore may be

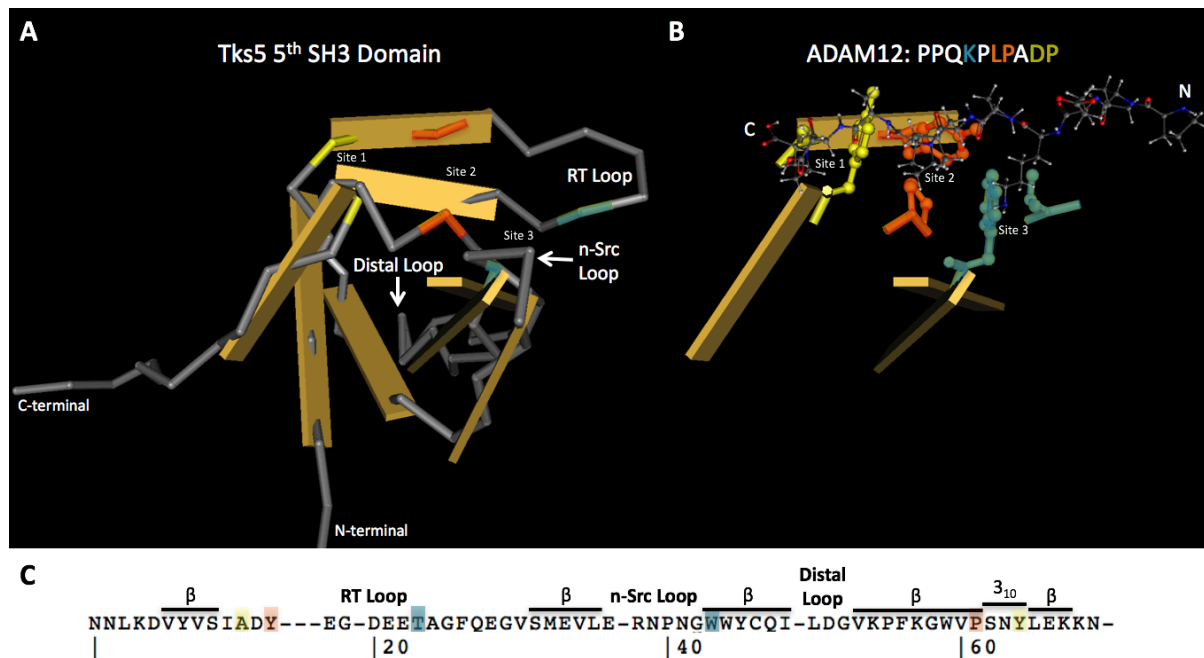


**Figure 20. Modeling SH3 domain binding between Tks5 and ADAM12.** (A) Structure of Tks5 5<sup>th</sup> SH3 domain adapted from NCBI Conserved Domain Database using Cn3D software. (B) Side chains of the specific residues involved in binding the 5<sup>th</sup> SH3 domain of Tks5 to the poly-proline motif of ADAM12. Modeled using Cn3D and Avogadro software. The ADAM12 poly-proline motif is represented by a grey ball and stick model. The residues involved in binding are highlighted according to the binding site they reside in. (C) Sequence of Tks5 fifth SH3 domain with residues involved in binding highlighted: site 1 (yellow), site 2 (orange), and the site 3 specificity pocket (teal).

more accurately referred to as the specificity zone (Saksela and Permi, 2012). The variability of the loops in sequence and structure is what confers binding specificity (Carducci et al., 2012). The RT and n-Src loops face the ligand and mediate protein interactions with terminal positively charged residues such as arginine and lysine. Conversely, the distal loop is located

on the opposite face of the SH3 domain and may contact other regions of the interacting protein (Mayer and Eck, 1995).

The positively charged arginine and lysine residues found in class I and class II poly-proline motifs are thought to provide binding stability through ligand orientation and electrostatic interactions (Carducci et al., 2012). For example, the arginine present in a class I sequence can form a salt bridge with the conserved acidic residue found in the specificity pocket of SH3 domains (Cohen et al., 1995; Mayer and Eck, 1995). Since SH3 domains only bind weakly to PXXP core motifs, any mutation in a proline, arginine, or lysine residue within the sequence has the ability to disrupt binding. Moreover, substitution of as few as two or three residues in the specificity pocket, while not necessarily changing the ability of the SH3 domain to bind poly-proline motifs, can easily alter its specificity (Li, 2005).

#### *Non-Consensus Ligands*

Some SH3 domains bind to other proteins in an atypical manner, such as in the case of the adaptor protein Grb2 and its regulation of the Vav guanine nucleotide exchange factor. In this case binding occurs between the C-terminal SH3 domain of Grb2 and the N-terminal SH3 domain of Vav, thus occurring through a complementary interface of both SH3 domains rather than through standard poly-proline motif binding (Li, 2005). Additionally, some SH3 domains bind non-consensus sequences. For example, the SH3 domain of Eps8 binds PXXDY, the SH3 domain of Fyn/Fyb binds RKXXYXXY, and the SH3 domain of Pex13p binds to an  $\alpha$  helix formed by a WXXXFXXLE while simultaneously binding a conventional poly-proline motif on the opposite face (Li, 2005). A characteristic feature of non-consensus

ligand binding is the extensive use of contacts with the SH3 specificity pocket (Saksela and Permi, 2012).

In a more comprehensive study, some SH3 domains did not provide an interpretable binding pattern, suggesting the presence of uncharacterized non-consensus sequences (Carducci et al., 2012). In addition, most of the SH3 domains in the human genome do not have a characterized ligand, which may skew the perception of consensus sequences and the prevalence of consensus binding (Saksela and Permi, 2012).

### *SH3 Domain Prevalence in Cancer*

SH3 domain-containing adaptor proteins are common in signal transduction pathways. The modular structure of adaptor proteins allows binding to multiple molecules simultaneously. Signaling results in the transient formation of the large macromolecular assemblies capable of specifying the spatiotemporal features of signal transduction pathways (Cohen et al., 1995; Csiszar, 2006). Different signaling events employ unique combinations of adaptors allowing for regulation of network assembly. Additionally, cell type-specific receptors influence tissue-dependent outcomes. The composition of adaptors at the entry sites of signals can determine whether the signal gets transmitted or degraded. This combinatorial control allows for tight regulation of compartment specificity and duration of signals (Csiszar, 2006).

SH3 domains can also relay phosphorylation signals. Activation of signal transduction pathways can occur through open and closed conformations of adaptor proteins, which allows for liberation or masking of binding surfaces. These conformational changes can be triggered by post-translational modifications (Csiszar, 2006). One example of this is

seen in the NADPH oxidase, a protein complex responsible for superoxide production. One component of the NADPH oxidase, p47phox, is held in a closed, inactive conformation through interactions between its C-terminal SH3 domain and its N-terminal PX domain, which contains a poly-proline motif within its primary sequence (Figure 21). When inactive,

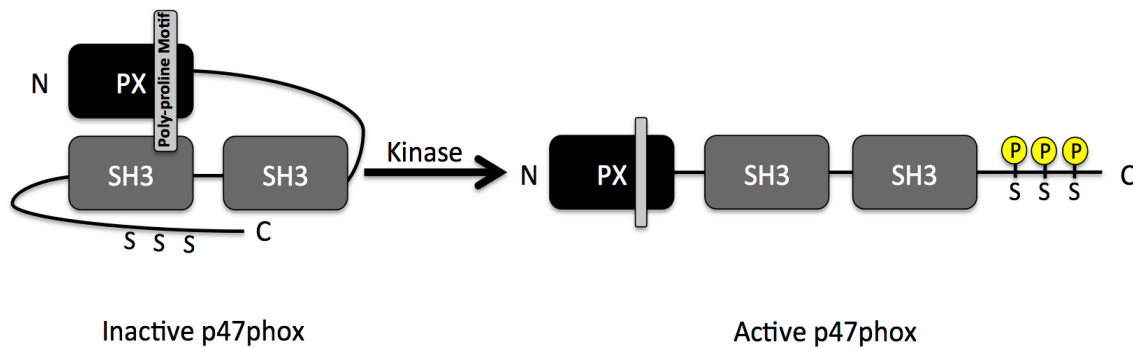


**Figure 21. Activation of p47phox.** Inactive p47phox is characterized by intramolecular binding between a poly-proline motif within its PX domain and its C-terminal SH3 domain. Upon phosphorylation this binding is disrupted, resulting in an open, active conformation. This mechanism allows for transduction of phosphorylation signals through SH3 domain function.

the protein is unable to interact with its SH3 domain-binding partners and the lipid binding surface of the PX domain is masked. The protein becomes activated when it is phosphorylated on serine residues in its polybasic region, presumably by PKC. It is thought that the presence of the phosphate groups disrupts the electrostatic interaction network mediated by the acidic residues of the SH3 domain. This disruption unfolds the protein and renders it accessible to its binding partners (Li, 2005). It is likely that SH3 domain-containing proteins commonly have both inactive, intramolecularly bound and active, binding-competent conformations (Mayer and Eck, 1995). A similar mechanism may be employed by Tks5 (see Discussion).

SH3 domain-containing adaptor proteins function as hubs in signaling networks while regulating basic aspects of cellular organization through protein-protein interactions (Csiszar, 2006; Thalappilly et al., 2008). The important roles that SH3 domain-containing proteins play in signal transduction suggest they may be good therapeutic targets for cancer cells.

### *SH3 Domain Targeting in Cancer Therapeutics*

The issue with traditional cancer therapies such as chemotherapy is the lack of specificity. In addition, the prevention of metastasis, the leading cause of death in cancer patients, is an aspect of cancer that has not been well addressed. Identifying new targets in cancer signaling pathways is a promising approach to effective treatments for this disease. Inhibition of signaling could allow for cytostatic therapies rather than the widely used cytotoxic therapies, resulting in fewer side effects. Some of these inhibitors could also target metastasis leading to a new avenue for cancer therapeutics (Vidal et al., 2001).

SH3 domain-containing proteins have been shown to be essential in several signaling pathways leading to cell division, differentiation, and cytoskeletal reorganization in response to growth signals. There is evidence of deregulation of some of these proteins in tumors, which could explain the malignant phenotypes seen in cancer cells (Vidal et al., 2001). According to a search using UniProt Knowledgebase, there are approximately 120 oncogenic human proteins that contain SH3 domains. For these reasons, SH3 domains have attracted attention as potential targets for new anti-proliferative drugs (Smithgall, 1995).

Interestingly enough, many SH3 domain-containing adaptor proteins are targets of caspases, proteases that shut off signal transduction during apoptosis. Additionally, E3 ubiquitin ligases can target proteins with SH3 domains to irreversibly downregulate signal

transduction activity through proteasomal degradation. Therefore, targeting SH3 domains appears to be a feasible means of halting cell growth or invasion and should be able to have wide implications in cancer treatment (Csiszar, 2006).

SH3 domain interactions have been analyzed in order to design agents with antitumor activity (Vidal et al., 2001). The specificity pockets of SH3 domains are very complex and variable, which allows for more specific inhibition of SH3 domains of interest (Saksela and Permi, 2012). In cancer cells, ligands designed around the sequences recognized by specific SH3 domains have shown promise in inhibiting signaling pathways that are constitutively activated by tyrosine kinases (Vidal et al., 2001). The use of synthetic peptides based on natural target sequences has been effective in blocking ligand binding to SH3 domains. These inhibitors may have utility in controlling cancer-associated signaling pathways (Smithgall, 1995).

For example, activation of the small GTPase Ras is implicated in transmission of tyrosine kinase signaling for stimulation of cell proliferation (Smithgall, 1995). Deregulation of Ras activity can result in cellular transformation. Inhibitors of tyrosine kinases disrupt deregulated Ras signaling and show antitumor potential. Within this Ras signaling pathway is the SH3 domain-containing protein Grb2 (Vidal et al., 2001). As previously discussed, activation of a receptor tyrosine kinase creates binding sites for Grb2, bringing it to the plasma membrane (Figure 22). The SH3 domain of Grb2 interacts with a poly-proline motif on Sos (Son of Sevenless), recruiting Sos to the plasma membrane and allowing it to be located in close proximity to Ras. Sos has the ability to activate Ras (Smithgall, 1995). Grb2 is not oncogenic, however its overexpression has been shown to occur in breast cancer (Vidal et al., 2001). For this reason, it has been studied as a potential target in this signaling

pathway without directly targeting Ras. This avenue has shown some success, with dominant negative expression of Grb2 SH3 domain mutants effectively blocking mitogenic signaling (Tanaka et al., 1995). In a similar study, dominant negative expression of Grb2 with deletion of either one of its SH3 domains inhibited Grb2/Sos signaling complex

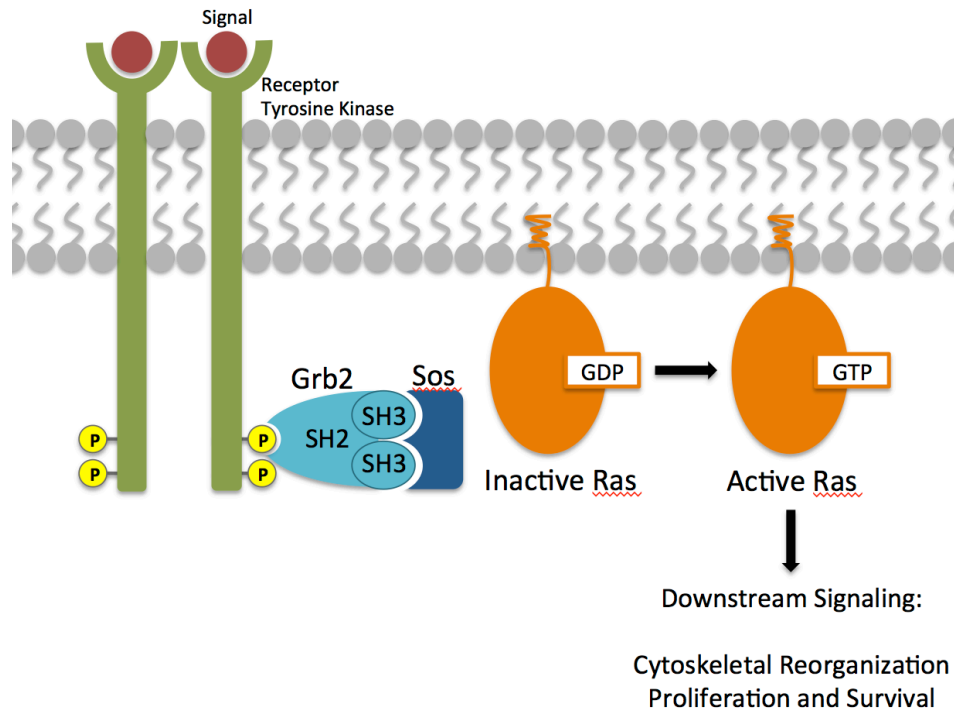


**Figure 22. The Role of Grb2 in Ras Signaling.** The SH2 domain of Grb2 binds to phosphorylated receptor tyrosine kinases. The SH3 domains of Grb2 are bound to Sos, recruiting it to the plasma membrane. When in close proximity to Ras, Sos, as a guanine nucleotide exchange factor, is able to catalyze GTP/GDP exchange, resulting in Ras activation.

formation and reversed transformation in cells. In still another approach, the dominant negative expression of a Sos mutant containing only the poly-proline motif necessary for binding Grb2 resulted in the inability to create functional signaling complexes (Vidal et al., 2001). In a more recent study, a variety of small molecules were tested in a virtual screen for their abilities to inhibit the interaction between the C-terminal SH3 domain of Grb2 and the

docking protein Gab2. Some of the molecules tested were able to inhibit this interaction with moderate affinity, and the most promising candidates were based on a dihydro-s-triazine scaffold showing the possibility of inhibiting SH3 domain interactions without the use of poly-proline motifs or SH3 domain mutants (Simister et al., 2013). These examples verify the successful targeting of the Grb2 SH3 domain, thus supporting the concept that SH3 domains within other signal transduction pathways may be similarly targeted without having to inhibit kinase signaling pathways directly.

Some SH3 domain inhibitors may specifically suppress the metastatic properties of cancer cells. For example, the binding of the SH3 domain of cortactin to AMAP1, an Arf GTPase activating protein, is a potential therapeutic option. Use of a cell-permeable peptide identical to the AMAP1 proline-rich region and designed to bind two cortactin molecules was effective in preventing this interaction. This inhibitor decreased cancer cell invasion and metastasis without affecting cell viability (Hashimoto et al., 2006).

As it might seem difficult to inhibit SH3 domain interactions due to their relatively low binding affinities, some studies have been more focused on designing inhibitors that are not identical to natural ligands in order to increase binding affinity. Use of an inhibitor with increased binding affinity could more easily displace the natural ligand allowing for more effective inhibition of SH3 domain function (Vidal et al., 2001). The development of poly-proline motifs with non-natural N-substituted amino acids in the place of prolines has been shown to increase binding affinity to SH3 domains in some cases, suggesting a possible route for inhibitor design (Nguyen et al., 1998). Another example of increasing binding affinity involved a Grb2 inhibitor that was synthesized to contain two linked proline-rich sequences. This approach resulted in the creation of a dimer with greater binding affinity than a single

motif. The dimer bound to two Grb2 SH3 domains simultaneously, improving the disruption of the interaction between Grb2 and Sos and leading to effective inhibition of Ras activation (Cussac et al., 1999).

Approaches similar to the aforementioned examples could be tested for their efficacies in suppressing Tks5 interactions and invadopodia-mediated invasion. Each Tks5 SH3 domain is structurally different, allowing for targeting of individual SH3 domains to disrupt the specific interactions necessary for these processes (Figure 23). A potential drawback to SH3 domain targeting could be the inability of agents to discriminate between normal and cancerous cells. However, through better understanding of the roles that SH3 domains play within these pathways, any potential issues might be easily alleviated. Use of correct doses may suppress tumor cell proliferation without completely inhibiting normal cell proliferation. Additionally, normal cells respond to multiple pathways, so inhibition of a single pathway might not affect proliferation and differentiation (Smithgall, 1995). Targeting a specific SH3 domain function is a viable means of disrupting the unregulated proliferation and invasion signaling pathways in cancer cells without being detrimental to the processes necessary for normal cell signaling. Further study of Tks5 SH3 domain function alongside testing of dominant negative expression of Tks5 SH3 mutants or small molecule inhibitors designed to displace ligands could provide a means of preventing cancer metastasis.

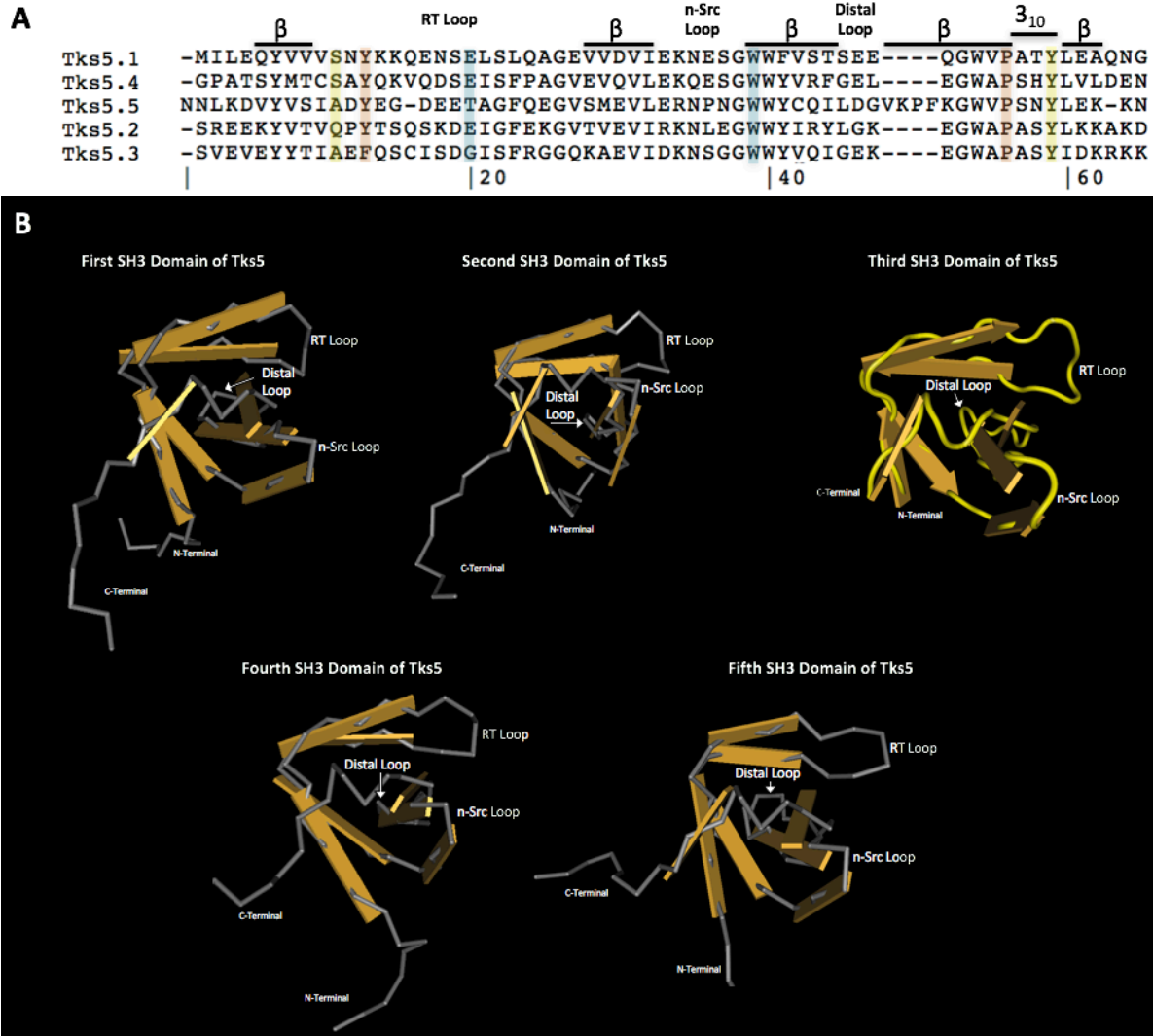


**Figure 23. Structures of the five SH3 domains of Tks5.** (A) Sequence alignment of the SH3 domains of Tks5. Residues involved in binding are highlighted: site 1 (yellow), site 2 (orange), and the site 3 specificity pocket (teal). Sequence alignment constructed using WebPRANK. (B) Tks5 SH3 domain structures, adapted from NCBI Conserved Domain Database using Cn3D software. The solution structure for the third SH3 domain of Tks5 is not currently available. The image shown was modeled using SWISS-MODEL structure homology software and adapted for Cn3D using VAST software.

## Objectives

Tks5 activation is accomplished through Src-mediated tyrosine phosphorylation, leading to Tks5 localization at the plasma membrane and binding of its PX domain to PI(3,4)P<sub>2</sub>. Once at the plasma membrane, Tks5 has been shown to be instrumental to the assembly of invadopodia precursor complexes. This activity by Tks5 is accomplished through its scaffolding function, as invadopodia-associated proteins are recruited to these sites by binding to the five SH3 domains of Tks5.

While the importance of Tks5 in invadopodia formation has been investigated, not much is known about the specific roles that the individual SH3 domains of Tks5 play in these processes. Additionally, there is little understanding of the mechanism by which Src phosphorylation leads to Tks5 activation. Furthermore, the regulation of Tks5 SH3 domain interactions is poorly understood. Better characterization of the SH3 domains of Tks5 might allow for identification of an interaction that could potentially be inhibited as a therapeutic option for metastatic disease.

We hypothesize that the SH3 domains of Tks5 influence the development of invadopodia through alterations in Tks5 cellular localization and regulation of Tks5 activation status. We address this hypothesis through the following specific aims. First, we will identify the specific SH3 domains of Tks5 that are necessary for ECM degradation associated with invadopodia formation. Second, we will determine how Tks5 SH3 domain mutants affect the ability of Tks5 to be activated through phosphorylation by Src tyrosine kinase and/or conformational changes. And third, we will examine the localization of these Tks5 SH3 domain mutants in invadopodia-competent cells. Presumably the alterations we expect to see in matrix degradation, activation, and localization will depend on the proteins in

which Tks5 interacts, thus making an analysis of Tks5-protein interactions a long-term goal of this study as well.

## Methods and Materials

### Construct Design and Verification

In previous work in the Seals lab, murine Tks5 cDNAs had been introduced into the pSGT mammalian expression vector and point mutations created in each of the SH3 domains by site-directed mutagenesis such that the first tryptophan within a conserved pair was converted to an alanine (WW → AW). This is a common strategy for interfering with the protein-binding properties of each SH3 domain, and was applied here in order to study the function of each SH3 domain in Tks5 (Nguyen et al., 1998; Li, 2005; Tanaka et al., 1995) (Table I and Figure 24). In preparation for the studies in this thesis project, an experiment

**Table I. Point Mutations in Tks5 Constructs**

<b>Tks5 Construct</b>	<b>Mutation*</b>
M1	W188A
M2	W260A
M3	W441A
M4	W827A
M5	W1056A

\*Position of mutations based on short form of Tks5

was undertaken to compare the expression of Tks5 from the pSGT vector, which uses an SV40 promoter, and the pcDNA3 vector, which uses a CMV promoter. The expression of

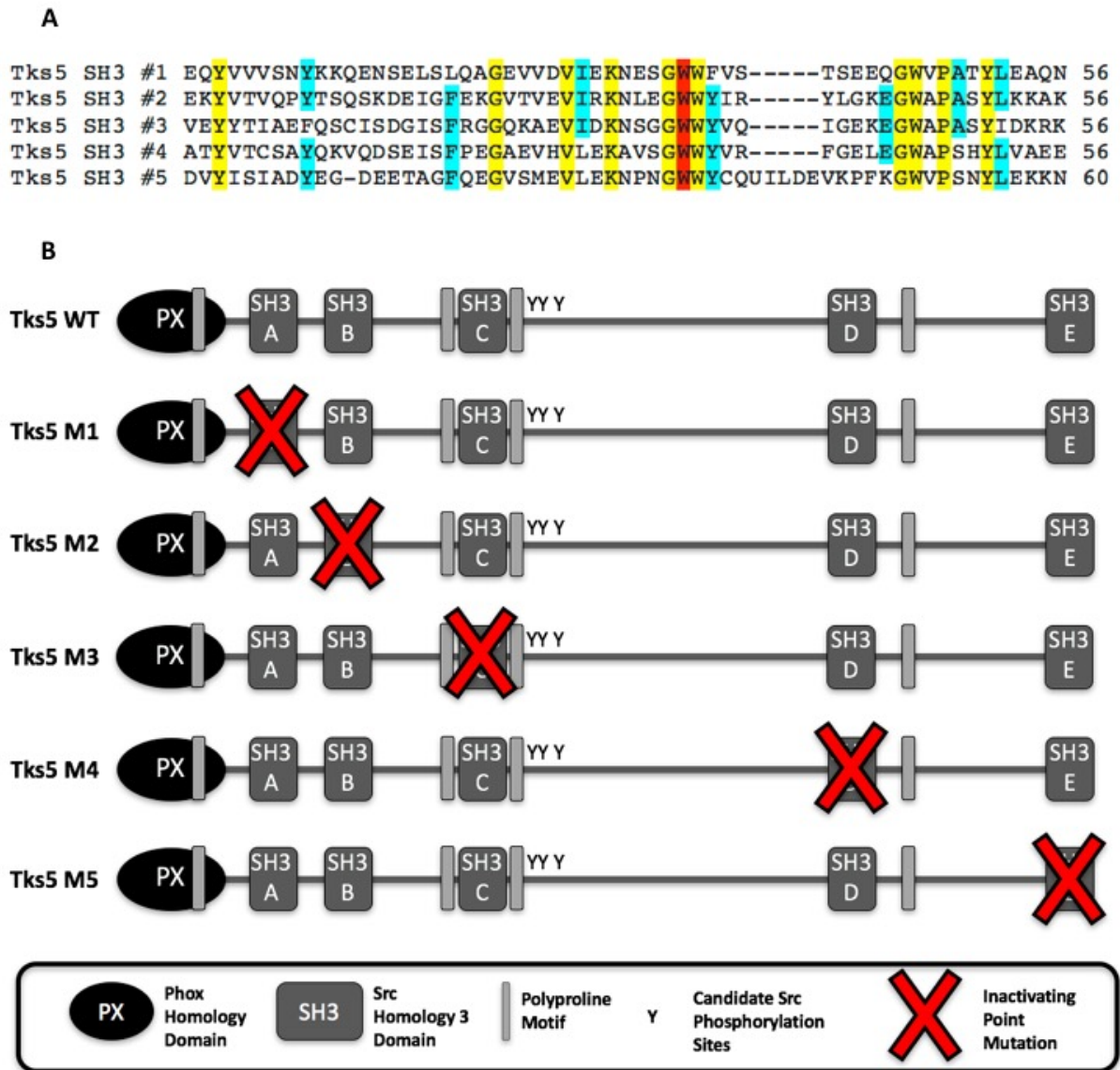


**Figure 24. Inactivation of Tks5 SH3 domains.** (A) Amino acid alignment of Tks5 SH3 domains. Yellow: conserved; blue: mostly conserved; red: tryptophan mutated to an alanine. (B) Schematic representation of Tks5 showing location of inactivating SH3 domain point mutations for the constructs used in this study.

ectopic Tks5 based on the expression vector was compared following immunoblotting (Figure 25). The results of this experiment indicated far more robust Tks5 expression from the pcDNA3 vector. We therefore decided to alter the wild-type version of Tks5 in pcDNA3

to create four new constructs (M1-M4) harboring the SH3 domain point mutations described above. This was accomplished by replacing the regions surrounding each SH3 domain in the

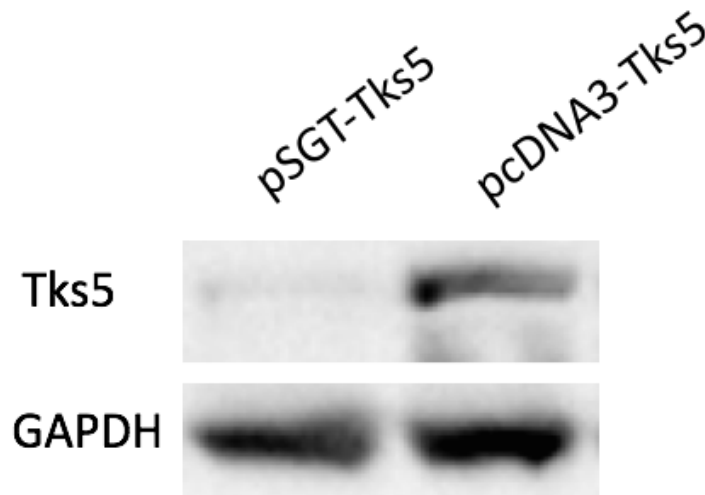


**Figure 25. Immunoblot analysis of Tks5 expression based on expression vector.** LNCaP cells were transfected with wild-type Tks5 constructs made in pSGT or pcDNA3 mammalian expression vectors. Lysates were subjected to immunoblotting for Tks5 to compare protein expression levels. GAPDH (glyceraldehyde-3-phosphate dehydrogenase) served as a loading control.

pcDNA3 vector with the mutant form previously created in the pSGT vector. The M5 construct had already been cloned into the pcDNA3 vector long before this thesis project. Large-scale preparations of wild-type and mutant DNA constructs were generated (Qiagen, ThermoFisher) and the mutations confirmed by DNA sequencing (GeneWiz).

### Cell Culture

The human prostate carcinoma cell line called LNCaP was cultured at 37°C and 5% CO<sub>2</sub> in RPMI-1640 media (Hyclone) formulated with 2 mM L-glutamine, 10 mM HEPES,

and 100 mg/L sodium pyruvate, and supplemented to a final concentration of 10% fetal bovine serum (Sigma-Aldrich) and 1% penicillin/streptomycin (Hyclone).

Src-transformed fibroblasts (Src-3T3 cells), COS-7 cells, and HEK293 cells were cultured at 37°C and 5% CO<sub>2</sub> in DMEM media (Sigma-Aldrich) formulated with 110 mg/L sodium pyruvate and 2 mM L-glutamine, and supplemented to a final concentration of 10% fetal bovine serum and 1% penicillin/streptomycin.

### **Nucleofection/Electroporation**

Each Tks5 construct was individually introduced into LNCaP cells according to previously defined protocols by Nucleofection<sup>TM</sup> (Lonza), a proprietary electroporation technique (Burger et al., 2014). Briefly,  $2 \times 10^6$  LNCaP cells were mixed with 3-10 µg of plasmid DNA and solutions from Nucleofector Kit R to a final volume of 100 µL.

Nucleofection was carried out using program T-009. After nucleofection, cells were allowed to recover for 15-30 minutes in 500 µL of pre-warmed media before being plated for further experimentation as defined below. Cells nucleofected with wild-type Tks5 and with an empty pcDNA3 vector served as positive and negative controls, respectively.

### **Lipid-based Transfections**

Approximately  $2 \times 10^6$  cells were seeded in 6-cm dishes. At 70% confluency, the cells were transfected with Tks5 constructs in the pcDNA3 vector, Src Y527F in the pSGT vector, and/or the PX domain of Tks5 in the pEGFP-N1 vector using Lipofectamine<sup>TM</sup> 3000 reagent (ThermoFisher) according to manufacturer protocol. Briefly, two separate 250 µL aliquots of Opti-MEM<sup>®</sup> reduced serum media (ThermoFisher) were mixed with 3.75 µL and

7.5  $\mu\text{L}$  Lipofectamine 3000, respectively. A 500  $\mu\text{L}$  aliquot of Opti-MEM was mixed with 10  $\mu\text{L}$  P3000<sup>TM</sup> reagent and 7  $\mu\text{g}$  plasmids. The 500  $\mu\text{L}$  aliquot was then split between the tubes containing Lipofectamine 3000 and incubated at room temperature for 10 minutes. Both aliquots were then added to cells in 6-cm dishes, and then the cells were incubated 48 hours at 37°C.

### **Invadopodia Activity**

LNCaP cells were grown at 37°C in a 12-well plate with approximately  $3.2 \times 10^5$  cells per well. Each well contained a glass coverslip coated with poly-L-lysine (50  $\mu\text{g}/\text{mL}$ ) and Oregon Green 488-labeled gelatin (111  $\mu\text{g}/\text{mL}$ ), a denatured form of the extracellular matrix protein collagen, as previously described (Martin et al., 2012). After 48 hours, the cells on the coverslips were fixed with 0.3% formaldehyde, permeabilized with 0.4% Triton X-100, stained with AlexaFluor 594-conjugated phalloidin (1:200; Invitrogen) and 5% donkey serum/PBS, and mounted using small aliquots of ProLong<sup>TM</sup> Gold Antifade Mountant with DAPI (Life Technologies). Using an Olympus BX51 microscope (OPELCO) equipped with a Retiga EXi Fast 1394 camera (QImaging), ten random images were collected for each experimental condition with each image containing an average of 30 cells. Image processing was conducted with Q-Capture 64 Suite software. The area of gelatin degradation was quantified using ImageJ 1.49 software for each image and then normalized based on the number of cells within each image.

Transfected Src-3T3 cells were allowed to recover for 24-48 hours before being lifted and re-plated into 12-well plates containing the same kind of poly-L-lysine/Oregon Green 488-labeled gelatin coated coverslips as mentioned above. Four hours after plating cells, the

coverslips were fixed and stained for Tks5 as described in the Invadopodia Localization section of the Methods and Materials. Quantification of gelatin degradation was carried out using a 100X objective and Type F Immersion Oil (Olympus).

### **Cell Lysates**

During the cell lysis procedure, all plates and buffers were kept on ice. Cultured cells were washed twice with 0.6 volumes of 1 mM sodium orthovanadate in PBS, then lysed using 0.05 volumes of NP40 lysis buffer composed of 20mM Hepes, 110 mM sodium chloride, 40 mM sodium fluoride, 1% NP40, 1 mM sodium orthovanadate, 10 µg/mL aprotinin, 10 µg/mL benzamidine, 10 µg/mL leupeptin, 10 µg/mL pepstatin, and 1 mM PMSF. The cells were scraped from the dish, incubated on ice for 10 minutes, and the cellular debris removed by centrifugation at 10,000 x g for 10 minutes at 4°C. Total protein was determined using a detergent-compatible protein assay kit according to manufacturer protocol (Bio-Rad), and by measuring absorbance at 750 nm on a SpectraMax Pro (Molecular Devices) relative to known BSA standards.

### **SDS-PAGE/Immunoblotting**

For immunoblotting, 35 to 55 µg of whole cell lysate protein were first loaded on a denaturing 7.5% polyacrylamide gel, separated at 150-200 V for approximately 1 hour, and then transferred to a 0.45 µm nitrocellulose membrane (Bio-Rad). After blocking in 5% milk/0.5% BSA in 0.1% PBST, the membrane was incubated overnight at 4°C with a primary antibody specific to Tks5 (1:1000; #sc-30122; Santa Cruz), phosphotyrosine (1:1000; Clone 4G10; Millipore), GFP (1:1000; sc-9996; Santa Cruz), c-Myc (1:1000; clone

4A6; Millipore), HA (1:1000; clone 12CA5; Roche Life Science), phospho-Src Y416 (1:1000; #2101; Cell Signaling Technology), or GAPDH (1:1000; #sc-25778; Santa Cruz) in 10% blocking buffer. This was followed by incubation in a species-specific peroxidase-conjugated secondary antibody (1:2500; NA9340V; NA931V; GE Healthcare, Piscataway, NJ) for 30 minutes at room temperature. Proteins were visualized using Western Lightning Plus Chemiluminescence reagent (PerkinElmer) or SuperSignal<sup>TM</sup> West Dura Extended Duration Substrate (ThermoFisher Scientific) and a ChemiDoc imaging system (Bio-Rad). Expression was quantified using Image Lab<sup>TM</sup> Software 5.1 (Bio-Rad).

### **Immunoprecipitation**

Cells were lysed and protein was quantified as described previously. Lysates containing 200-500 µg protein were then diluted to a final volume of 500 µL using NP40 lysis buffer. One microliter of a Tks5 polyclonal antibody (1736.9; reactive to the 4th SH3 domain of Tks5), 5 µL c-Myc antibody (clone 4A6; Millipore), or 2 µL GFP antibody (sc-9996; Santa Cruz) were added to each sample and mixed on a rotator at 4°C for 2 hours. Antibodies bound to their target proteins were then separated from unbound proteins by mixing with 10 µL protein A-conjugated Sepharose 4G beads (#101041; Life Technologies) or immobilized protein G beads (#30399; Pierce) on a rotator at 4°C for 1 hour. Beads were then washed three times in 500 µL of NP40 lysis buffer by addition, centrifugation at 1000 x g for 1 min at 4°C, and removal of the supernatant. Precipitated proteins were eluted from the beads with 50 µL SDS-PAGE gel loading buffer containing DTT by boiling for 5 minutes at 95°C. Precipitated proteins were separated using SDS-PAGE and visualized by immunoblotting as described above for Tks5, phosphotyrosine, or GFP detection.

## **Invadopodia Localization**

Untagged Tks5 constructs (wild-type, M1-M5) in the pcDNA3 vector, carboxy terminal, Myc-tagged Tks5 constructs in the pSGT vector, and/or the FYVE domain of Hrs in the pEGFP vector were introduced into cells. Coverslips were transferred to a 12-well plate for processing at 48 hours after transfection. The coverslips were fixed with 0.3% formaldehyde, permeabilized with 0.4% Triton X-100, and incubated with a primary antibody specific to the Myc tag (1:1000; clone 4A6; Millipore) in 5% donkey serum/PBS for three hours. The coverslips were then incubated for one hour with the appropriate fluorescent-conjugated secondary antibody (1:2000; AlexaFluor 488-anti-mouse; GE Healthcare) and AlexaFluor 594-conjugated phalloidin (1:200; Invitrogen) to visualize Myc-tagged Tks5 and F-actin, respectively. When studying co-localization, coverslips were incubated with primary antibodies to Tks5 (1:1000; #sc-30122; Santa Cruz), EEA1 (1:1000; #610456; BD Transduction Labs<sup>TM</sup>), total Src (1:1000; #2108; Cell Signaling), or cortactin (1:1000; #05-180; Millipore) in 5% donkey serum/PBS for three hours. The coverslips were then incubated for one hour with the appropriate fluorescent-conjugated secondary antibodies (1:2000; AlexaFluor 488-anti-rabbit; GE Healthcare) (1:2000; AlexaFluor 594-anti-mouse; GE Healthcare). Coverslips were mounted using small aliquots of ProLong<sup>TM</sup> Gold Antifade Mountant with DAPI and imaged as described above. Oil immersion microscopy was carried out for LNCaP localization and Src-3T3 co-localization imaging as described above, using a 100X objective and Type F Immersion Oil (Olympus).

## **Bioinformatic Procedures**

### *Retrieval of Human Proteins*

A list of human proteins containing SH3 domains was compiled using the UniProt Knowledge Base (<http://www.uniprot.org/>). Briefly, an advanced search was carried out for “SH3” using the domain search and “*Homo sapiens*” using the organism search. This resulted in a list of 220 proteins in this knowledge base to be used for further analysis.

### *Retrieval of Domain Sequences*

PX and SH3 domain sequences were obtained from the NCBI Protein Database (<http://www.ncbi.nlm.nih.gov/protein/>). Searches were carried out using UniProt entry identifiers in order to access information pages specific to the proteins of interest. Under the “Features” section, regions containing the PX domain and SH3 domain sequences were identified. Selecting regions allowed for highlighting of the domain sequence of interest in the sequence located under the “Origin” section. These sequences were transferred to a document and translated to FASTA format for further analysis.

### *Multiple Sequence Alignment*

Multiple sequence alignments were formulated using webPRANK (<http://www.ebi.ac.uk/goldman-srv/webprank/>), Clustal Omega (<http://www.ebi.ac.uk/Tools/msa/clustalo/>), and MUSCLE (<http://www.ebi.ac.uk/Tools/msa/muscle/>). Default parameters were used for each

program. Sequences of interest were submitted in FASTA format and each program aligned the sequences and produced distance trees showing sequence similarity.

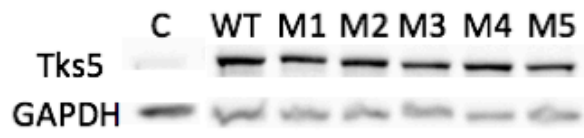
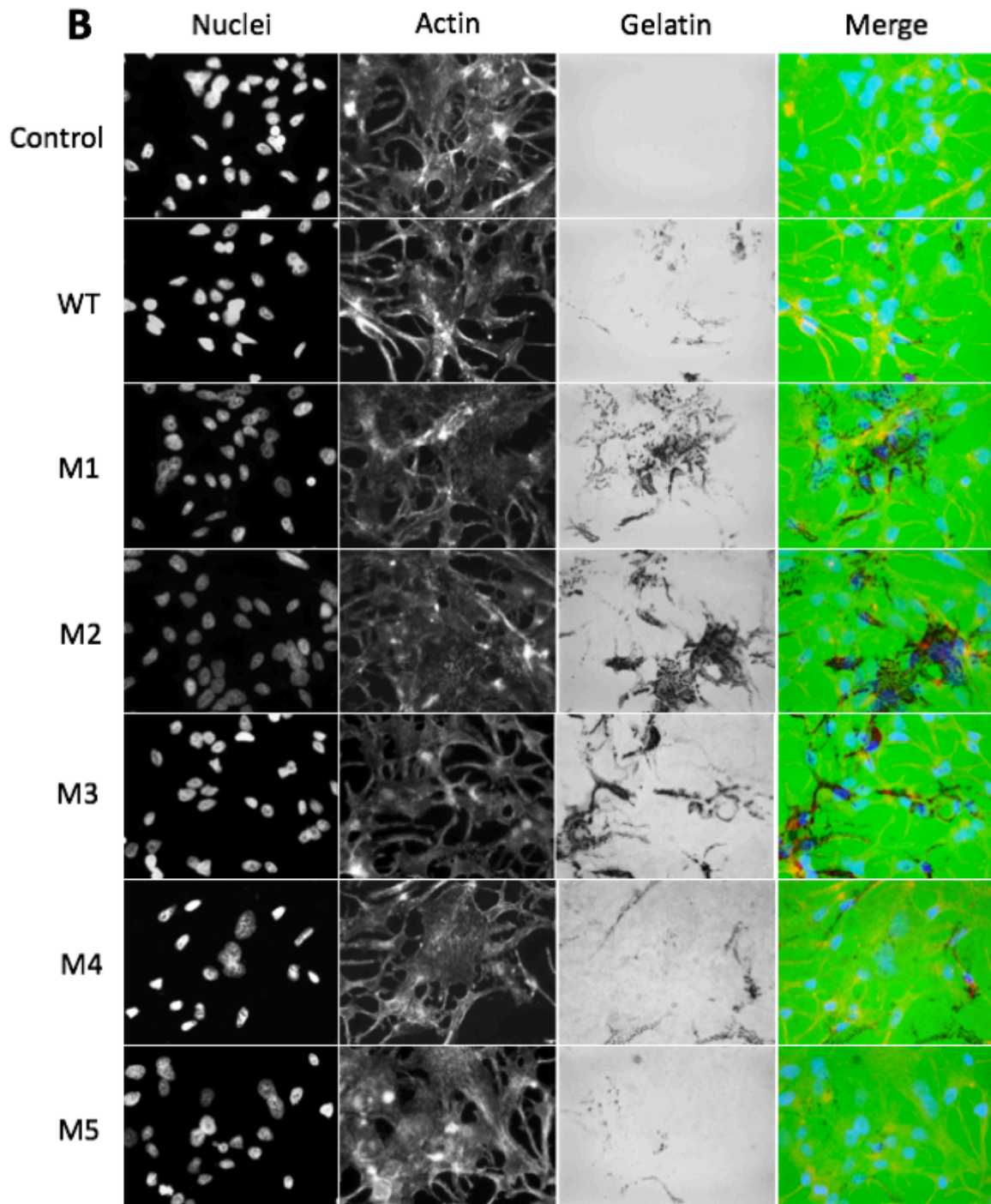
#### *Poly-proline Motif Scan*

PX domain sequences were scanned for poly-proline motifs using ScanProsite (<http://prosite.expasy.org/scanprosite/>). “Option 3” was selected in order to search known domain sequences for a motif of interest. The sequences were entered in FASTA format. Common poly-proline motifs were searched against these sequences, specifically (K/R)xxPxxP, PxxPx(R/K), and RxxK.

## Results

### **Tks5 SH3 Domain Mutations Result in Differential Effects on ECM Degradation in LNCaP Cells**

Previous research has shown that the introduction of ectopic Tks5 into LNCaP cells, a cell line largely deficient in this protein, can induce invadopodia development and invadopodia-associated gelatin degradation activity (Burger et al., 2014). We wanted to determine the role of Tks5 SH3 domain mutations in invadopodia development using this model system. This was accomplished using Tks5 constructs with SH3 domain mutations (WW → AW) that would be expected to disrupt the binding of Tks5 to other proteins at these sites. To that end, we introduced wild-type or mutant Tks5 from the pcDNA3 mammalian expression vector into LNCaP cells to comparable expression levels with GAPDH serving as a gel loading control (Figure 26A). The nucleofected cells were also grown on coverslips coated with fluorescently-labeled gelatin in order to determine the extent of matrix-degrading invadopodia activity in these cells (Figures 26B and 26C). In this assay, matrix degradation is seen as cleared zones ('holes') in the fluorescent gelatin monolayer with the average degradation per cell represented in terms of a fold-change in activity relative to wild-type Tks5. Our results showed surprising differential changes in invadopodia activity exerted by the Tks5 mutants. Disruption of the 4th or 5th SH3 domain of Tks5 (M4-W827A, M5-W1056A) resulted in what appeared to be a slight decrease in the ability of the cells to degrade gelatin relative to wild-type (WT) Tks5. Conversely, disruption of the 1<sup>st</sup> (M1-W188A), 2<sup>nd</sup> (M2-W260A), or 3<sup>rd</sup> (M3-W441A) SH3 domain resulted in a 2.5- to 4-fold

**A****B**

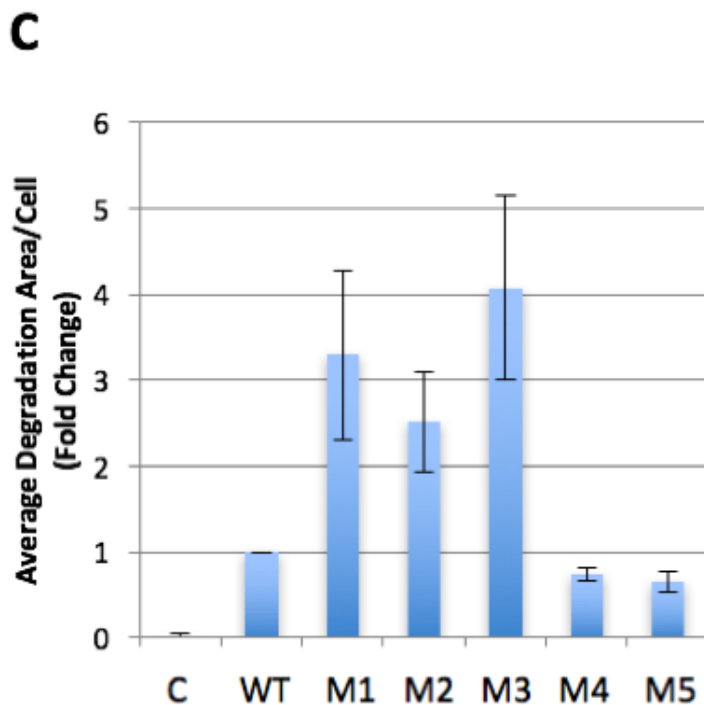


**Figure 26. Effects of Tks5 SH3 Domain Mutations on Invadopodia-associated Gelatin Degradation by LNCaP cells.** (A) Nucleofected LNCaP cells expressing wild-type (WT) Tks5 or Tks5 mutants (M1-M5) were analyzed for Tks5 and GAPDH protein levels in total cell lysates by immunoblotting. (B) Representative images taken at 40X magnification showing gelatin degradation in the nucleofected LNCaP cells. (C) Quantification of gelatin degradation area per cell. Error bars represent standard error.

increase in gelatin degradation. We speculated at the time that these results may reflect either a down-regulatory control mechanism exerted on Tks5 by other proteins that bind to these domains, an increased ability to be activated by Src phosphorylation including potential Tks5 conformational changes, or an increase in translocation of Tks5 to invadopodia when these first three SH3 domains are disrupted.

### **Tks5 SH3 Domain Mutants Are Uniformly Distributed in LNCaP Cells**

Tks5 has been shown to localize to punctate invadopodia formed by LNCaP cells, though in the past this depended on the stable overexpression of Tks5 (Burger et al., 2014).

In order to investigate the hypothesis that the localization of the transiently expressed Tks5 mutants plays a role in the observed differences in degradation ability, the mutants were again introduced into LNCaP cells by nucleofection and this time the cells were transferred to uncoated glass coverslips. After 48 hours, the coverslips were fixed and stained for actin and Tks5 (Figure 27). Interestingly, no overt differences were observed in the distribution of Tks5 within these cells. That is, the LNCaP cells transiently nucleofected with Tks5, unlike the Tks5 overexpressing stable LNCaP cell line, all had a similar morphology and did not form any obvious actin-rich invadopodial structures, despite their ability to degrade gelatin in an invadopodia-like manner (Figure 27). This is consistent with previous observations (Burger et al., 2014), and suggests that Tks5 localization did not likely play a role in the degradation ability of these cells. In sum, the localization of Tks5 mutants within the cells and the appearance of the cells themselves did not vary between any of the tested conditions leading us to explore other hypotheses beyond the enhanced ability to localize to invadopodial structures.

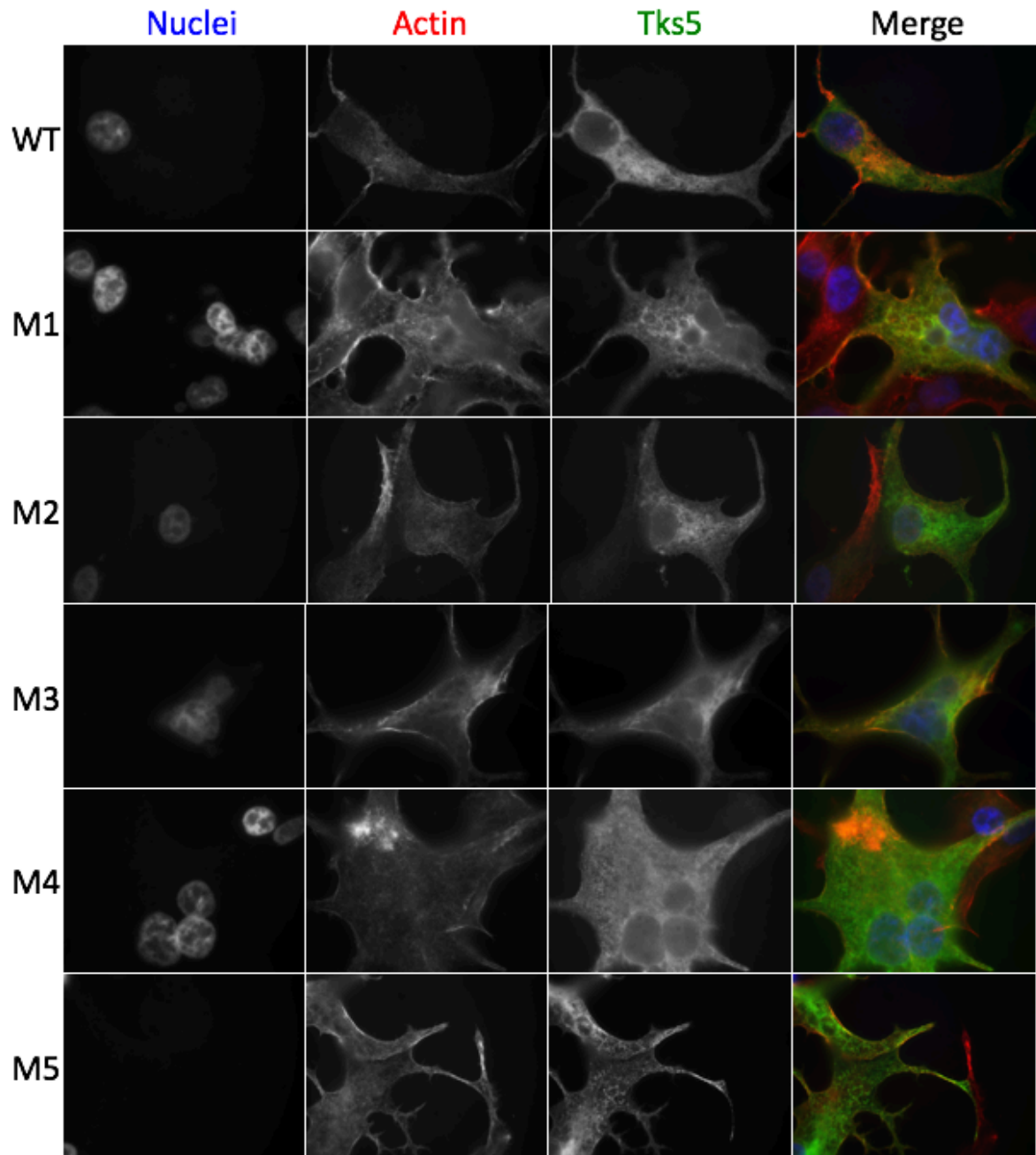


**Figure 27. Effects of SH3 domain mutations on Tks5 localization in LNCaP cells.** Representative images show localization of nuclei (blue), F-actin (red), and Tks5 (green) 48 hours post-nucleofection of LNCaP cells by fluorescent microscopy. Images were taken at 100X magnification.

## **COS-7 Cells as a Model for Investigations Surrounding Tks5 SH3 Domain Mutations**

Previous studies have shown that Tks5 activity within a cell is directly linked to the ability of Tks5 to be phosphorylated by Src tyrosine kinase (Burger et al., 2014). Mutation of Y557 and Y619 result in a diminished ability of Tks5 to be phosphorylated by Src. And introduction of these mutants into LNCaP cells results in a significantly diminished ability of the cells to degrade gelatin (Burger et al., 2014). It could be speculated that any disruption in the binding of proteins to any of the first three SH3 domains of Tks5 could allow for easier access to these tyrosine residues by Src, and thus allow for increased phosphorylation and Tks5 activity. We thus hypothesized that the ability of these Tks5 SH3 domain mutants to be phosphorylated within the LNCaP cells may be affecting their ability to degrade gelatin films.

In order to detect Tks5 phosphorylation, LNCaP cells were nucleofected with Tks5 and constitutively active Src Y527F constructs. Whole cell lysates were subject to immunoprecipitation using an antibody specific to Tks5 and then analyzed for tyrosine phosphorylation by immunoblotting with a phosphotyrosine-specific antibody. Both Tks5 and activated Src, monitored with an antibody that detected Src phosphorylation at Y416 (p-Src), were detectable in the transiently nucleofected LNCaP cells. However, detection of Tks5 phosphorylation proved more difficult with this cell line despite past screens with the assay being successful (Burger et al., 2014).

To potentially remedy the situation, we turned to COS-7 cells as they are a relatively easier cell line to transfect (Figure 28). Relative to LNCaP cells, COS-7 cells showed detectable tyrosine phosphorylation of Tks5 and were therefore adopted for analysis of Tks5

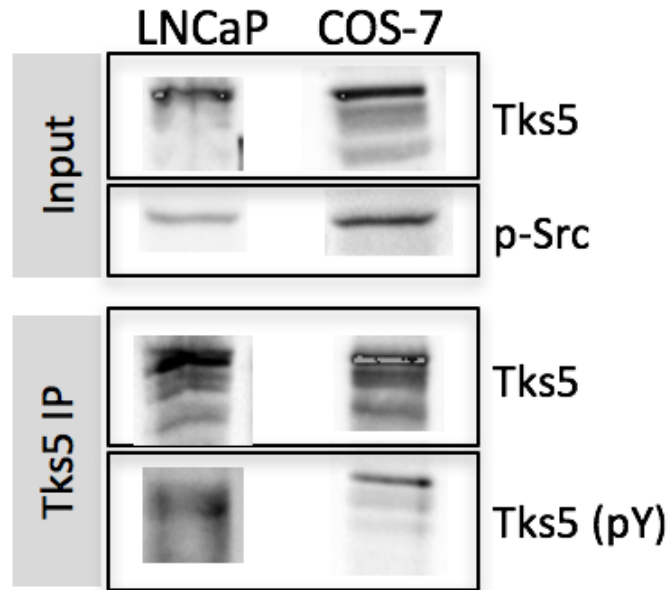


**Figure 28. Detection of Tks5 phosphorylation in LNCaP and COS-7 cells.** The top panel depicts the total cell lysates (input) from LNCaP and COS-7 cells transiently expressing Tks5 and Src Y527F based on immunoblot analysis with antibodies to Tks5 and p-Src. The lower panel depicts the lysates following immunoprecipitation (IP) with a Tks5 antibody and analyzed for either Tks5 or Tks5 tyrosine phosphorylation (pY) by immunoblot analysis.

SH3 domain mutant phosphorylation studies. To that end, Tks5 SH3 domain mutants were introduced into COS-7 cells alongside Src Y527F and after 48 hours were analyzed for tyrosine phosphorylation (Figure 29). Unfortunately, difficulties arose with this assay, as some transfections appeared to be toxic to the COS-7 cells producing undetectable levels of Src and Tks5 expression. When phosphorylation was detectable, all Tks5 SH3 domain mutants appeared to have the capacity to be phosphorylated by Src, however the results overall were largely inconclusive. Due to inability to effectively assess tyrosine phosphorylation or to detect any changes in phosphorylation as a result of SH3 domain mutations, this hypothesis was not pursued further.

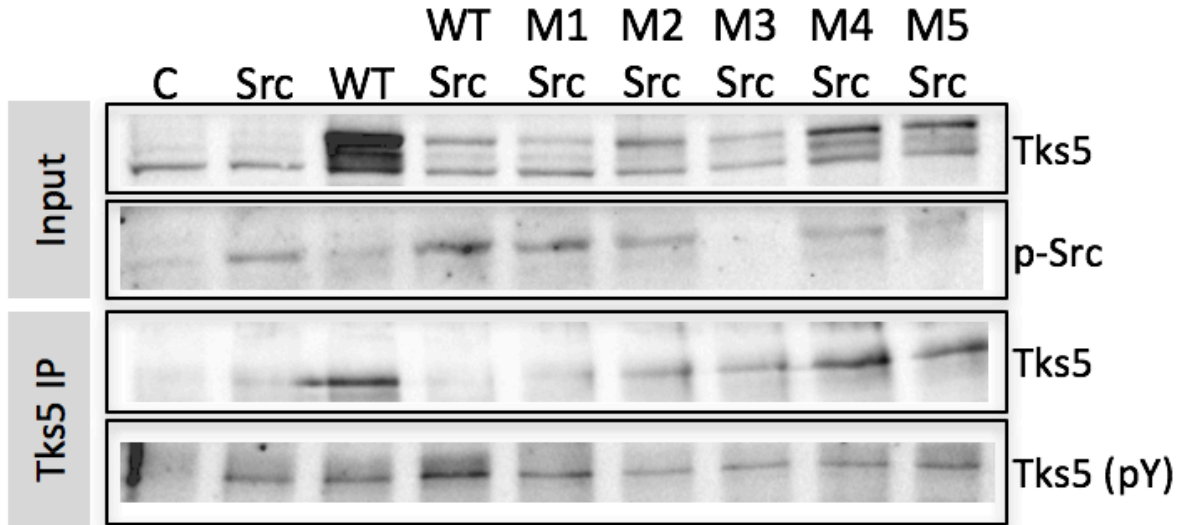


**Figure 29. Effects of Tks5 SH3 domain mutations on Tks5 tyrosine phosphorylation in COS-7 cells co-expressing Src Y527F.** Input lysates from transiently transfected COS-7 cells were analyzed for Tks5 and p-Src by immunoblot analysis. Lysates were also immunoprecipitated (IP) with a Tks5 antibody and analyzed for Tks5 and Tks5 tyrosine phosphorylation (pY) by immunoblot analysis.

COS-7 cells were also explored for their use as a model system for Tks5 mutant localization, cell morphology, and matrix degradation. In this case, COS-7 cells were transiently transfected with wild-type Tks5, constitutively active Src Y527F, or both constructs. Cells were then grown on glass coverslips or coverslips coated with Oregon Green 488 gelatin for 48 hours (Figure 30). COS-7 cells transiently expressing Src Y527F and wild-type Tks5 appeared to develop invadopodia-like structures (Figure 30A). These structures remained largely punctate with coincident staining of Src, Tks5, and F-actin, though some cells acquired the ability to form more developed crescent- or ring-shaped invadopodial structures as well. COS-7 cells transiently expressing Src Y527F alone also appeared to have the ability to form actin-based invadopodial structures, so while the formation of invadopodia by COS-7 cells appears to be Src-dependent, it may or may not be Tks5-dependent depending on the endogenous Tks5 protein levels in this cell line (Figure 30A). Despite the morphological changes to the transfected COS-7 cells, none of them

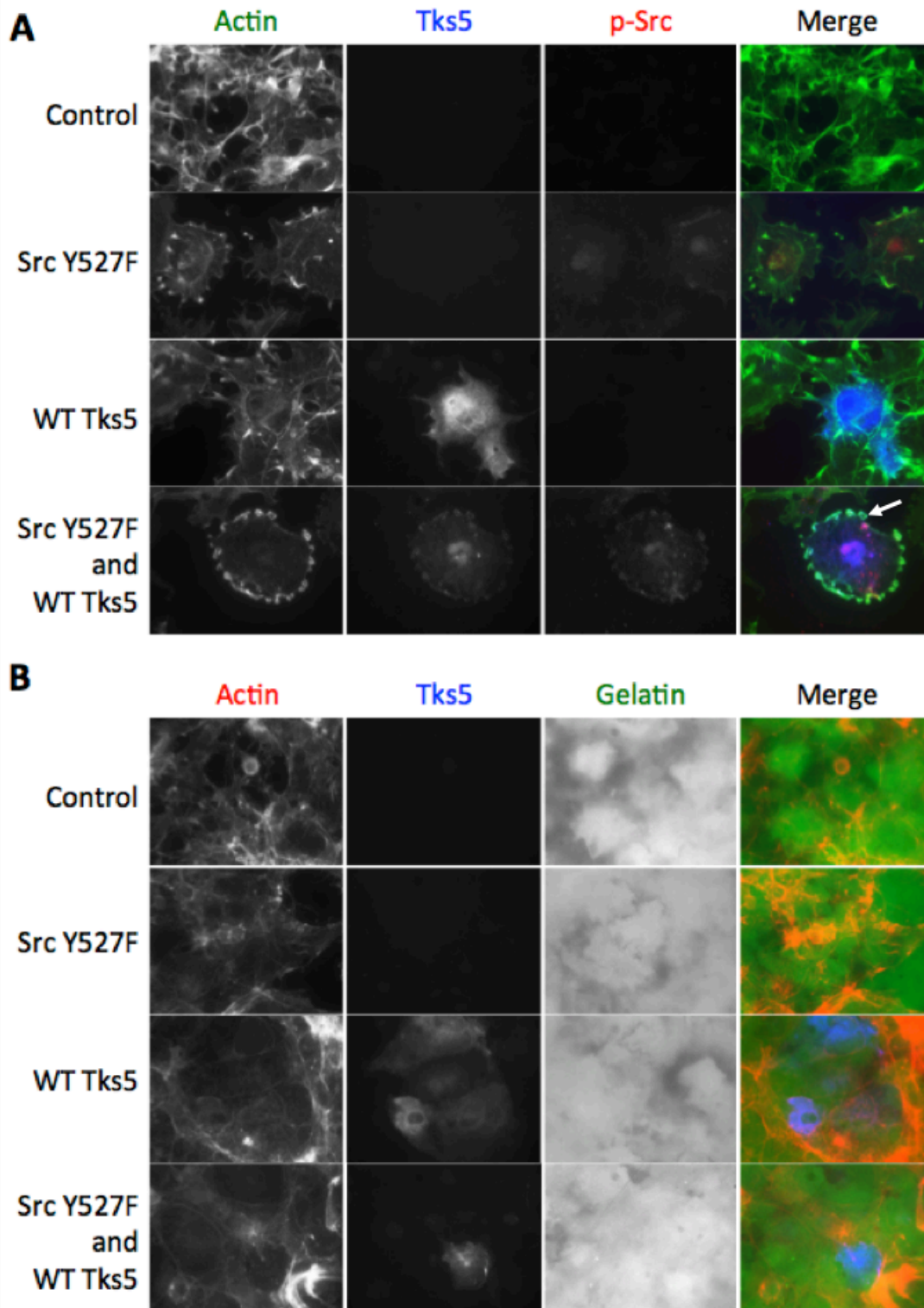


**Figure 30. Morphology (A) and matrix degradation (B) by COS-7 cells transiently expressing wild-type Tks5, Src Y527F, or both constructs.** Images were taken at 40X magnification by fluorescent microscopy using antibodies for Tks5 and Src as well as phalloidin for F-actin. The arrow points to an invadopodia-like structure in a cell transfected with both Tks5 and Src Y527F.

appeared to acquire the ability to degrade gelatin in ways seen previously for LNCaP cells, so the ultimate use of this cell line for studies of matrix degradation did not seem feasible (Figure 30B). Previous work with COS-7 cells had also alluded to the inability of this cell line to degrade matrix (Crowley et al., 2009).

Due to the formation of actin-rich structures in COS-7 cells co-expressing of Src Y527F and Tks5, further studies were carried out to investigate the morphology of COS-7 cells co-expressing Src Y527F and the Tks5 SH3 domain mutants (Figure 31). While the cells continued to form actin-rich structures, no overt differences were observed based on Tks5 SH3 domain mutation. It is likely that Src Y527F alone is sufficient to induce these morphological changes, and when combined with the lack of matrix degradation in this cell line, it was decided that the COS-7 model system would no longer be utilized for experimentation.

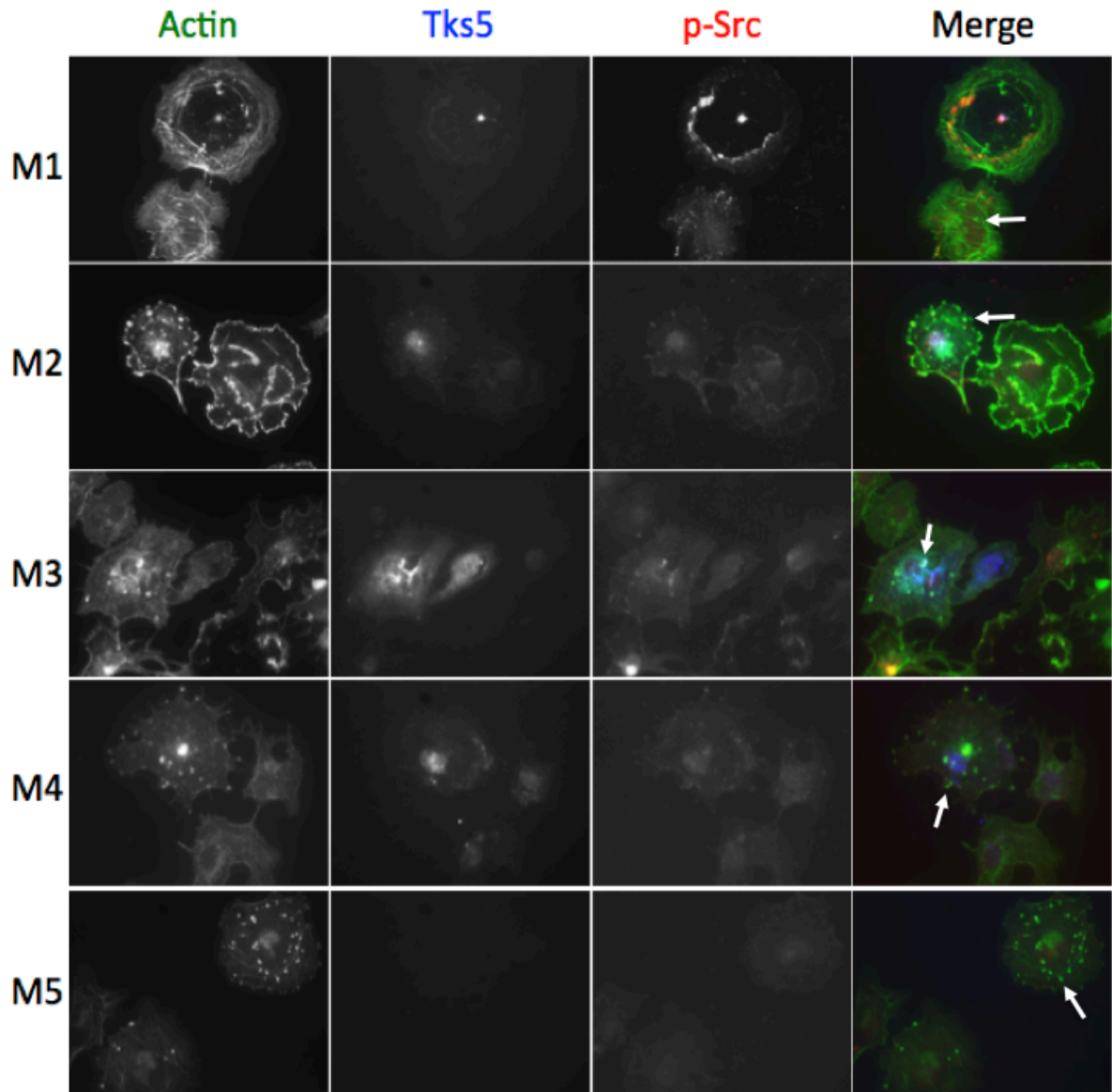


**Figure 31. Morphology of COS-7 cells co-expressing Src Y527F and Tks5 SH3 domain mutants.** COS-7 cells were transiently transfected with Src Y527F and Tks5 SH3 domain mutants (M1-M5) and then analyzed by fluorescent microscopy using antibodies for the detection of Tks5 and Src alone with phalloidin for F-actin. The arrows point to invadopodia-like structures in the merged images. Images were taken at 40X magnification.

## **Tks5 SH3 Domain Mutations Affect Tks5 Localization and Invadopodia Formation in Src-3T3 Cells**

Use of the LNCaP and COS-7 cell lines was unable to provide any conclusive results regarding Tks5 localization and cell morphology. In order to better investigate these aspects of Tks5 function, we began experimentation with Src-3T3 cells. Src-3T3 cells carry stable expression of a constitutively active form of Src and thus develop robust invadopodia in the form of superstructures called “rosettes”. Src-3T3 cells also have high levels of endogenous Tks5, and Tks5 localizes to these rosettes (Seals et al., 2005). Mutants carrying a Myc epitope tag were introduced into these cells to provide easy detection of transiently expressed, ectopic Tks5 using a Myc antibody. This was done to determine the effects of these mutations on cell morphology were explored alongside the localization of Tks5 mutants relative to invadopodia. Src-3T3 cells were transfected with the Tks5 mutants, and stained for actin and Tks5-Myc 48 hours post-transfection (Figure 32). Based on the results in LNCaP cells (Figure 26) we hypothesized that that Tks5 harboring mutations in the first (M1), second (M2), or third (M3) SH3 domains might exhibit robust localization to invadopodia, but instead these mutant constructs resulted in nearly a complete loss in invadopodia formation. Additionally, these mutants appeared to aggregate in the cytoplasm in the region surrounding the nucleus. In contrast, the Tks5 harboring mutations in the fourth (M4) and fifth (M5) SH3 domains did not appear to affect invadopodia formation, and these mutants were further able to localize to rosettes to the same extent as wild-type Tks5.

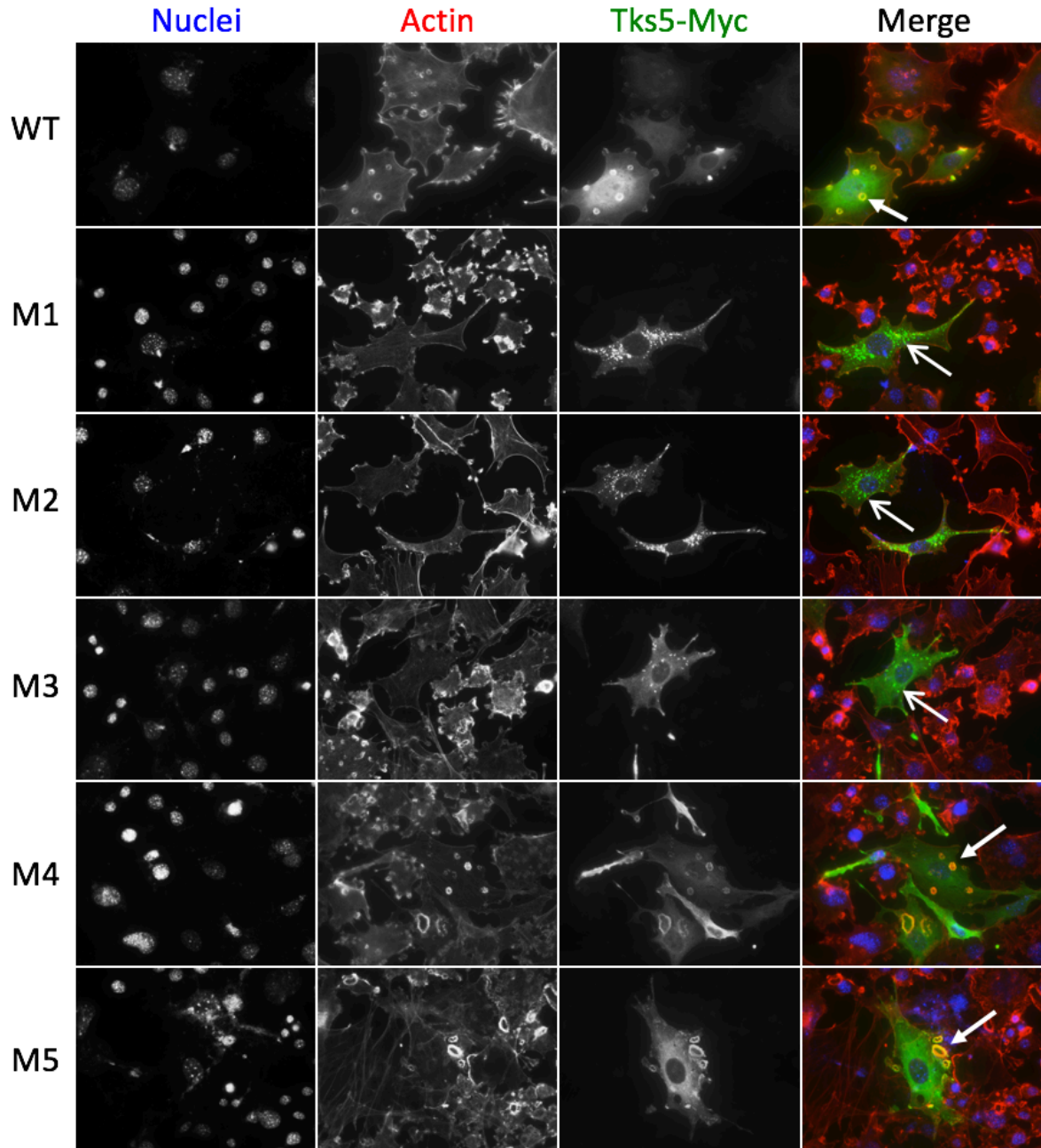


**Figure 32. Effects of Tks5 SH3 domain mutations on Src-3T3 cell morphology and Tks5 localization.** Src-3T3 cells were transiently transfected with wild-type (WT) Tks5 or Tks5 SH3 domain mutants (M1-M5) and then analyzed for morphology and Tks5 localization by fluorescent microscopy. Ectopic Tks5 was monitored with an antibody to the Myc epitope. Representative images show localization of nuclei (blue), actin (red), and the Myc epitope of Tks5 (green) 48 hours post-transfection. Closed arrows point to rosette-shaped invadopodia structures. Open arrows point to mis-localized M1, M2, and M3 Tks5 constructs to peri-nuclear aggregates. Images were taken at 40X magnification.

### **Tks5 SH3 Domain Mutations Affect ECM Degradation Efficiency by Src-3T3 Cells**

Using the LNCaP model, the M1, M2, and M3 mutant Tks5 constructs result in an increase in invadopodia-associated matrix degradation activity, however they obliterate invadopodia integrity in Src-3T3 cells. Additionally, the aggregates formed by these mutants in Src-3T3 cells did not co-localize with actin, suggesting that the F-actin that did exist did not possess the ability to degrade matrix proteins. To test this hypothesis, Src-3T3 cells expressing Tks5 SH3 domain mutants were analyzed for their ability to degrade gelatin films. Tks5 mutants were introduced into Src-3T3 cells, and 48 hours post-transfection the cells were lifted and re-plated onto Oregon Green 488 gelatin coated coverslips for an additional 4 hours, after which the cells were fixed and stained for Tks5-Myc (Figure 34). In some cases, the cells expressing M1, M2, or M3 Tks5 mutants appeared to lose their ability to degrade gelatin in the shorter time frame of this assay. For those cells that retained some ability to degrade gelatin, the degradation pattern appeared to lack focalization, occurring diffusely underneath the entire span of the cell in a pattern similar to that exhibited by LNCaP cells transiently expressing Tks5 (Figure 26B). This was contrary to the degradation patterns made by Src-3T3 cells expressing wild-type Tks5, or the M4 or M5 Tks5 mutants, which all showed more focalized gelatin degradation at sites of invadopodia formation (Figure 33). By focusing matrix degradation where it is needed, more efficient invasion may be maintained (Mukhopadhyay et al., 2009). Loss of invadopodia formation thus appeared to impair the ability of these cells to efficiently degrade matrix through a loss of focalized gelatin degradation.

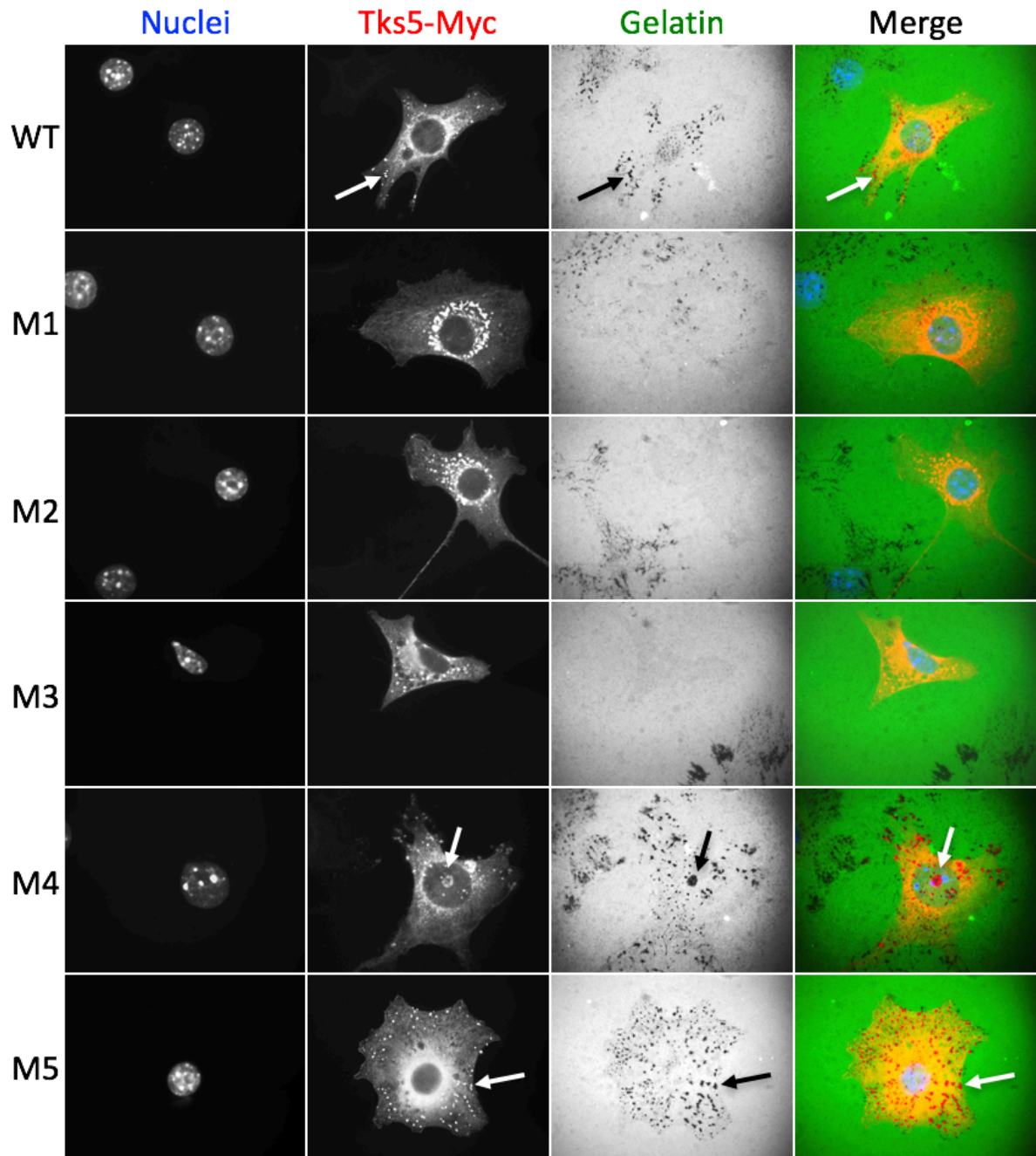


**Figure 33. Effects of Tks5 SH3 domain mutations on invadopodia-mediated gelatin degradation by Src-3T3 cells.** Src-3T3 cells were transiently transfected with wild-type (WT) Tks5 or Tks5 SH3 domain mutants (M1-M5) and then analyzed for gelatin degradation by fluorescent microscopy. Ectopic Tks5 in transfected cells was monitored with an antibody to the Myc epitope. Representative images show nuclei (blue), the Myc epitope tag of Tks5 (red), and gelatin (green) after a 4 hour degradation period. Arrows point to focalized sites of degradation. Images were taken at 100X magnification.

It is noteworthy that the nonspecific gelatin degradation patterns observed in LNCaP cells transiently expressing Tks5 (Figure 26) was similar to that of Src-3T3 cells expressing M1, M2, or M3 Tks5 SH3 domain mutants (Figure 33). It is possible that these diffuse gelatin degradation patterns represent some sort of compromise in the ability to fully focalize gelatin degradation in ways seen in cells fully competent for invadopodia formation. It is possible that LNCaP cells lack all the requisite components for focalized matrix degradation, whereas the Src-3T3 cells, which have them, become compromised in their functionality, thus leading to more inefficient invadopodia-associated matrix degradation patterns.

### **Tks5 Constructs with M1-M3 Mutations Co-localize with Early Endosome Markers in Src-3T3 Cells**

We noted that the aggregates formed by the M1, M2, and M3 mutant Tks5 constructs were highly reminiscent of the punctate distribution of the isolated PX domain of Tks5 when introduced into normal NIH3T3 fibroblasts (Abram et al., 2003). As the PX domain of Tks5 is used for lipid interactions, it was hypothesized that the isolated PX domain was associated with early endosomes which are rich in PI(3)P (Abram et al., 2003). We further hypothesized that the PX domain of Tks5 might also be responsible for localizing the M1, M2, and M3 Tks5 mutants to endosomes. In order to determine the nature of the aggregates formed by these Tks5 mutants, Src-3T3 cells were transfected with each Tks5 SH3 domain mutant construct and 48 hours post-transfection were stained for the Myc epitope of Tks5 and for early endosomal antigen 1 (EEA1), a protein with a lipid-binding FYVE domain that is often used as an early endosomal marker (Stenmark et al., 1996) (Figure 34). As

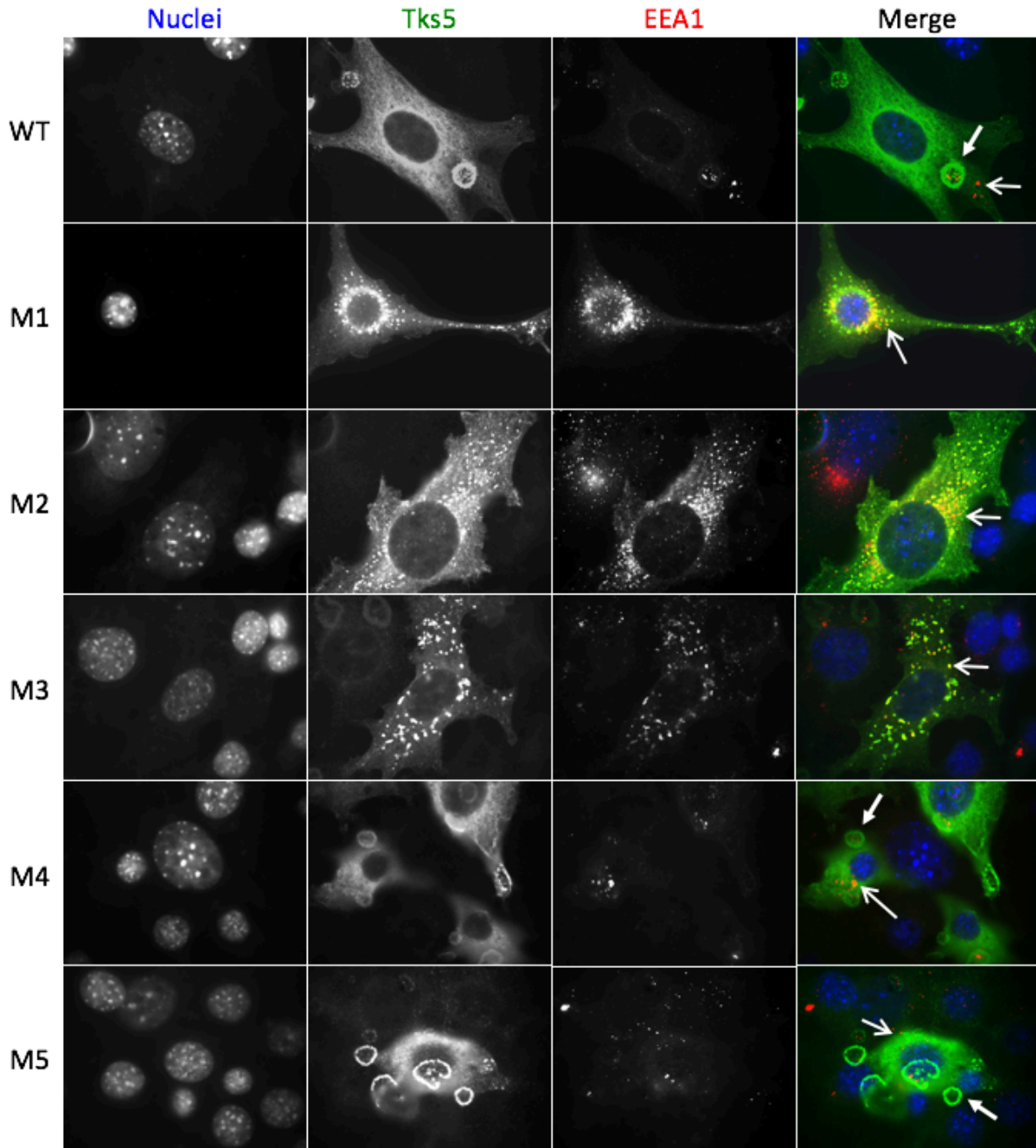


**Figure 34. Localization of Tks5 SH3 domain mutants and EEA1 in Src-3T3 cells.** Src-3T3 cells were transiently transfected with wild-type (WT) Tks5 or Tks5 SH3 domain mutants (M1-M5) and then analyzed for Tks5 and EEA1 localization by fluorescent microscopy. Ectopic Tks5 in transfected cells was monitored with an antibody to the Myc epitope. Representative images show localization of nuclei (blue), Tks5 (green), and EEA1 (red) 48 hours post-transfection. Closed arrows point to invadopodia rosettes. Open arrows point to endosomes. Images were taken at 100X magnification.

anticipated, each of the M1, M2, and M3 mutations created a version of Tks5 that co-localized with EEA1, suggesting that these mutants may be mis-localizing due to interactions between the PX domain and endosomal membranes, thus resulting in the aggregates observed in the previous experiment (Figure 32).

In order to confirm these results, the localization pattern of the lipid-binding FYVE domain of the early endosomal protein Hrs was also compared with the Tks5 SH3 domain mutants in Src-3T3 cells (Figure 35). Consistent with the previous results, the FYVE domain co-localized with the M1, M2, and M3 mutant Tks5 constructs at organelles patterned similar to that of endosomes. This suggests that by disrupting the protein-binding capacity of the 1<sup>st</sup>, 2<sup>nd</sup>, or 3<sup>rd</sup> SH3 domains, the full-length Tks5 protein is able to interact with these subcellular structures. As the FYVE domain of Hrs is responsible for localizing the protein through interactions with phosphoinositides, it appears possible that the PX domain of Tks5 in each of these mutants is ultimately responsible for the localization to and quite possibly the exaggerated formation of endosomes within these cells.

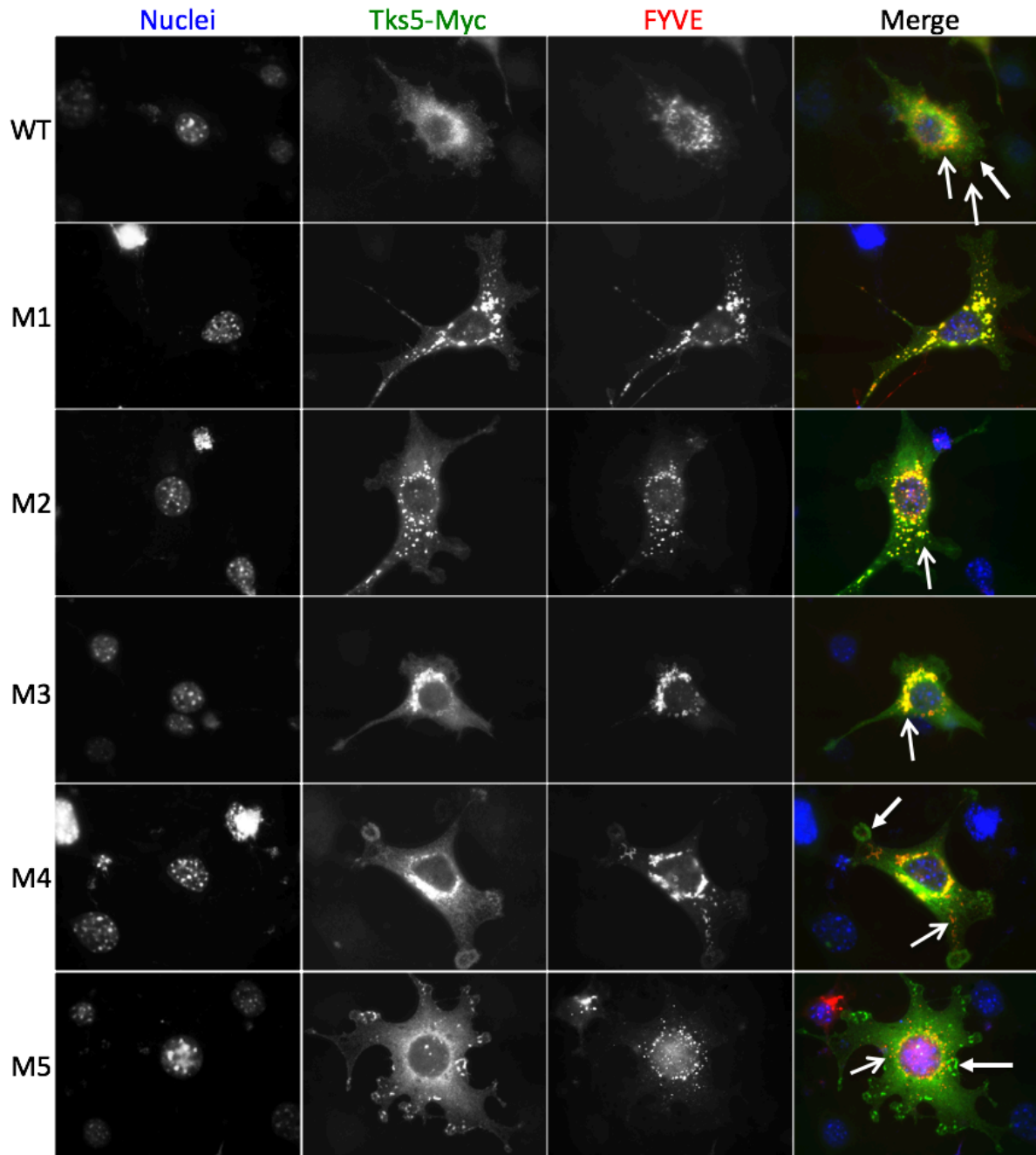


**Figure 35. Localization of the FYVE domain of Hrs and Tks5 SH3 domain mutants in Src-3T3 cells.** Src-3T3 cells were transiently transfected with wild-type (WT) Tks5 or Tks5 SH3 domain mutants (M1-M5) along with the FYVE domain of Hrs tagged with GFP before being analyzed by fluorescent microscopy. Ectopic Tks5 in transfected cells was monitored with an antibody to the Myc epitope. Representative images show localization of nuclei (blue), Tks5-Myc (green), and the FYVE domain of Hrs (red) 48 hours post-transfection. Closed arrows point to invadopodia rosettes. Open arrows point to endosomes. Images were taken at 100X magnification.

## **Mutations in the First, Second, and Third SH3 Domains of Tks5 Mis-localize Src in Src-3T3 Cells**

The invadopodia formed by Src-3T3 cells have been shown to be dependent on Tks5 expression, as silencing of Tks5 in these cells leads to invadopodia disassembly and a loss in gelatin degradation (Seals et al., 2005). Src-3T3 cells expressing the M1, M2, and M3 mutant Tks5 constructs exhibit a more diffuse gelatin degradation pattern that might be explained by the localization of Tks5 to early endosomes. However, these cells still express endogenous Tks5, which should be able to function normally in driving invadopodia formation. For this reason, it was hypothesized that the loss of invadopodia formation and more diffuse gelatin degradation pattern could be due to mis-localization of invadopodia-associated Tks5 binding partners to these organelles. In order to test this hypothesis, we first tested the potential co-localization of these Tks5 mutants with the Tks5 binding partner cortactin. The fifth SH3 domain had been previously shown to mediate binding between Tks5 and cortactin at the invadopodia-related podosomes of vascular smooth muscle cells (Crimaldi et al., 2009). In invadopodia-competent Src-3T3 cells expressing wild-type, M4, or M5 Tks5 constructs, both Tks5 and cortactin localized to invadopodia (Figure 36). However, while the M1, M2, and M3 Tks5 constructs still localized to endosomes, cortactin did not appear to strongly co-localize with these mutants and remained largely cytoplasmic with some sporadic localization at edges of the plasma membrane. This may be explained by the fact that in a recent study, cortactin was shown to localize to sites of invadopodia

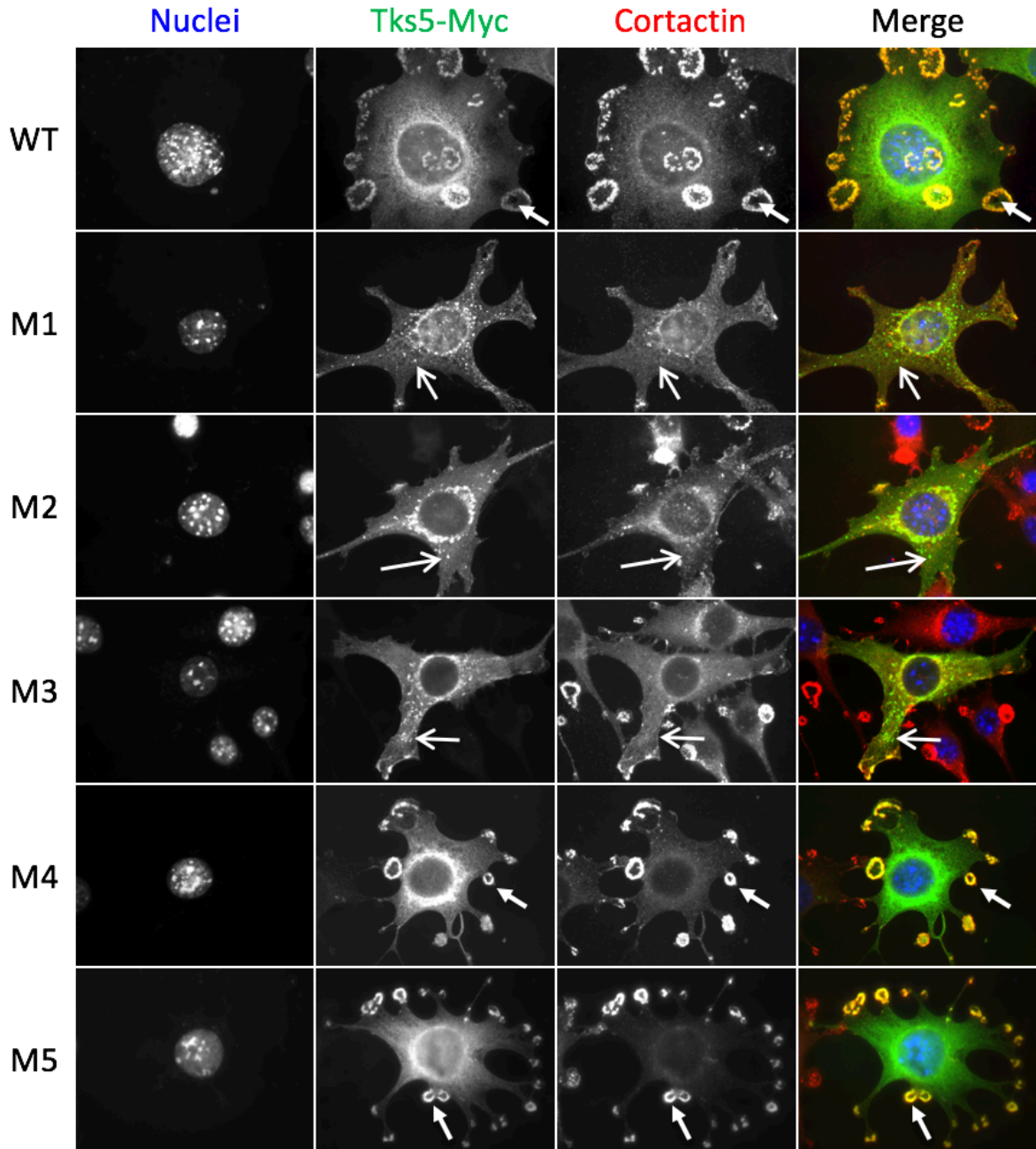


**Figure 36. Localization of Tks5 SH3 domain mutants and cortactin in Src-3T3 cells.** Src-3T3 cells were transiently transfected with wild-type (WT) Tks5 or Tks5 SH3 domain mutants (M1-M5) and then analyzed for Tks5 and cortactin localization by fluorescence microscopy. Ectopic Tks5 in transfected cells was monitored with an antibody to the Myc epitope. Representative images show localization of nuclei (blue), Tks5-Myc (green), and cortactin (red) 48 hours post-transfection. Closed arrows point to Tks5 and cortactin co-localization at invadopodia rosettes. Open arrows point to mis-localized M1, M2, and M3 constructs without cortactin co-localization. Images were taken at 100X magnification.

formation prior to Tks5. Thus cortactin localization was not be affected by the localization of these Tks5 mutants (Sharma et al., 2013).

As Src is responsible for the activation of many invadopodial proteins and for invadopodia formation (Boateng and Huttenlocher, 2012), the localization of Src was also studied in Src-3T3 cells expressing the M1, M2, and M3 mutant Tks5 constructs. Like cortactin before, wild-type Tks5 and the M4 and M5 Tks5 mutants all co-localized with Src at invadopodia (Figure 37). However, unlike cortactin, Src also co-localized with the M1, M2, and M3 Tks5 mutants at endosomal structures. Since Src was mis-localized in these cells, invadopodia-associated Src substrates may be unable to be activated at the plasma membrane, thus providing a possible explanation for the loss of invadopodia formation.

Previous research has demonstrated that inactive Src co-localizes with endosomal markers in the perinuclear region (Sandilands and Frame, 2008). Src is then delivered through endosomal trafficking to the plasma membrane for activation by receptor tyrosine kinases. Disruption of endosomal trafficking machinery results in an inability of Src to be translocated to the plasma membrane, and, therefore, Src is retained at cytoplasmic endosomes (Sandilands and Frame, 2008). Since a similar phenotype was seen in this study with the introduction of M1, M2, or M3 mutant Tks5 constructs in Src-3T3 cells, it is possible that Tks5 regulates Src trafficking. Thus, the mis-localization of Tks5 away from the plasma membrane may disrupt targeting of Src to the plasma membrane, resulting in sequestration of the kinase in cytoplasmic endosomes.

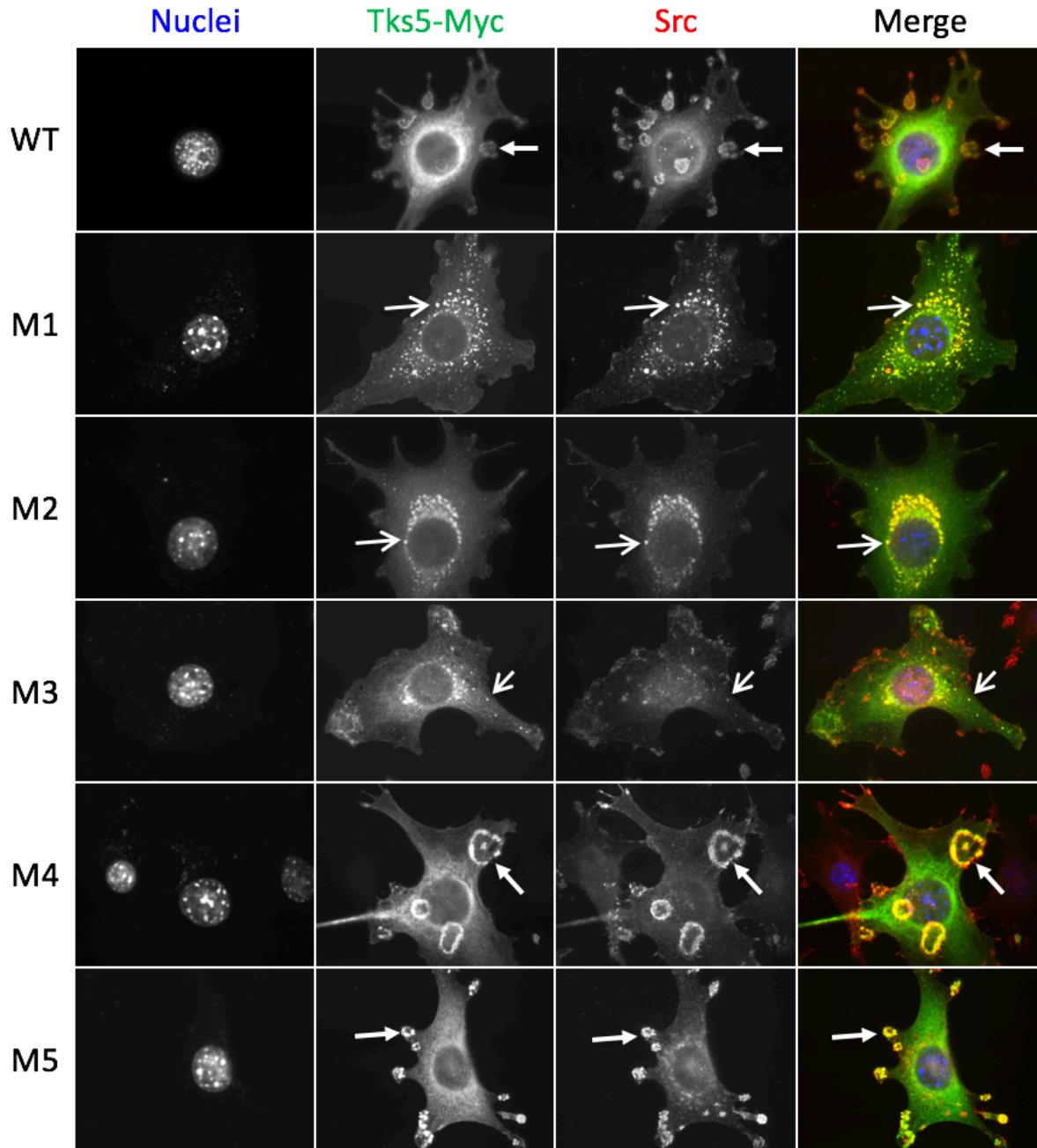


**Figure 37. Co-localization of Tks5 SH3 domain mutants and Src in Src-3T3 cells.** Src-3T3 cells were transiently transfected with wild-type (WT) Tks5 or Tks5 SH3 domain mutants (M1-M5) and then analyzed for Tks5 and Src localization by fluorescence microscopy. Ectopic Tks5 in transfected cells was monitored with an antibody to the Myc epitope. Representative images show nuclei (blue), Tks5-Myc (green), and total Src (red) 48 hours post-transfection. Closed arrows point to Tks5 and Src co-localization at invadopodia rosettes. Open arrows point to mislocalized M1, M2, and M3 constructs with Src co-localization. Images were taken at 100X magnification.

### **SH3 Domains Hold Tks5 in an Inactive Masked Conformation**

Since the M1, M2, and M3 mutant Tks5 constructs localize to phosphoinositide-rich endosomes, it appears that these forms of Tks5 have a PX domain that is more accessible to interacting with endosomal membranes. Interactions within or between Tks5 molecules have been proposed in the past. Tks5 has been suggested to have a closed intramolecular conformation that masks the PX domain until the protein is properly localized at sites of active Src at the plasma membrane (Abram et al., 2003). More recently, a Tks5 dimer was proposed that might also keep the PX domain from promiscuous lipid-binding within the cell (Oikawa et al., 2012). In order to distinguish between these two models, it is useful to compare Tks5 sequences to well-characterized proteins.

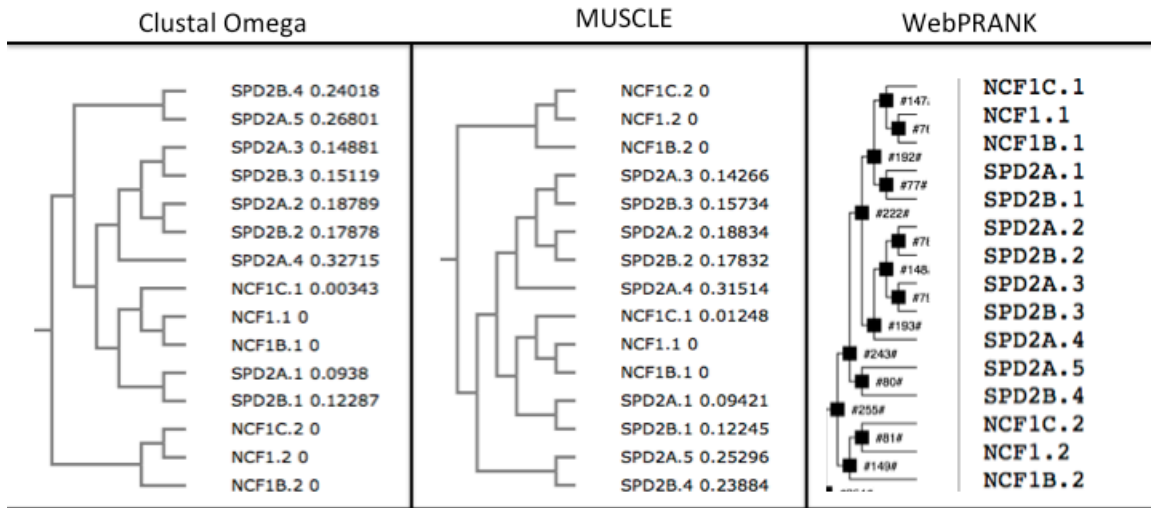
In order to compare the SH3 domains of Tks5 to other well-characterized SH3 domains, a search was carried out using the UniProt Knowledge and NCBI Protein Databases to identify the 220 human proteins with SH3 domains and 283 unique SH3 domain sequences (Table II). The sequences for the total 283 SH3 domains were aligned using Clustal Omega,

**Table II. Human proteins containing SH3 domains.** Listed by mnemonic identifier of UniProtKB entry. The identifier for Tks5 is noted in red.

ABI1	ASPP1	CSKI2	MYO1E	ITSN2*	MPP5	OBSCN	RHG32	SH3G3	SPT13	UBS3B
ABI2	ASPP2	CSKP	ES8L3	JIP1	MPP6	OSTF1	RHG33	SH3K1*	SPTA1	VAV*
ABI3	BAIP2	DBNL	FBP1L	JIP2	MPP7	OTOR	RHG42	SH3R1*	SPTN1	VAV2*
ABL1	BCAR1	DESP	FCSD1*	KALRN*	MY15B	P85A	RIM3A*	SH3R2*	SRBS1*	VAV3*
ABL2	BI2L1	DLG1	FCSD2*	LASP1	MYO15	P85B	RIM3B*	SH3R3*	SRBS2*	VINEX*
ACK1	BI2L2	DLG2	FGR	LCK	MYO7A	PACN1	RIM3C*	SH3Y1	SRC8	YES
AHI1	BIN1	DLG3	FNBP1	LYN	MYO7B*	PACN2	RIMB1*	SHAN1	SRC	ZO1
AMPH	BLK	DLG4	FRK	M3K9	NCF1*	PACN3	RIMB2*	SHAN2	SRGP1	ZO2
ANM2	BTK	DLG5	FUT8	M3K10	NCF1B*	PEX13	RUSC1	SHAN3	SRGP2	ZO3
ARH37*	CACB1	DNMBP*	FYB	M3K11	NCF1C*	PLCG1	RUSC2	SHLB1	SRGP3	MYO1F
ARH38 *	CACB2	DOCK1	FYN	M3KL4	NCF2*	PLCG2	S3TC1	SHLB2	SRMS	
ARHG4	CACB3	DOCK2	GAS7	MACC1	NCF4	PPIP1	S3TC2	SKAP1	STAC	
ARHG5	CACB4	DOCK3	GRAP*	MACF1	NCK1*	PRAM	SAMN1	SKAP2	STAC2	
ARHG6	CASL	DOCK4	GRAP2*	MATK	NCK2*	PTK6	SASH1	SLAP1	STAC3*	
ARHG7	CASS4	DOCK5	GRAPL	MCF2L	NEBL	RASA1	SASH3	SLAP2	STAM1	
ARHG9	CD2AP*	DYST	GRB2*	MIA	NEBU	RHG04	SGSM3	SNX18	STAM2	
ARHGG	CIP4	EFS	HCK	MIA2	NGEF	RHG09	SH319*	SNX33	TEC	
ARHGJ	CRK*	EM55	HCLS1	MIA3	NOSTN	RHG10	SH321	SNX9	TNK1	
ARHGQ	CRKL*	EPS8	IASPP	MPP2	NOXA1	RHG12	SH3B4	SPD2A*	TRIO*	
ASAP1	CSK	ES8L1	ITK	MPP3	NOXO1*	RHG26	SH3G1	SPD2B*	TXK	
ASAP2	CSK11	ES8L2	ITSN1*	MPP4	NPHP1	RHG27	SH3G2	SPN90	UBS3A	

\*Contains multiple SH3 domains

MUSCLE, and WebPRANK. Results from multiple programs were compared in order to ensure accuracy. Distance trees were constructed by these programs for the 283 SH3 domain sequences, and are depicted, in part, in Figure 38. For each of these programs, the sequences for the five SH3 domains of Tks5 were consistently grouped with the four SH3 domains of Tks4 and the two SH3 domains of neutrophil cytosol factor 1 (p47-phox). This consistent grouping suggests that the structures of the SH3 domains present in these proteins are related.



SPD2A- Tks5  
 SPD2B- Tks4  
 NCF1- Neutrophil cytosol factor 1 (p47-phox)  
 NCF1B- Putative neutrophil cytosol factor 1B (p47-phox pseudogene)  
 NCF1C- Putative neutrophil cytosol factor 1C (p47-phox pseudogene)

**Figure 38. Subset of SH3 domain multiple sequence alignments containing the five SH3 domains of Tks5.** Alignments are based on the Clustal Omega, MUSCLE, and WebPRANK databases as shown.

The domain architecture of these proteins containing the most similar SH3 domains to Tks5 was investigated using NCBI Conserved Domain Database (Figure 39). The domain architecture comparison demonstrated that each of these proteins contains an amino-terminal PX domain in addition to the SH3 domains.

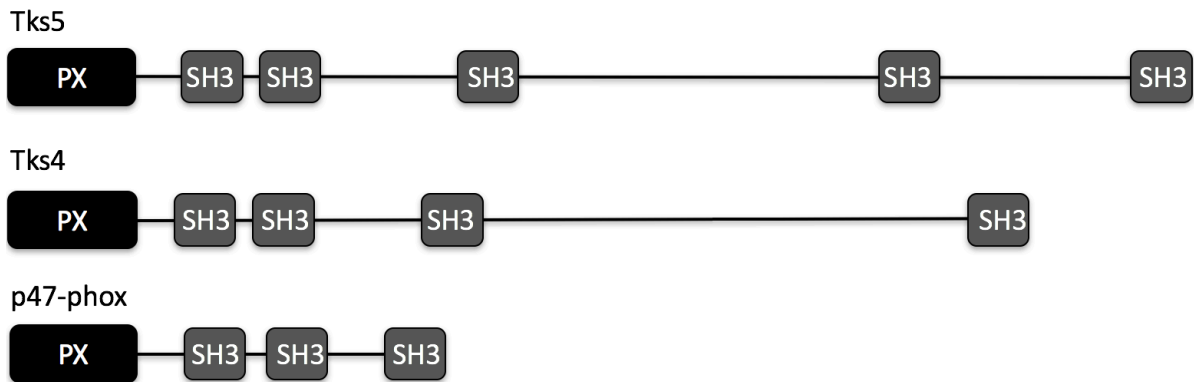


**Figure 39. Domain architecture of Tks5, Tks4, and p47-phox.** Adapted from NCBI Conserved Domain Database.

In order to investigate the significance of the PX domain in the structure of these SH3 domain-containing proteins, other human proteins containing SH3 domains and PX domains were identified. The 220 human proteins identified as containing SH3 domains (Table 1I) were searched for PX domains by using the NCBI Protein Database. This resulted in identification of 12 human proteins containing at least one SH3 domain and a PX domain (Table III). The sequences for these PX domains were retrieved using the NCBI Protein

**Table III. SH3 domain containing human proteins with a PX domain.** Listed by mnemonic identifier of UniProtKB entry.

NCF1C	NCF4	RHG33	SNX9
NCF1	NOXO1	SNX18	SPD2A
NCF1B	RHG32	SNX33	SPD2B

Database and aligned using Clustal Omega, MUSCLE, and WebPRANK. Distance trees were constructed by each program in order to identify similarities in sequence (Figure 40). Again, the distance trees produced by these programs consistently resulted in grouping of Tks5, Tks4, and p47-phox. The PX domain structure similarity suggests a similarity in the domain architecture of these proteins, with quite possibly similar functional implications.

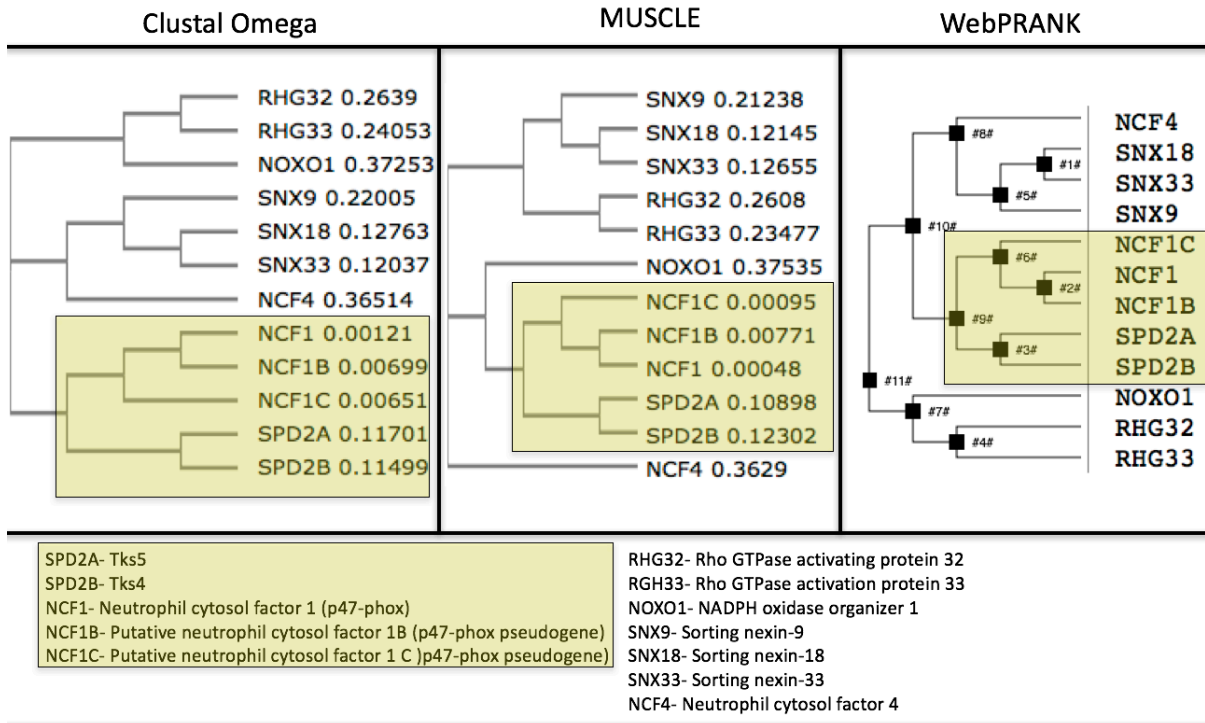


**Figure 40. PX domain multiple sequence alignments for SH3 domain-containing proteins.** Highlighted are the groupings containing Tks5, Tks4, and p47-phox.

Following the identification of sequence similarities between the SH3 domains and PX domains of Tks5, Tks4, and p47-phox, the binding properties of the characterized domains were investigated. As the Tks4 SH3 domain interactions remain relatively uncharacterized, the SH3 domain interactions of p47-phox were focused on for this investigation. p47-phox is a component of the NADPH oxidase, an enzyme complex responsible for superoxide production during phagocytosis (Ago et al., 2003). p47-phox is known to exist in two conformations (Figure 21). The inactive conformation is formed when a poly-proline motif in the N-terminal PX domain of p47-phox is bound to its C-terminal SH3 domain. This renders both the PX and SH3 domains inaccessible and inhibits the

function of p47-phox. However, three serine residues on the C-terminal end of the protein can be phosphorylated by protein kinases in order to induce a conformational change in p47-phox. This allows for the PX domain to disassociate from the SH3 domain, the PX domain to bind phosphoinositides, and the protein to be relocated to the plasma membrane where it is catalytically active (Ago et al., 2003).

In order to investigate whether a similar, inactive conformation might exist for Tks5, the PX domain was scanned for poly-proline motifs, sequences allowing for binding to an SH3 domain (Table IV). The PX domain of Tks5 contains a Class I poly-proline motif similar in position and sequence to those found in the PX domains of p47-phox and Tks4.

**Table IV. Poly-proline motifs located in PX domains.**

<b>Poly-proline Motif</b>	<b>Protein</b>	<b>Sequence</b>	<b>Position in PX Domain</b>
RxxPxxP (Class I)	NCF1C	RiiPhlP	46-52
	NCF1	RiiPhlP	67-73
	NCF1B	RiiPhlP	71-77
	SHPD2A	RiiPflP	67-73
	SHPD2B	RiiPflP	67-73
PxxPxK (Class II)	NCF4	PtlPaK	69-74
	SNX18	PhlPeK	58-63
	SNX33	PhlPeK	58-63
	SNX9	PslPdK	59-64
	SHPD2A	PflPgK	70-75
	SHPD2B	PflPgK	70-75

In addition, the poly-proline motif identified in p47-phox is the motif used to bind the PX domain to the SH3 domain (Hiroaki et al., 2001) (Figure 41). These results suggest that the structural similarity between Tks5 and p47-phox may lend itself to functional similarity. As p47-phox undergoes an intramolecular interaction due to its structure, it may also be true that an SH3 domain of Tks5 may have the ability to bind its own PX domain.



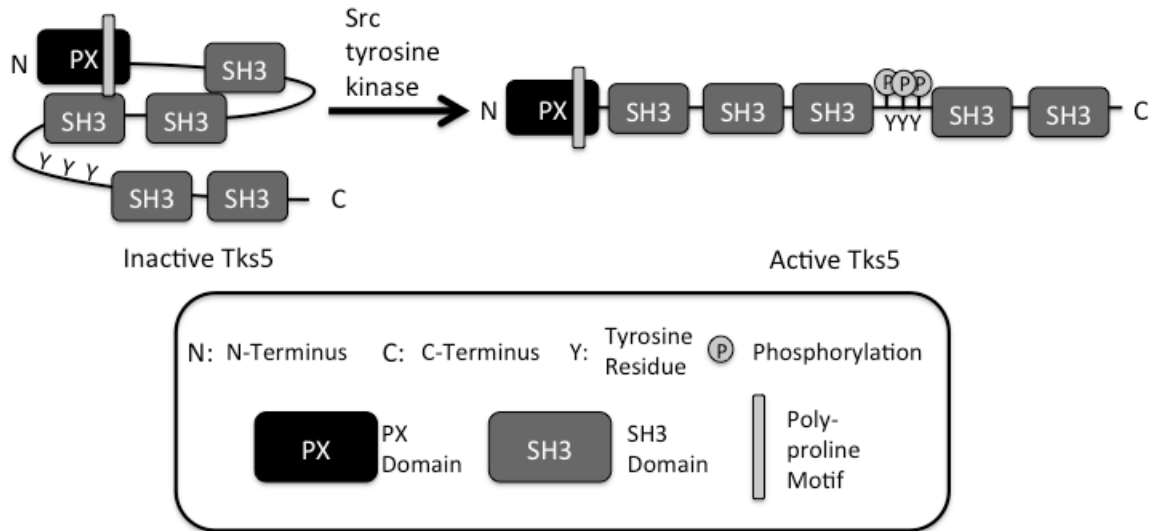


**Figure 43. Proposed Tks5 inactive conformation model.** In this model, Tks5 remains in an inactive conformation with its third SH3 domain bound to the poly-proline motif present in its PX domain. When phosphorylated by Src tyrosine kinase on the three tyrosine residues located in close proximity to this SH3 domain, the protein undergoes a conformational change. This allows for dissociation of the PX domain and an open, active conformation.

Tks5 contains three tyrosine residues downstream of its third SH3 domain, which are known to be phosphorylated by Src tyrosine kinase during Tks5 activation (Burger et al., 2014). Phosphorylation of these tyrosine residues may result in a conformational change reminiscent to that of p47-phox on its three serine residues located downstream of its C-terminal SH3 domain. Based on this observation, it is proposed that the intramolecular binding that Tks5 exhibits in this model takes place between the PX domain and the third SH3 domain.

In order to validate this model, further experimentation will need to be done. Binding assays, specifically GST pull down assays and co-immunoprecipitation assays, can be implemented to address the possible interaction between the PX domain and the third SH3 domain of Tks5. Preliminary studies using co-immunoprecipitation assays have been carried

out and provide promising results regarding the efficacies of binding assays in providing evidence of this interaction (see Future Directions).

## Discussion

### Conclusions

In this study, inactivating point mutations were introduced into each of the SH3 domains of Tks5 to study the role that each individual SH3 domain of Tks5 plays in invadopodia development and activity. We identified the first, second, and third SH3 domains of Tks5 as being instrumental to the regulation of its activity within the cell. Disrupting binding to these SH3 domains allowed for a 2.5- to 4-fold increase in matrix degradation in LNCaP cells. However, in Src-3T3 cells there was a mis-localization of Tks5 to intracellular structures and co-localization with endosome marker proteins leading to a loss of invadopodia formation and focalized degradation. In the Src-3T3 cells expressing the M1, M2, or M3 mutant Tks5 constructs, Src was unable to be properly delivered to the plasma membrane, instead being retained at the same perinuclear endosome structures as Tks5. This observation may explain the loss of invadopodia in these cells. Mechanistically, the presence of a poly-proline motif in the PX domain of Tks5 may confer binding to one of its own SH3 domains, suggesting a possible intramolecular or intermolecular interaction that governs Tks5 activity, invadopodia development, and the invasive phenotype of cancer cells.

### Tks5 Inactive Conformation Model Pertaining to Model Cell Lines

The existence of an interaction between the PX domain and the 3<sup>rd</sup> SH3 domain of Tks5 could provide an explanation for the results observed in this study. The LNCaP cells have little Tks5 or active Src expression (Burger et al., 2014). Any Tks5 that is introduced into these cells may be activated when in close proximity to the basal levels of PI(3,4)P<sub>2</sub> and/or Src at the plasma membrane, thus allowing for Tks5 phosphorylation, lipid binding,

and an opening of the protein's structure (Sharma et al., 2013). Once bound, Tks5 may function to recruit other invadopodia-associated proteins to the plasma membrane, thus allowing for the low and diffuse levels of matrix degradation observed by LNCaP cells transiently expressing Tks5 (Burger et al., 2014). Mutations in any of the first three SH3 domains of Tks5 could disrupt the intramolecular binding that masks the PX domain, thus allowing for increased binding of Tks5 to phosphoinositides at the plasma membrane and an increase in the observed matrix degradation (Figure 44). Interestingly, LNCaP cells stably

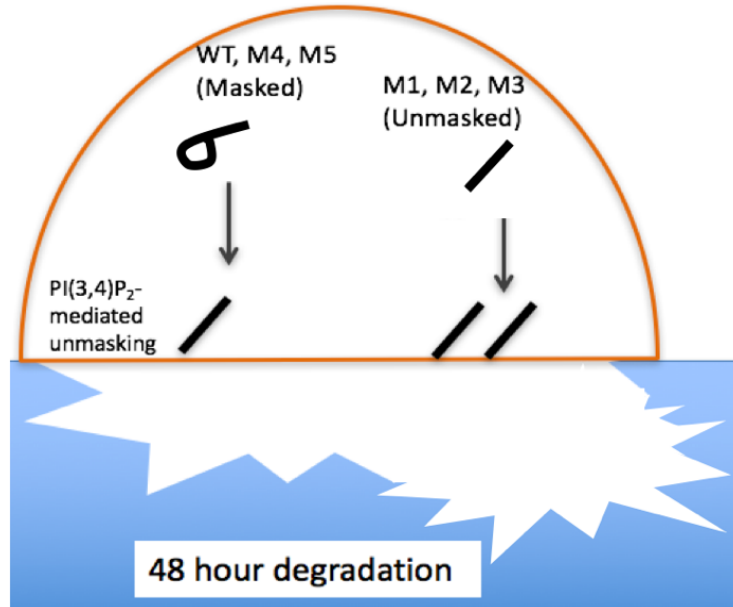


**Figure 44. Inactive conformation model in LNCaP cells.** The Tks5 M1, M2, and M3 SH3 domain mutants have a PX domain that is accessible for lipid binding, thus allowing for enhanced matrix degradation activity within the cells. Wild-type (WT) Tks5 and the Tks5 M4 and M5 mutants have a PX domain that is only made available for interaction upon close proximity to the plasma membrane, where Src is localized. However, since activated Src levels are relatively low, there is less overall Tks5 activity and matrix degradation.

expressing Tks5 have been shown to form punctate invadopodia that are capable of focalized degradation (Burger et al., 2014). It is possible then that, over longer periods of time, LNCaP cells transiently expressing Tks5 might also be able to adjust to efficiently form mature invadopodial structures.

Src-3T3 cells have high levels of Tks5 and activated Src is expressed constitutively. Disrupted binding to any of the first three SH3 domains of Tks5 led to the accumulation of Tks5 in aggregates near the nucleus and without degradative capabilities. These aggregates were reminiscent of the punctate staining of the isolated PX domain of Tks5 in normal NIH-3T3 fibroblasts (Abram et al., 2003). As the PX domain of Tks5 is known to bind to PI(3)P, a lipid found extensively at endosomes, the mutants were studied for co-localization with early endosomal markers. Indeed, both EEA1 and the lipid-binding FYVE domain of Hrs seemed to partially co-localize at the aggregates, suggesting that the Tks5 M1, M2, and M3 mutant constructs localize to these organelles. It is possible that disrupted binding to these first three SH3 domains of Tks5 allows for an open conformation. In unmasking the PX domain, Tks5 is available for promiscuous binding to phosphoinositide-rich organelles like endosomes (Figure 45). In contrast, wild-type Tks5 and the Tks5 M4 and M5 mutant constructs localize correctly as they maintain a closed conformation until in close proximity to active Src. Once phosphorylated, conformational changes allow for unfolding of Tks5 and its proper localization to the plasma membrane via its lipid-binding PX domain. This provides a mechanism for how Src phosphorylation leads to Tks5 activity.

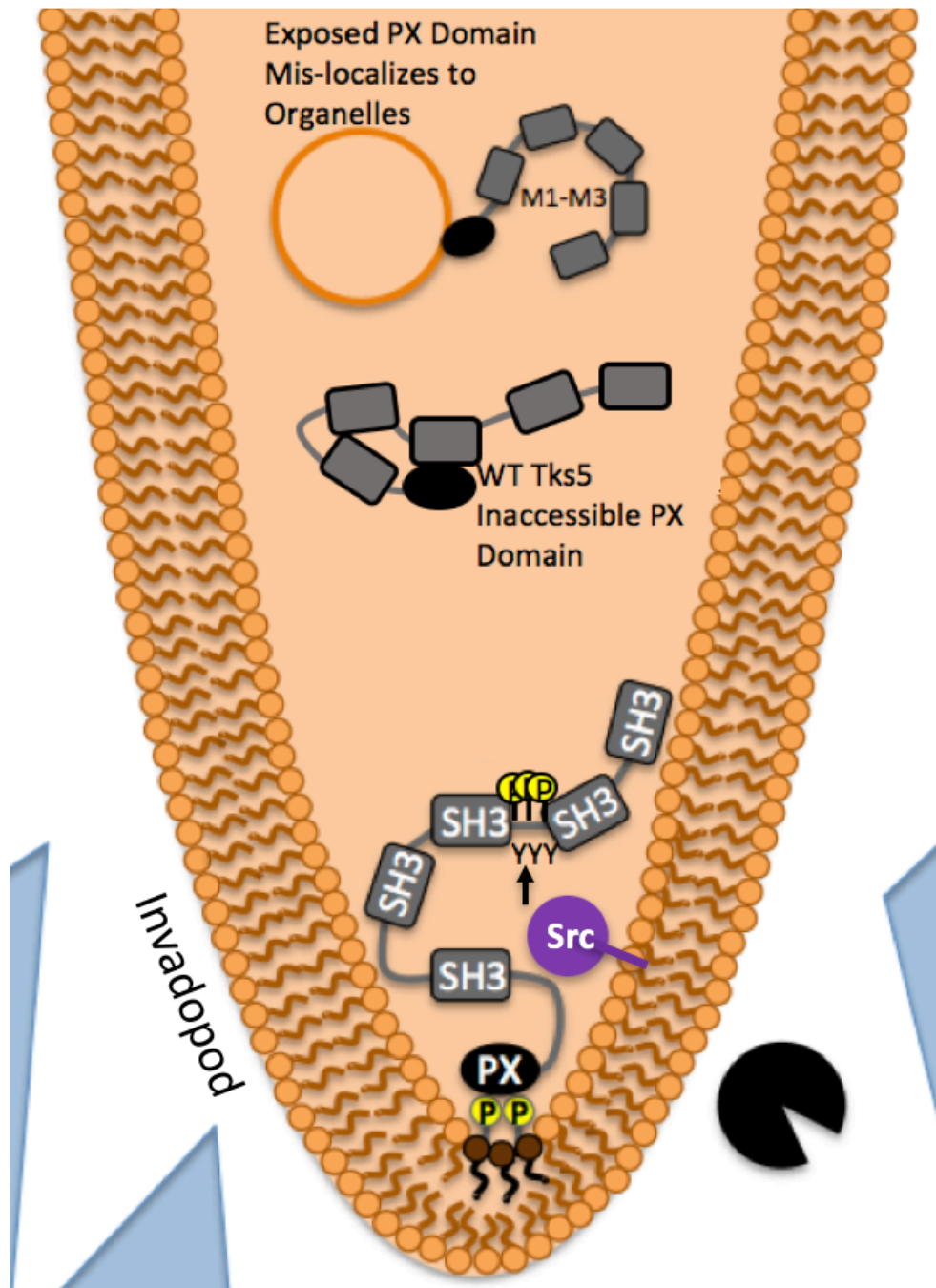


**Figure 45. Proposed model for endosomal mis-localization of Tks5 M1, M2, and M3.** The M1-M3 mutations of Tks5 have an exposed PX domain that is available for promiscuous binding. Wild-type (WT) Tks5 and the M4 and M5 Tks5 mutants have a masked PX domain that is not available for lipid binding until activated by Src at the plasma membrane.

Src-3T3 cells are also known to create robust invadopodia in the form of super-structures termed rosettes. However, expression of the M1, M2, or M3 Tks5 mutants had a dominant-negative effect on invadopodia formation. And while the cells still maintained the ability to degrade, the degradation pattern was no longer focused. Additionally, Src co-localized with the Tks5 M1, M2, or M3 mutant constructs at endosomal compartments. Src is known to be delivered to invadopodia through endosomal trafficking (Figure 46). And

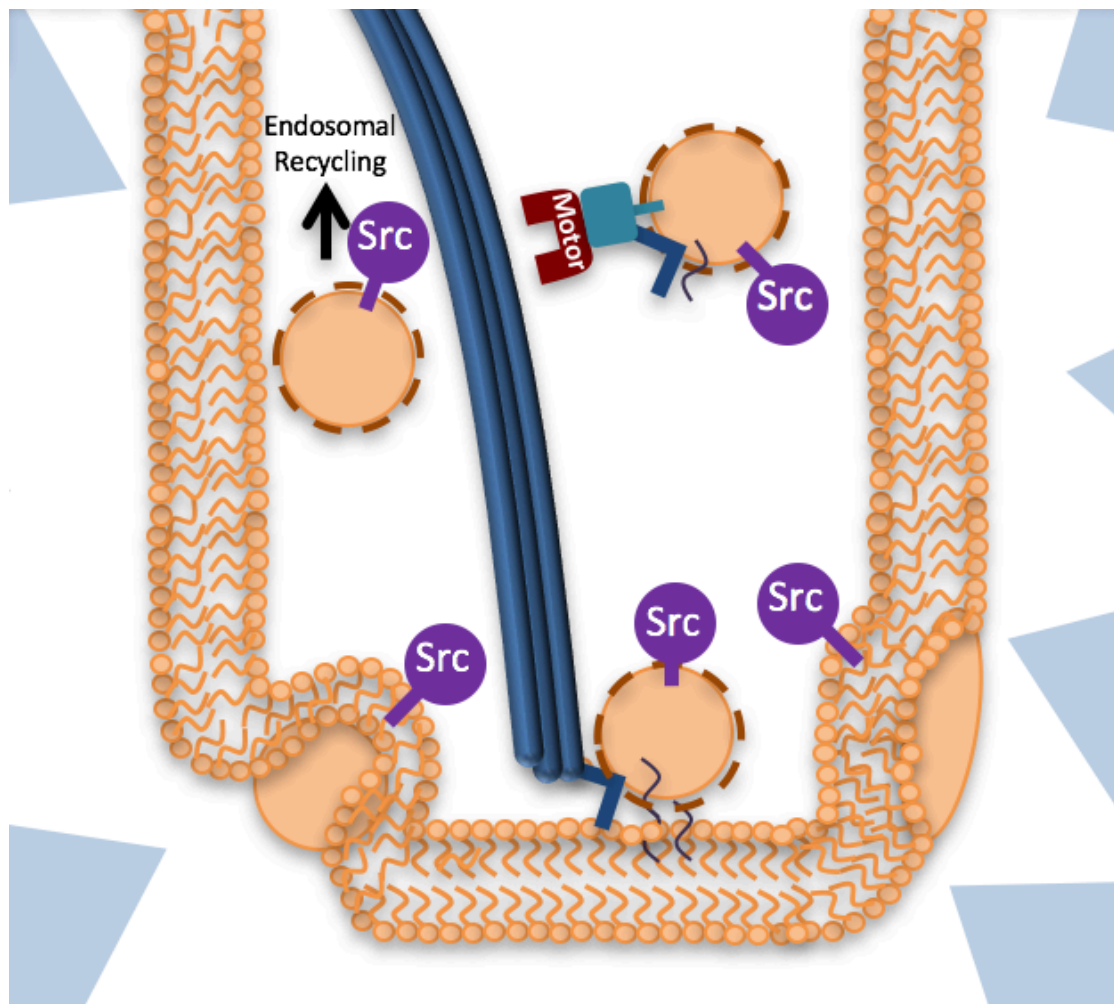


**Figure 46. Endosomal trafficking of Src tyrosine kinase in an invadopod.** Src is delivered to invadopodia through endosomal trafficking. Inactive Src is internalized through endocytosis where it may be recycled for redelivery to these sites. Motor proteins (red), Rabs (teal), the exocyst complex (dark blue), and SNARE proteins (black squiggly lines) are involved in trafficking Src through use of microtubules (large blue lines).

disruption of trafficking machinery (*e.g.*, with Rab mutants) results in the retention of Src at endosomes within the cell (Sandilands and Frame, 2008). A study done in MDA-MB-231 cells also showed that an inhibition of SNARE trafficking machinery, specifically syntaxin13 and SNAP23, resulted in a decrease in the number of invadopodia formed by these cells as well as in the amount of Src found at the plasma membrane (Williams and Coppolino, 2014). Also, when observing focal adhesions in HeLa cells and fibroblasts, depletion of the endocytic regulatory protein MICAL-L1 resulted in a loss of active Src at focal adhesions and a decrease in cell migration (Reinecke et al., 2014). These studies suggest that a disruption in Src endosomal trafficking machinery may impair the ability of cells to form invadopodia, much as was observed here.

As this phenotype was observed in cells expressing the M1, M2, or M3 Tks5 SH3 domain mutations, it is possible that Tks5 is involved in endosomal trafficking of Src (Figure 47). In support of this, the adaptor protein Tks4, the closest homolog to Tks5, has been shown to be involved in the delivery of MT1-MMP to invadopodia, though the precise mechanism behind this is unknown (Buschman et al., 2009). Interestingly, there is evidence that Tks5 can bind to endosomal trafficking machinery, such as the kinesin Eg5 (Stylli et al., 2009) (Figure 8B). Evidence has also been found of Tks5 interacting with myosin light polypeptide 6, a subunit of myosin, myosin regulatory light chain 2, and the microtubule subunit tubulin (Stylli et al., 2009) (Figure 8). Microtubules provide a mechanical scaffold for protein sorting, while motor proteins allow for movement of cargo across the cytoskeleton (Murray and Wolkoff, 2003). Kinesins are known to bind microtubules and hydrolyze ATP to produce movement of cargo, including vesicles. Myosins are actin-associated motor proteins, some of which are also known to drive vesicle transport along

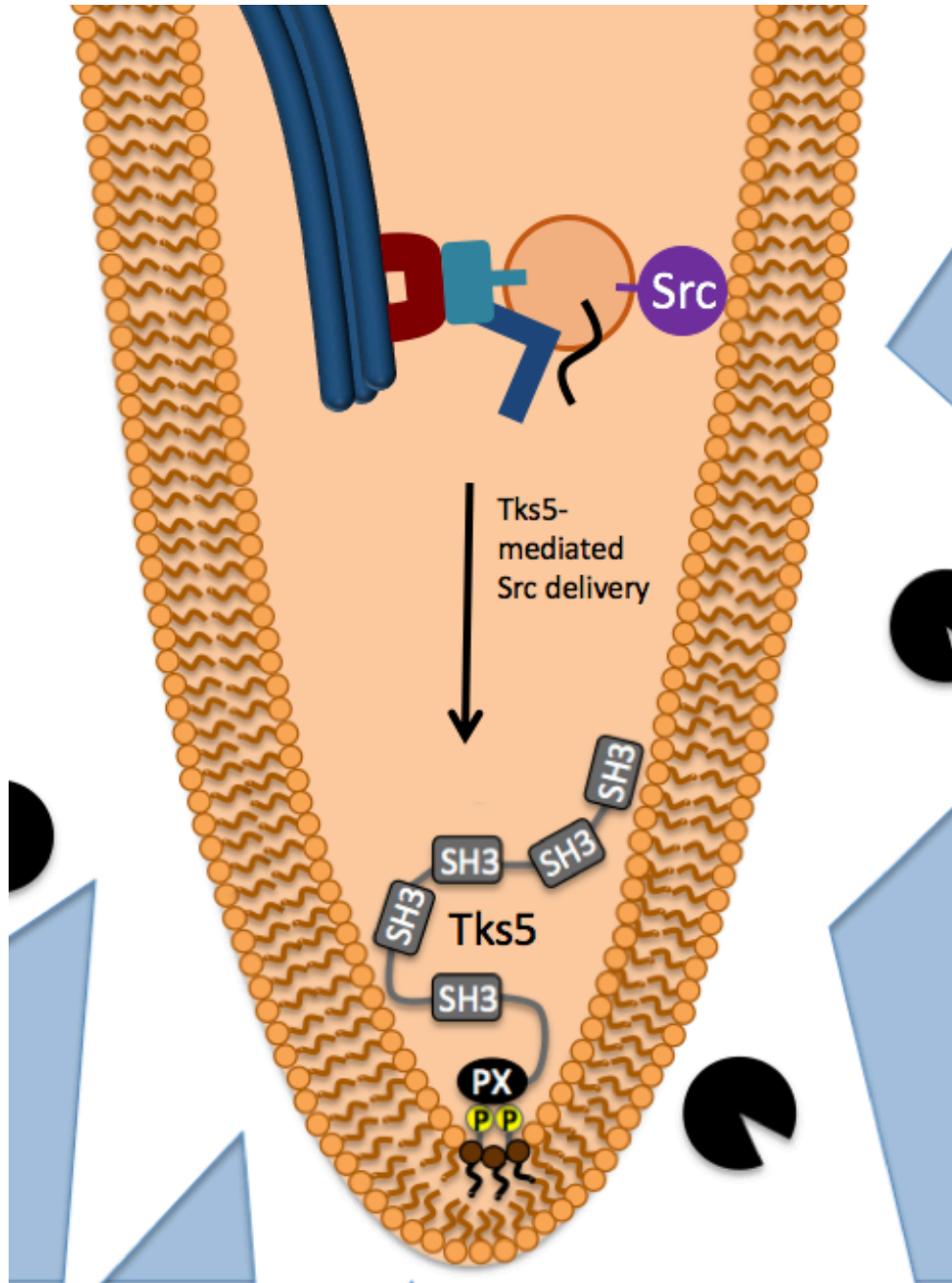


**Figure 47. Proposed model for the role of Tks5 in Src delivery to the plasma membrane.** Tks5 appears to play a role in targeting Src vesicle delivery to sites of invadopodia formation. Tks5 has been shown to interact with motor proteins (red) and microtubules (large blue lines). Other trafficking machinery includes Rabs (teal), the exocyst complex (dark blue), and SNARE proteins (black squiggly line).

microtubules (Murray and Wolkoff, 2003). For these reasons, it remains possible that Tks5 may play a role in the motor protein driven vesicular trafficking of Src and potentially other invadopodial proteins. When Tks5 is mis-localized to phosphoinositide-rich organelles, this trafficking system appears to be disrupted and Src is unable to be properly delivered to the plasma membrane, resulting in a loss of invadopodia formation (Figure 48).

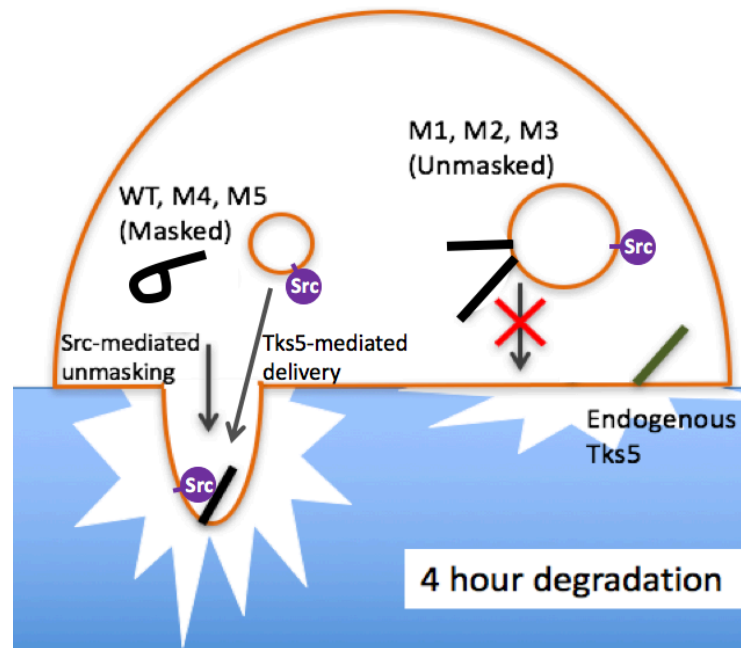


**Figure 48. Tks5 inactive conformation in Src-3T3 cells.** Wild-type (WT) Tks5 and the M4 and M5 Tks5 mutants are activated upon close proximity to active Src at the plasma membrane where they may function in the targeting delivery of Src-containing vesicles to sites of invadopodia formation. The Tks5 M1, M2, and M3 mutants, however, have an open conformation and a promiscuous PX domain capable of binding to endosomes. As Tks5 is no longer at the plasma membrane, Src delivery is also disrupted and invadopodia are unable to be formed.

This new model of Tks5 may provide better understanding of how Tks5 is regulated within cells. Tks5 may exist in a closed conformation with an inaccessible PX domain until in close proximity to Src. Once phosphorylated by Src, conformational changes allow for opening of the Tks5 structure and for normal Tks5 functioning within the cell. One of these

functions may be in the endosomal trafficking of Src to invadopodia. In this way, Tks5 may function both upstream and downstream of Src allowing for a positive feedback loop in invadopodia development and maturation.

### **Tks5 Function in Tumor Growth**

Understanding the regulation of Tks5 may have further applications outside of cancer cell invasion. Tks5 has been shown in several studies to play a role in tumor growth. For example, Tks5 silencing has been shown to decrease total cellular ROS in Src-transformed fibroblasts and SCC61 head and neck cancer cells. The protein p22-phox, a component of the NADPH oxidase, was shown to associate with full length Tks5 as well as with a truncated “PX-SH3A-SH3B” version of Tks5, suggesting this association may allow for Tks5 regulation of ROS production (Figure 8B) (Diaz et al., 2009).

Tks5 silencing in MDA-MB-231 cells has also been shown to impair primary tumor growth in a mouse model through both an increase in apoptosis and a decrease in proliferation. The authors also noted that when the cells lacking Tks5 were introduced directly into circulation, metastatic growth in the lungs was inhibited. The tumors lacking Tks5 expression were hypoxic and associated with thin, leaky blood vessels, possibly accounting for the decrease in tumor size, however the mechanisms behind this are still largely unknown (Blouw et al., 2015).

The 5<sup>th</sup> SH3 domain of Tks5 has been shown to interact with the N-terminus of XB130, an adaptor protein linked with BEAS-2B human bronchial epithelial cell growth, survival, and migration (Figure 8A). Tks5 and XB130 also appear to form a complex with Src. This particular interaction seems to play a role in cell proliferation and survival,

specifically in regulation of the G1 (resting) phase checkpoint. Downregulation of XB130 and Tks5 resulted in a decrease in Src activation, suggesting a possible mechanism for the effect of this interaction on proliferation (Moodley et al., 2015). Interestingly, this study concluded that Tks5 may play a role upstream of Src activation, and this is consistent with our findings here. It may be that the XB130 and Tks5 interaction mediate the vesicle trafficking of Src to the plasma membrane.

### **Non-cancer Tks5 Function**

Further understanding of the regulation of Tks5 may have application in normal cellular function as well. For example, Tks5 has been shown to be a key component of podosomes. Podosomes are proteolytic structures similar to invadopodia but found in normal, but often professionally invasive, cell types, including osteoclasts, macrophages, endothelial cells, and vascular smooth muscle cells (Courtneidge et al., 2005).

Osteoclasts, the cells that resorb the bone matrix, organize podosomes in a superstructure called the “sealing zone” in order to carry out this function. Tks5 has been shown to be essential for osteoclast podosome formation as well as podosome-mediated osteoclast fusion downstream of a signaling pathway regulated by TGF- $\beta$ , PI3K, and Src. This process was also shown to mediate the fusion of osteoclasts with cancer cells, possibly allowing for immune system evasion in sites of bone metastases. Binding partners of Tks5 in osteoclasts include the actin-binding gelsolin precursor protein, actin-regulating filamin-A, a homolog of the transcriptional activator flightless 1, the actin capping protein tropomodulin3, the actin-plasma membrane linker protein moesin, and cofilin. Interestingly, Tks5 $\Delta$ PX was also able to bind to the actin-plasma membrane linker protein radixin, Abl interactor 1

(Abi1), WIP, WASp family member 2 (WAVE2), WASp itself, Grb2, and filamin-B (Figure 8B) (Oikawa et al., 2012).

Macrophages form podosomes in order to navigate the ECM of various tissues and remove microorganisms and debris from the body. Tks5 has also been shown to be necessary for proper function of these structures through regulation of adhesion, motility, ECM degradation, and MMP expression and activity (Burger et al., 2011). Similar to osteoclasts, cancer cell-macrophage hybrids have been found *in vivo* and may contribute to the ability of cancer cells to escape immune surveillance (Oikawa et al., 2013).

Aortic endothelial cells and vascular smooth muscle cells also form podosomes in order to invade tissues during angiogenesis (Gimona et al., 2003; Varon et al., 2006). Similarly, myoblasts form podosomes to develop muscle. Tks5 and  $\beta$ -dystroglycan, a ubiquitous transmembrane laminin-binding protein, are known to localize at these structures in myoblasts. A dystroglycan-Src complex was found to bind to the 3<sup>rd</sup> SH3 domain of Tks5 within these cells (Figure 8A) (Thompson et al., 2008).

The Src-Tks5 signaling pathway has also been shown to be necessary during embryonic development. Zebrafish one-cell stage embryos were injected with morpholinos designed to suppress Tks5 expression. At 48 hours post fertilization, these embryos were unable to fully develop and displayed small heads, small eyes, edema around the heart, and a delay in pigment cell appearance in their tails. These defects were attributed to faulty migration of neural crest cells, multipotent cells that arise from the embryonic ectoderm. Further investigation demonstrated that TGF- $\beta$  stimulation of murine neural crest stem cells leads to Src and Tks5 activation as well as podosome formation (Murphy et al., 2011).

The role of Tks5 in development was further investigated in a mouse model. Homozygous disruption of the gene was carried out through insertion of a trapping cassette containing a transcriptional termination sequence between exons 1 and 2 of the *SH3PXD2A* gene, a method known as “gene-trapping.” This technique resulted in neonatal death and a cleft palate. It was hypothesized that interference with cell migration affected palatogenesis (Cejudo-Martin et al., 2014).

Tks5 is also known to play a role in diseases outside of cancer. For example, Tks5 phosphorylation has been found to be associated with Alzheimer’s disease. Alzheimer’s is caused by amyloid- $\beta$  peptide accumulation leading to neuronal death. Tks5 appears to be involved in this neurotoxic signaling by amyloid- $\beta$ . Furthermore, Tks5 associated neurotoxicity has been shown to be ADAM12 dependent. Disruption of Tks5 and ADAM12 activity enables protection against amyloid- $\beta$  induced cell death (Malinin et al., 2005).

Finally, Tks5 has been shown to be recruited to enteropathogenic *Escherichia coli* (EPEC) infection sites. EPEC secrete effector proteins into the underlying intestinal lumen to trigger formation of podosome-like structures referred to as pedestals. The pedestals facilitate attachment of the bacteria to the intestinal lumen. Tks5 localization to these areas was recently discovered, though pedestals are still able to be formed by intestinal cells expressing Tks5 $\Delta$ PX. Thus, the significance of Tks5 to these processes remains unknown (Jensen et al., 2015).

## **Future Directions**

### **Validation of Tks5 Closed Conformation through SH3 Domain Interactions with PX**

#### **Domain**

In order to address possible inactive conformations of Tks5, the ability of the SH3 domains of Tks5 to bind to its PX domain can be tested through GST pull down assays. Briefly, an HA tagged Tks5 PX domain will be introduced into cells with low levels of endogenous Tks5. The lysates will then be run down a column with glutathione Sepharose beads coupled to GST fusion proteins of each Tks5 SH3 domain. Bound proteins will be eluted, then separated using SDS-PAGE before being blotted for the HA-tagged PX domain. This will elucidate any binding between the PX domain and any of the SH3 domains of Tks5. A previous experiment has suggested binding between HA-PX and the third SH3 domain of Tks5, but this requires further substantiation (data not shown).

The interaction between the PX and SH3 domains of Tks5 may also be investigated through co-immunoprecipitation. A preliminary experiment of this nature has been conducted in which HEK293 cells were co-transfected with the Tks5 SH3 domain mutants and the isolated PX domain of Tks5 containing a GFP tag. After a 48-hour incubation period, cells were lysed and co-immunoprecipitations were carried out using an antibody specific to the GFP epitope tag of the isolated PX domain of Tks5 and analyzing for Tks5 using an antibody specific to the fourth SH3 domain of Tks5 (Figure 49). Preliminary results point to a decrease in Tks5 domain interaction with the M3 Tks5 mutant construct, which is consistent with the modeled interaction of the PX domain with the third SH3 domain. These results also appear to show an increase in Tks5 PX domain interaction with the M1 and M2 Tks5 mutant constructs. This is consistent with the suggested open conformation of these

constructs, allowing for accessibility of the third SH3 domain to bind to the PX domain of Tks5. However, consistent expression levels of GFP-tagged PX domain and the Tks5 SH3 domain mutant constructs were not obtained in this experiment, and thus the results overall remain promising, but ultimately inconclusive.

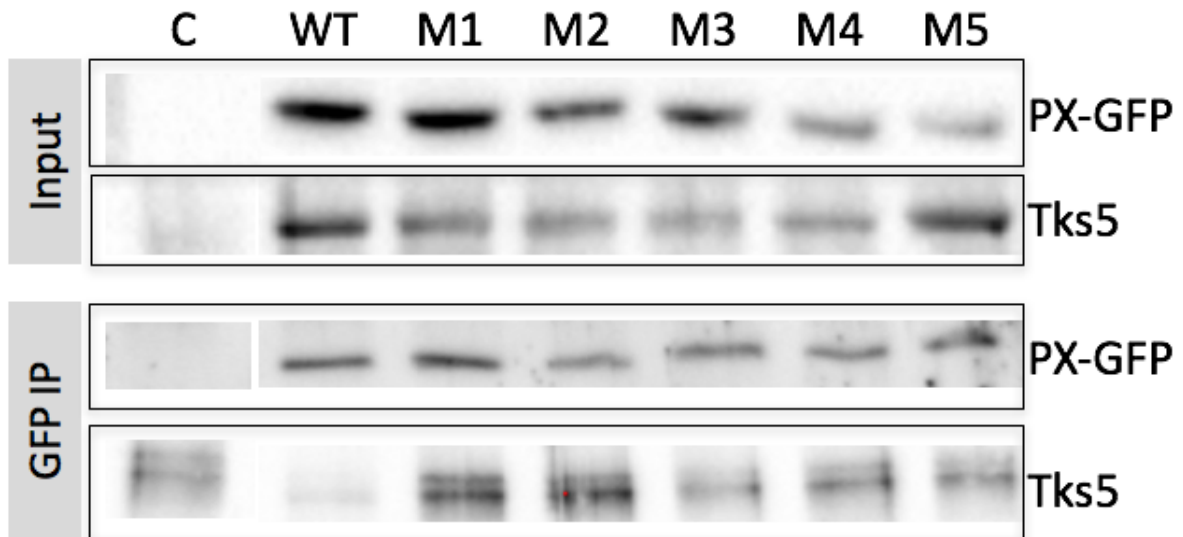


**Figure 49. Co-immunoprecipitation of the isolated PX domain of Tks5 containing a GFP epitope tag and Tks5 SH3 domain mutant constructs in HEK293 cells.** Total cell lysates (input) were analyzed for the GFP tag on the isolated PX domain of Tks5 and for the Tks5 SH3 domain mutant constructs by immunoblot analysis. Lysates were also immunoprecipitated (IP) with a GFP antibody and analyzed for Tks5 PX-GFP and the Tks5 SH3 domain mutants by immunoblot analysis.

### Validation of Tks5 Closed Conformation through PX Domain Characterization

Future experimentation will investigate the validity of the Tks5 masked conformation model. The Tks5 SH3 domain mutants can be subjected to a phosphatidylinositol phosphate binding assay that tests for their ability to bind PI(3)P and PI(3,4)P<sub>2</sub>. Presumably, those

mutants containing an accessible PX domain (Tks5 M1, M2, and M3) should show stronger binding to these lipids.

For identification of any binding that is occurring *in vitro*, the poly-proline motif in the PX domain of Tks5 could also be mutated to disrupt interactions with SH3 domains.

This mutant construct of Tks5 can then be introduced into cells to study its effects such as binding has on the activation of Tks5 and invadopodia formation and activity.

Characterization of the binding properties and activation mechanisms behind the function of Tks5 can contribute to further understanding of cancer cell invasion leading to cancer metastasis as well as for the proposed roles of Tks5 in other diseases or in normal invasive cell types of the body.

### **Investigating Tks5 Binding Partners using Tks5 SH3 Domain Mutants**

Further studies may also elucidate the binding partners of Tks5 along with their locations of binding. Binding partners have often been identified using isolated, GST-tagged SH3 domains, however this does not allow for how such binding might change in the context of the full length protein (Abram et al., 2003; Oikawa et al., 2008). Using the Tks5 SH3 domain mutants, it may be possible to further identify specific Tks5 binding partners. In order to confirm the efficacy of this assay, an example of this was performed using dynamin2. Dynamin2 is a protein shown to be involved in invadopodia formation through vesicle formation and actin filament organization regulation (Baldassarre et al., 2003). Tks5 has been suggested to bind to dynamin2 through its 1<sup>st</sup> and 2<sup>nd</sup> SH3 domains, which function together as a superSH3 domain, as well as through its 5<sup>th</sup> SH3 domain (Oikawa et al., 2008; Rufer et al., 2009). Tks5 mutants were introduced into LNCaP cells alongside dynamin2.

After an incubation time of 48 hours, Tks5 was immunoprecipitated from the cells and analyzed for an interaction with dynamin2 through immunoblot analysis (Figure 50). An interaction between Tks5 and dynamin2 was detected, and this interaction appeared to be diminished when the 2<sup>nd</sup> and 5<sup>th</sup> SH3 domains of Tks5 were disrupted. This supports previous research done using GST-tagged SH3 domains demonstrating dynamin2 binding to the 1<sup>st</sup> and 2<sup>nd</sup> superSH3 and the 5<sup>th</sup> SH3 domains of Tks5 (Figure 8A). However, a repeat of

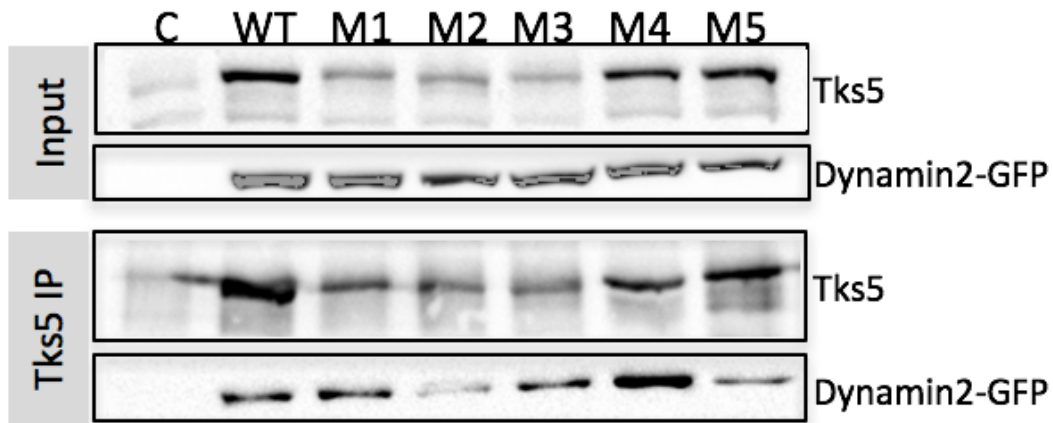


**Figure 50. Co-immunoprecipitation of dynamin2 with Tks5 SH3 domain mutants in LNCaP cells.** Total cell lysates (Input) were analyzed for Tks5 and GFP-tagged dynamin2 by immunoblot (IB). Lysates were also immunoprecipitated (IP) with a Tks5 antibody and analyzed for Tks5 and the GFP tag on dynamin2 by immunoblot as indicated.

this experiment produced contradictory results, in which the M2 and M3 mutant Tks5 constructs appeared to bind more strongly to dynamin2 (data not shown). Clearly there are technical issues that need to be resolved in these immunoprecipitation assays before meaningful data can be obtained, but they nevertheless also point to the feasibility of identifying and characterizing the potentially important Tks5 conformations and associations likely to be necessary for invadopodia development as well. In particular, if this assay is

successful, further study of any binding partners involved in Src endosomal trafficking could provide validation of the role of Tks5 in this specific aspect of invadopodia formation.

## References

- Abram, C.L., Seals, D.F., Pass, I., Salinsky, D., Maurer, L., Roth, T.M., and Courtneidge, S.A. (2003). The adaptor protein Fish associates with members of the ADAMs family and localizes to podosomes of Src-transformed cells. *J. Biol. Chem.* *278*, 16844-16851.
- Ago, T., Kuribayashi, F., Hiroaki, H., Takeya, R., Ito, T., Kohda, D., and Sumimoto, H. (2003). Phosphorylation of p47phox directs phox homology domain from SH3 domain toward phosphoinositides, leading to phagocyte NADPH oxidase activation. *Proc. Natl. Acad. Sci. USA* *100*, 4474-9.
- Albiges-Rizo, C., Destaing, O., Fourcade, B., Planus, E., and Block, M.R. (2009). Actin machinery and mechanosensitivity in invadopodia, podosomes, and focal adhesions. *J. Cell Sci.* *122*, 3037-3049.
- Badowski, C., Pawlak, G., Grichine, A., Chabadel, A., Oddou, C., Jurdic, P., Pfaff, M., Albiges-Rizo, C., and Block, M.R. (2008). Paxillin phosphorylation controls invadopodia/podosomes spatiotemporal organization. *Mol. Biol. Cell* *19*, 633-645.
- Baldassarre, M., Pompeo, A., Beznoussenko, F., Castaldi, C., Cortellino, S., McNiven, M.A., Luini, A., and Buccione, R. (2003). Dynamin participates in focal extracellular matrix degradation by invasive cells. *Mol. Biol. Cell* *14*, 1074-1084.
- Beaty, B.T., Sharma, V.P., Bravo-Cordero, J.J., Simpson, M.A., Eddy, R.J., Koleske, A.J., and Condeelis, J. (2013).  $\beta$ 1 integrin regulates Arg to promote invadopodial maturation and matrix degradation. *Mol. Biol. Cell* *24*, 1661-1675.

- Blouw, B., Patel, M., Iizuka, S., Abdullah, C., You, W.K., Huang, X., Li, J.L., Diaz, B., Stallcup, W.B., and Courtneidge, S.A. (2015). The invadopodia scaffold protein Tks5 is required for the growth of human breast cancer cells in vitro and in vivo. *PLoS One* *10*, e0121003.
- Boateng, L.R., and Huttenlocher, A. (2012). Spatiotemporal regulation of Src and its substrates at invadosomes. *Eur. J. Cell Biol.* *91*, 878-888.
- Branch, K.M., Hoshino, D., and Weaver, A.M. (2012). Adhesion rings surround invadopodia and promote maturation. *Biology Open* *1*, 711-722.
- Bravo-Cordero, J.J., Oser, M., Chen, X., Eddy, R., Hodgson, L., and Condeelis, J. (2011). A novel spatiotemporal RhoC activation pathway locally regulates cofilin activity at invadopodia. *Curr. Biol.* *21*, 635-644.
- Burger, K.L., Davis, A.L., Isom, S., Mishra, N., and Seals, D.F. (2011). The podosome marker protein Tks5 regulates macrophage invasive behavior. *Cytoskeleton* *68*, 694-711.
- Burger, K.L., Learman, B.S., Boucherle, A.K., Sirintrapun, S.J., Isom, S., Díaz, B., Courtneidge, S.A., and Seals, D.F. (2014). Src-dependent Tks5 phosphorylation regulates invadopodia-associated invasion in prostate cancer cells. *The Prostate* *74*, 134-148.
- Buschman, M.D., Bromann, P.A., Cejudo-Martin, P., Wen, F., Pass, I., and Courtneidge, S.A. (2009). The novel adaptor protein Tks4 (SH3PXD2B) is required for functional podosome formation. *Mol. Biol. Cell* *20*, 1302-1311.

- Carducci, M., Perfetto, L., Briganti, L., Paoluzi, S., Costa, S., Zerweck, J., Schutkowski, M., Castagnoli, L., and Cesareni, G. (2012). The protein interaction network mediated by human SH3 domains. *Biotech. Adv.* *30*, 4-15.
- Cejudo-Martin, P., Yuen, A., Vlahovich, N., Lock, P., and Courtneidge, S.A. (2014). Genetic Disruption of the *Sh3pxd2a* gene reveals an essential role in mouse development and the existence of a novel isoform of Tks5. *PLoS One* *9*, e107674.
- Chang, C., and Werb, Z. (2001). The many faces of metalloproteases: Cell growth, invasion, angiogenesis and metastasis. *Trends Cell Biol.* *11*, S37-S43.
- Chebrek, R., Leonard, S., de Brevern, A.G., and Gelly, J-C. (2014). PolyprOnline: polyproline helix II and secondary structure assignment database. *Database* *2014*, article ID bau102.
- Chen, W.T. (1989). Proteolytic activity of specialized surface protrusions formed at rosette contact sites of transformed cells. *J. Exp. Zool.* *251*, 167-185.
- Chen, W.T. (1996). Proteases associated with invadopodia, and their role in degradation of extracellular matrix. *Enzyme Protein* *49*, 59-71.
- Chen, W.T., Chen, J.M., Parsons, S.J., and Parsons, J.T. (1985). Local degradation of fibronectin at sites of expression of the transforming gene product pp60<sup>src</sup>. *Nature* *316*, 156-158.
- Chen, W.T., Olden, K., Bernard, B.A., and Chu, F. (1984). Expression of transformation-associated protease(s) that degrade fibronectin at cell contact sites. *J. Cell Biol.* *98*, 1546-1555.

- Clark, E.S., Whigham, A.S., and Yargrough, W.G. (2007). Cortactin is an essential regulator of matrix metalloproteinase secretion and extracellular matrix degradation in invadopodia. *Cancer Res.* *67*, 4227-4235.
- Cohen, G.B., Ren, R., and Baltimore, D. (1995). Modular binding domains in signal transduction proteins. *Cell* *80*, 237-248.
- Cortesio, C.L., Chan, K.T., Perrin, B.J., Burton, N.O., Zhang, S., Zhang, Z., and Huttenlocker, A. (2008). Calpain 2 and PTP1B function in a novel pathway with Src to regulate invadopodia dynamics and breast cancer cell invasion. *J. Cell Biol.* *180*, 957-971.
- Courtneidge, S.A. (2012). Cell migration and invasion in human disease: the Tks adaptor proteins. *Biochem. Soc. Trans.* *40*, 129-132.
- Courtneidge, S.A., Azucena, E.F., Pass, I., Seals, D.F., and Tesfay, L. (2005). The SRC substrate Tks5, podosomes (invadopodia), and cancer cell invasion. *Cold Spring Harb Symp Quant Biol.* *70*, 167-71.
- Crimaldi, L., Courtneidge, S.A., and Gimona, M. (2009). Tks5 recruits AFAP-110, p190RhoGAP, and cortactin for podosome formation. *Exp. Cell Res.* *315*, 2581-2592.
- Crowley, J.L., Smith, T.C., Fang, Z., Takizawa, N., and Luna, E.J. (2009). Supervillin reorganizes the actin cytoskeleton and increases invadopodial efficiency. *Mol. Biol. Cell* *20*, 948-62.
- Csiszar, A. (2006). Structural and functional diversity of adaptor proteins involved in tyrosine kinase signalling. *BioEssays* *28*, 465-479.

- Cussac, D., Vidal, M., Leprince, C., Liu, W., Cornille, F., Tiraboschi, G., Roques, B.P., and Garbay, C. (1999). A Sos-derived peptidimer blocks the Ras signaling pathway by binding both Grb2 SH3 domains and displays antiproliferative activity. *FASEB J.* *13*, 31-38.
- David-Pfeuty, T., and Singer, S.J. (1980). Altered distributions of the cytoskeletal proteins vinculin and alpha-actinin in cultured fibroblasts transformed by Rous sarcoma virus. *Proc. Natl. Acad. Sci. USA* *77*, 6687-6691.
- Diaz, B., Shani, G., Pass, I., Anderson, D., Quintavalle, M., and Courtneidge, S.A. (2009). Tks5-dependent, Nox-mediated generation of reactive oxygen species is necessary for invadopodia formation. *Sci. Signal.* *2*, ra53.
- Diaz, B., Yuen, A., Iizuka, S., Higashiyama, S., and Courtneide, S.A. (2013). Notch increases the shedding of HB-EGF by ADAM12 to potentiate invadopodia formation in hypoxia. *J. Cell. Biol.* *201*, 279-292.
- Eckert, M.A., Lwin, T.M., Chang, A.T., Kim, J., Danis, E., Ohno-Machado, L., and Yang, J. (2011). Twist1-induced invadopodia formation promotes tumor metastasis. *Cancer Cell* *19*, 372-386.
- Frame, M.C. (2002). Src in cancer: deregulation and consequences for cell behaviour. *Biochim. Biophys. Acta.* *1602*, 114-130.
- Franco, S.J., and Huttenlocher, A. (2005). Regulating cell migration: calpains make the cut. *J. Cell Sci.* *118*, 3829-3838.
- Friedl, P., and Wolf, K. (2003). Tumour-cell invasion and migration: Diversity and escape mechanisms. *Nat. Rev. Cancer* *3*, 362-374.

- Garcia, E., Jones, G.E., Machesky, L.M., and Anton, I.M. (2012). WIP: WASP-interacting proteins at invadopodia and podosomes. *Eur. J. Cell Biol.* *91*, 869-877.
- Gatesman, A., Walker, V.G., Baisden, J.M., Weed, S.A., and Flynn, D.C. (2004). Protein Kinase C $\alpha$  activates c-Src and induces podosome formation via AFAP-110. *Mol. Cell Biol.* *24*, 7578-7597.
- Gimona, M., Kaverina, I., Resch, G.P., Vignal, E., and Burgstaller, G. (2003). Calponin repeats regulate actin filament stability and formation of podosomes in smooth muscle cells. *Mol. Biol. Cell* *14*, 2482-2491.
- Goertzen, C.G., Dragan, M., Turley, E., Babwah, A.V., and Bhattacharya, M. (2015). KISS1R signaling promotes invadopodia formation in human breast cancer cell via  $\beta$ -arrestin2/ERK. *Cell. Signal.* *28*, 165-176.
- Halier, A., Grunewald, T.GP., Orth, M., Reiss, C., Kneitz, B., Spahn, M., and Butt, E. (2014). Loss of tumor suppressor mir-203 mediates overexpression of LIM and SH3 Protein 1 (LASP1) in high-risk prostate cancer thereby increasing cell proliferation and migration. *Oncotarget* *5*, 4144-4153.
- Hashimoto, S., Hirose, M., Hashimoto, A., Morishige, M., Yamada, A., Hosaka, H., Akagi, K., Ogawa, E., Oneyama, C., Agatsuma, T., et al. (2006). Targeting AMAP1 and cortactin binding bearing an atypical src homology 3/proline interface for prevention of breast cancer invasion and metastasis. *PNAS* *103*, 7036-7041.
- Hiroaki, H., Ago, T., Ito, T., Sumimoto, H., and Kohda, D. (2001). Solution structure of the PX domain, a target of the SH3 domain. *Nat. Struct. Biol.* *8*, 526-30.
- Hoshino, D., Branch, K.M., and Weaver, A.M. (2013). Signaling inputs to invadopodia and podosomes. *J. Cell Signal.* *126*, 2979-2989.

- Hu, J., Mukhopadhyay, A., Truesdell, P., Chander, H., Mukhopadhyay, U.K., Mak, A.S., and Craig, A.W.B. (2011). Cdc42-interacting protein 4 is a Src substrate that regulates invadopodia and invasiveness of breast tumors by promoting MT1-MMP endocytosis. *J. Cell. Sci.* *124*, 1739-1751.
- Hughes, T., Briercheck, E.L., Freud, A.G., Trotta, R., McClory, S., Scoville, S.D., Keller, K., Deng, Y., Cole, J., Harrison, N., et al. (2014). The transcription factor AHR prevents the differentiation of a stage 3 innate lymphoid cell subset to natural killer cells. *Cell Rep.* *8*, 150-162.
- Jacob, A., Jing, J., Lee, J., Schedin, P., Gilbert, S.M., Peden, A.A., Junutula, J.R., and Prekeris, R. (2013). Rab40b regulates trafficking of MMP2 and MMP9 during invadopodia formation and invasion of breast cancer cell. *J. Cell. Sci.* *126*, 4647-4658.
- Jensen, H.H., Pedersen, H.N., Stenkjaer, E., Pedersen, G.A., Login, F.H., and Nejsum, L.N. (2015). Tir is essential for the recruitment of Tks5 to enteropathogenic *Escherichia coli* pedestals. *PLoS One* *10*, e0141871.
- Kobashigawa, Y., Sakai, M., Naito, M., Yokochi, M., Kumeta, H., Makino, Y., Ogura, K., Tanaka, S., and Inagaki, F. (2007). Structural basis for the transforming activity of human cancer-related signaling adaptor protein CRK. *Nat. Struct. Mol. Biol.* *14*, 503-510.
- Krutchen, A.E. and McNiven, M.A. (2006). Dynamin as a mover and pincher during cell migration and invasion. *J. Cell Sci.* *119*, 1683-1690.
- Langeberg, L.K., and Scott, J.D. (2015). Signalling scaffolds and local organization of cellular behaviour. *Nat. Rev. Mol. Cell. Biol.* *16*, 232-244).

- Larson, S.M., and Davidson, A.R. (2000). Identification of conserved interactions within the SH3 domain by alignment of sequences and structures. *Protein Sci.* *9*, 2170-2180.
- Lee, M.K., Pardoux, C., Hall, M.C., Lee, P.S., Warburton, D., Qing, J., Smith, S.M., and Derynck, R. (2007). TGF- $\beta$  activates Erk MAP kinase signaling through direct phosphorylation of ShcA. *EMBO J.*, *26*, 3957-3967.
- Li, C.M., Chen, G., Dayton, T.L., Kim-Kiselak, C., Hoersch, S., Whittaker, C.A., Bronson, R.T., Beer, D.G., Winslow, M.M., and Jacks, T. (2013). Differential Tks5 isoform expression contributes to metastatic invasion of lung adenocarcinoma. *Genes & Dev.* *27*, 1557-1567.
- Li, S.S.-C. (2005). Specificity and versatility of SH3 and other proline-recognition domains: structural basis and implications for cellular signal transduction. *Biochem. J.* *390*, 641-653.
- Linder, S., and Aepfelbacher, M. (2003). Podosomes: Adhesion hot-spots of invasive cells. *Trends Cell Biol.* *13*, 376-385.
- Liu, X., Zhang, Q., Zhang, D., Zhou, C., Xing, H., Tian, Z., Rao, Q., Wang, M., and Wang, J. (2009). Overexpression of an isoform of *AML1* in acute leukemia and its potential role in leukemogenesis. *Leukemia* *23*, 739-745.
- Lock, P., Abram, C.L., Gibson, T., and Courtneidge, S.A. (1998). A new method for isolating tyrosine kinase substrates used to identify Fish, an SH3 and PX domain-containing protein, and Src substrate. *EMBO J.* *17*, 4346-4357.

- Lu, K.V., Jong, K.A., Rajasekaran, A.K., Cloughesy, T.F., and Mischel, P.S. (2004). Upregulation of tissue inhibitor of metalloproteinases (TIMP)-2 promotes matrix metalloproteinase (MMP)-2 activation and cell invasion in a human glioblastoma cell line. *Lab. Invest.* *84*, 8-20.
- Malinin, N.L., Wright, S., Seubert, P., Schenk, D., and Griswold-Prenner, I. (2005). Amyloid-B neurotoxicity is mediated by FISH adapter protein and ADAM12 metalloprotease activity. *PNAS* *102*, 3058-3063.
- Martin, K.H., Hayes, K.E., Walk, E.L., Ammer, A.G., Markwell, S.M., and Weed, S.A. (2012). Quantitative measurement of invadopodia-mediated extracellular matrix proteolysis in single and multicellular contexts. *J. Vis. Exp.* *66*, e4119.
- Mayer, B.J., and Eck, M.J. (1995). Minding your p's and q's. *Curr. Biol.* *5*, 364-367.
- Mayer, B.J., Hamaguchi, M., and Hanafusa, H. (1988). A novel viral oncogene with structural similarity to phospholipase C. *Nature* *332*, 272-275.
- Min, L., Ruan, Y., Shen, Z., Jia, D., Wang, X., Zhao, J., Sun, Y., and Gu, J. (2015). Overexpression of Ras-GTPase-activating protein SH3 domain-binding protein 1 correlates with poor prognosis in gastric cancer patients. *Histopathology* *67*, 677-688.
- Monsky, W.L., Lin, C., Aoyama, A., Kelly, T., Akiyama, S.K., Mueller, S.C., and Chen, W. (1994). A potential marker protease of invasiveness, seprase, is localized on invadopodia of human malignant melanoma cells. *Cancer Res.* *54*, 5702-5710.
- Moodley, S., Bai, X.H., Kapus, A., Yang, B., and Liu, M. (2015). XB130/Tks5 scaffold protein interaction regulates Src-mediated cell proliferation and survival. *Mol. Biol. Cell* *26*, 4492-4502.

- Moon, S.K., Cha, B.Y., and Kim, C.H. (2004). ERK1/2 mediates TNF-alpha-induced matrix metalloproteinase-9 expression in human vascular smooth muscle cells via the regulation of NF-kB and AP-1: Involvement of the ras dependent pathway. *J. Cell. Physiol.* *198*, 417-427.
- Moroco, J.A., Craigo, J.K., Iacob, R.E., Wales, T.E., Engen, J.R., and Smithgall, T.E. (2014). Differential sensitivity of Src-family kinases to activation by SH3 domain displacement. *PLoS One* *9*, e105629.
- Moshfegh, Y., Bravo-Cordero, J.J., Mischkolci, V., Condeelis, J., and Hodgson, L. (2014). A Trio-Rac1-Pak1 signaling axis drives invadopodia disassembly. *Nat. Cell Biol.* *16*, 571-583.
- Mueller, S.C., Ghersi, G., Akiyama, S.K., Sang, Q.A., Howard, L., Pineiro-Sanchez, M., Nakahara, H., Yeh, Y., and Chen, W. (1999). A novel protease-docking function of integrin at invadopodia. *J. Biol. Chem.* *274*, 24947-24952.
- Mukhopadhyay, U.K., Eves, R., Jia, L., Mooney, P., and Mak, A.S. (2009). p53 suppresses Src-induced podosome and rosette formation and cellular invasiveness through the upregulation of caldesmon. *Mol. Cell. Biol.* *29*, 3088-3098.
- Murphy, D.A., and Courtneidge, S.A. (2011). The 'ins' and 'outs' of podosomes and invadopodia: characteristics, formation and function. *Nat. Rev. Mol. Cell Biol.* *12*, 413-426.
- Murphy, D.A., Diaz, B., Bromann, P.A., Tsai, J.H., Kawakami, Y., Maurer, J., Stewart, R.A., Izpisua-Belmonte, J.C., and Courtneidge, S.A. (2011). A Src-Tks5 pathway is required for neural crest cell migration during embryonic development. *PLoS One* *6*, e22499.

- Murray, J.W., and Wolkoff, A.W. (2003). Roles of the cytoskeleton and motor proteins in endocytic sorting. *Adv. Drug Deliv. Rev.* 55, 1385-1403.
- Nakahara, H., Howard, L., Thompson, E.W., Sato, H., Seiki, M., Yeh, Y., and Chen, W. (1997). Transmembrane/cytoplasmic domain-mediated membrane type 1-matrix metalloprotease docking to invadopodia is required for cell invasion. *Proc. Natl. Acad. Sci.* 94, 7959-7964.
- Neel, N.F., Rossman, K.L., Martin, T.D., Hayes, T.K., Yeh, J.J., and Der, C.J. (2012). The RalB small GTPase mediates formation of invadopodia through a GTPase-activation protein-independent function of the RalBP1-RLIP76 effector. *Mol. Cell. Biol.* 32, 1374-1386.
- Nguyen, J.T., Turck, C.W., Cohen, F.E., Zuckermann, R.N., and Lim, W.A. (1998). Exploiting the basis of proline recognition by SH3 and WW domains: design of N-substituted inhibitors. *Science* 282, 2088-2091.
- Oikawa, T., Itoh, T., and Takenawa, T. (2008). Sequential signals toward podosome formation in NIH-src cells. *J. Cell Biol.* 182, 157-169.
- Oikawa, T., Nakamura, A., Onishi, N., Yamada, T., Matsuo, K., and Saya, H. (2013). Acquired expression of NFATc1 downregulates E-cadherin and promotes cancer cell invasion. *Cancer Res.* 73, 5100-5109.
- Oikawa, T., Oyama, M., Kozuka-Hata, H., Uehara, S., Udagawa, N., Saya, H., and Matsuo, K. (2012). Tks5-dependent formation of circumferential podosomes/invadopodia mediates cell-cell fusion. *J. Cell Biol.* 197, 553-568.

- Osenkowski, P., Toth, M., and Fridman, R. (2004). Processing, shedding, and endocytosis of membrane type 1-matrix metalloproteinase (MT1-MMP). *J. Cell. Physiol.* *200*, 2-10.
- Pichot, C.S., Arvanitis, C., Hartig, S.M., Jensen, S.A., Bechill, J., Marzouk, S., Yu, J., Frost, J.A., and Corey, S.J. (2010). Cdc42-interacting protein 4 promotes breast cancer cell invasion and formation of invadopodia through activation of N-WASp. *Cancer Res* *70*, 8347-8356.
- Pignatelli, J., Tumbarello, D.A., and Schmidt, R.P. (2012). Hic-5 promotes invadopodia formation and invasion during TGF- $\beta$ -induced epithelial-mesenchymal transition. *J. Cell. Biol.* *197*, 421-437.
- Playford, M.P., and Schaller, M.D. (2004). The interplay between Src and integrins in normal and tumor biology. *Oncogene* *23*, 7928-7946.
- Poincloux, R., Lizarraga, F., and Chavrier, P. (2009). Matrix invasion by tumor cells: a focus on MT1-MMP trafficking to invadopodia. *J. Cell. Sci.* *122*, 3015-3024.
- Reinecke, J.B., Katafiasz, D., Naslavasky, N., and Caplan, S. (2014). Regulation of Src trafficking and activation by the endocytic regulatory proteins MICAL-L1 and EHD1. *J. Cell Sci.* *127*, 1684-98.
- Ren, R., Mayer, B.J., Cicchetti, P., and Baltimore, D. (1993). Identification of a ten-amino acid proline-rich SH3 binding site. *Science* *259*, 1157-1161.
- Reynolds, A.B., Kanner, S.B., Bouton, A.H., Schaller, M.D., Weed, S.A., Flynn, D.C., and Parsons, J.T. (2014). SRChing for the substrates of Src. *Oncogene* *33*, 4537-4547.
- Rohatgi, R., Ho, H.H., and Kirschner, M.W. (2000). Mechanism of N-WASp activation by Cdc42 and phosphatidylinositol 4,5-bisphosphate. *J. Cell. Biol.* *150*, 1299-1310.

- Roy, R., Wewer, U.M., Zurakowski, D., Pories, S.E., and Moses, M.A. (2004). ADAM12 cleaves extracellular matrix proteins and correlates with cancer status and stage. *J. Biol. Chem.* *279*, 51323-30.
- Rufer, A.C., Rumpf, J., von Holleben, M., Beer, S., Rittinger, K., and Groemping, Y. (2009). Isoform-selective interaction of the adaptor protein Tks5/FISH with Sos1 and dynamins. *J. Mol. Biol.* *390*, 939-950.
- Saksela, K., and Permi, P. (2012). SH3 domain ligand binding: what's the consensus and where's the specificity? *FEBS Letters* *586*, 2609-2614.
- Salah, Z., Itzhaki, E., and Aqeilan, R.I. (2014). The ubiquitin E3 ligase ITCH enhances breast tumor progression by inhibiting the Hippo tumor suppressor pathway. *Oncotarget* *5*, 10886-10900.
- Sandilands, E., and Frame, M.C. (2008). Endosomal trafficking of Src tyrosine kinase. *Trends Cell Biol.* *18*, 322-329.
- Sandoval, C.O., and Simmen, T. (2012). Rab proteins of the endoplasmic reticulum: functions and interactors. *Biochem. Soc. Trans.* *40*, 1426-1432.
- Schanda, K., Hermann, M., Stefanova, N., Gredler, V., Bandtlow, C., and Reindl, M. (2011). Nogo-B is associated with cytoskeletal structures in human monocyte-derived macrophages. *BMC Res. Notes* *4*.
- Schoumacher, M., Goldman, R.D., Louvard, D., and Vignjevic, D.M. (2010). Actin, microtubules, and vimentin intermediate filaments cooperate for elongation of invadopodia. *J. Cell. Biol.* *189*, 541-556.

- Seals, D.F., Azucena, E.F., Pass, I., Tesfay, L., Gordon, R., Woodrow, M., Resau, J.H., and Courtneidge, S.A. (2005). The adaptor protein Tks5/Fish is required for podosome formation and function, and for the protease-driven invasion of cancer cells. *Cancer Cell* 7, 155-165.
- Seals, D.F., and Courtneidge, S.A. (2003). The ADAMs family of metalloproteases: multidomain proteins with multiple functions. *Genes Dev.* 17, 7-30.
- Shao, W., and Espenshade, P.J. (2012). Expanding roles for SREBP in metabolism. *Cell Metab.* 16, 414-419.
- Sharma, V.P., Eddy, R., Entenberg, D., Kai, M., Gertler, F.B., and Condeelis, J. (2013). Tks5 and SHIP2 regulate invadopodium maturation, but not initiation, in breast carcinoma cells. *Curr. Biol.* 23, 2079-2089.
- Shi, F., and Sottile, J. (2011). MT1-MMP regulates the turnover and endocytosis of extracellular matrix fibronectin. *J. Cell. Sci.* 124, 4039-4050.
- Simister, P.C., Luccarelli, J., Thompson, S., Appella, D.H., Feller, S.M., and Hamilton, A.D. (2013). Novel inhibitors of a Grb2 SH3C domain interaction identified by a virtual screen. *Bioorg. Med. Chem.* 21, 4027-4033.
- Sjoblon, B., Salmazo, A., and Dijinovic-Carugo, K. (2008). Alpha-actinin structure and regulation. *Cell Mol. Life Sci.* 65, 2688-701.
- Skor, M.N., Wonder, E.L., Kocherginsky, M., Goyal, A., Hall, B.A., Cai, Y., and Conzen, S.D. (2013). Glucocorticoid receptor antagonism as a novel therapy for triple-negative breast cancer. *Clin. Cancer Res.* 19, 6163-6172.

- Smith-Pearson, P.S., Greuber, E.K., Yogalingam, G., and Pendergast, A.M. (2010). Abl kinases are required for invadopodia formation and chemokine-induced invasion. *J. Biol. Chem.* *285*, 40201-40211.
- Smithgall, T.E. (1995). SH2 and SH3 domains: potential targets for anti-cancer drug design. *J. Pharmacol. Toxicol. Methods* *34*, 125-132.
- Spector, D.H., Varmus, H.E., and Bishop, J.M. (1978). Nucleotide sequences related to the transforming gene of avian sarcoma virus are present in DNA of uninfected vertebrates. *Proc. Natl. Acad. Sci. USA* *75*, 4102-4106.
- Stautz, D., Sanjay, A., Hansen, M.T., Albrechtsen, R., Wewer, U.M., and Kveiborg, M. (2010). ADAM12 localizes with c-Src to actin-rich structures at the cell periphery and regulates Src kinase activity. *Exp. Cell Res.* *316*, 55-67.
- Stenmark, H., Aasland, R., Toh, B., and D-Arrigo, A. (1996). Endosomal localization of the autoantigen EEA1 is mediated by a Zinc-binding FYVE finger. *J. Biol. Chem.* *271*, 24048-24054.
- Stylli, S.S., Kaye, A.H., and Lock, P. (2008). Invadopodia: At the cutting edge of tumour invasion. *J. Clin. Neurosci.* *15*, 725-737.
- Stylli, S.S., Stacey, T.T., Verhagen, A.M., Xu, S.S., Pass, I., Courtneidge, S.A., and Lock, P. (2009). Nck adaptor proteins link Tks5 to invadopodia actin regulation and ECM degradation. *J. Cell. Sci.* *122*, 2727-40.
- Sun, M., Yang, L., Feldman, R.I., Sun, X., Bhalla, K.N., Jove, R., Nicosia, S.V., and Cheng, J.Q. (2003). Activation of Phosphatidylinositol 3-kinase/Akt pathway by androgen through interaction of p85a, androgen receptor, and Src. *JBC* *291*, 42992-43000.

- Sundararajan, V., Gengenbacher, N., Stemmler, M.P., Kleemann, J.A., Brabletz, T., and Brabletz, S. (2015). The ZEB1/miR-200c feedback loop regulates invasion via actin interacting proteins MYLK and TKS5. *Oncotarget* 6, 27083-27096.
- Synek, L., Sekeres, J., and Zarsky, V. (2014). The exocyst at the interface between cytoskeleton and membranes in eukaryotic cells. *Front. Plant Sci.* 4, 1-7.
- Takeya, T., and Hanafusa, H. (1983). Structure and sequence of the cellular gene homologous to the RSV *src* gene and the mechanism for generating the transforming virus. *Cell* 32, 881-890.
- Tanaka, M., Gupta, R., and Mayer, B.J. (1995). Differential inhibition of signaling pathways by dominant-negative SH2/SH3 adapter proteins. *Mol. Cell. Biol.* 15, 6829-6837.
- Tarone, G., Cirillo, D., Giancotti, F.G., Comoglio, P.M., and Marchisio, P.C. (1985). Rous sarcoma virus-transformed fibroblasts adhere primarily at discrete protrusions of the ventral membrane called podosomes. *Exp. Cell Res.* 159, 141-157.
- Thalappilly, S., Suliman, M., Gayet, O., Souveyran, P., Hermant, A., Lecine, P., Iovanna, J.L., and Dusetti, N.J. (2008). Identification of multi-SH3 domain-containing protein interactome in pancreatic cancer: A yeast two-hybrid approach. *Proteomics* 8, 3071-3081.
- Thompson, O., Kleino, I., Crimadli, L., Gimona, M., Saksela, K., and Winder, S.J. (2008). Dystroglycan, Tks5 and Src mediated assembly of podosomes in myoblasts. *PLoS One* 3, e3638.

- Varon, C., Tatin, F., Moreau, V., Obberghen-Schilling, E.V., Fernandez-Sauze, F., Reuzeau, E., Kramer, I., and Genot, E. (2006). Transforming growth factor B induces rosettes of podosomes in primary aortic endothelial cells. *Mol. Cell. Biol.* *26*, 3582-3594.
- Vidal, M., Gigoux, V., and Garbay, C. (2001). SH2 and SH3 domains as targets for anti-proliferative agents. *Crit. Rev. Oncol. Hematol.* *40*, 175-186.
- Wang, H., An, H., Wang, B., Liao, Q., Li, W., Jin, X., Cui, S., Zhang, Y., Ding, Y., and Zhao, L. (2013). miR-133a represses tumour growth and metastasis in colorectal cancer by targeting LIM and SH3 protein 1 and inhibiting the MAPK pathway. *Eur. J. Cancer* *49*, 3924-3935.
- Weaver, A.M. (2006). Invadopodia: specialized cell structures for cancer invasion. *Clin. Exp. Metastasis* *23*, 97-105.
- Wei, C., Wu, Q., Vega, V.B., Chiu, K.P., Ng, P., Zhang, T., Shahab, A., Yong, H.C., Fu, Y., Weng, Z., et al. (2006). A global map of p53 transcription-factor binding sites in the human genome. *Cell* *124*, 207-219.
- Williams, K.C., and Coppolino, M.G. (2014). SNARE-dependent interaction of Src, EGFR, and B1 integrin regulates invadopodia formation and tumor cell invasion. *J. Cell Sci.* *127*, 1712-25.
- Wishart, M.J., Taylor, G.S., and Dixon, J.E. (2001). Phoxy lipids: Revealing PX domains as phosphoinositides binding modules. *Cell* *105*, 817-820.
- Xiang, Y., Cheng, Y., Li, X., Xu, J., Zhang, J., Liu, Y., Xing, Q., Wang, L., He, L., and Zhao, X. (2013). Up-regulated expression and aberrant DNA methylation of LEP and SH3PXD2A in pre-eclampsia. *PLoS One* *8*, e59753.

- Yoshio, T., Mortia, T., Kimura, Y., Tsujii, M., Hayashi, N., and Sobue, K. (2007). Caldesmon suppresses cancer cell invasion by regulating podosome/invadopodium formation. *FEBS Let.* 581, 3777-3782.
- Zajac, M., Law, J., Cvetkovic, D.D., Pampillo, M., McColl, L., Pape, C., Guglielmo, G.M., Postovit, L.M., Babwah, A.V., and Bhattacharya, M. (2011). GPR54 (KISS1R) transactivates EGFR to promote breast cancer cell invasiveness. *PLoS ONE* 6, e21599.
- Zarrinpar, A., Bhattacharyya, R.P., and Lim, W.A. (2003). The structure and function of proline recognition domains. *Sci, STKE* 2003, RE8.
- Zhu, J., Pang, Z., and Yu, Y. (2012). Regulation of trophoblast invasion: the role of matrix metalloproteinases. *Rev. Obstet. Gynecol.* 5, e137-e143.

## Supplemental Information

**Supplementary Table SI. Tks5 associated proteins<sup>a</sup> categorized by function.**

<b>Categorical Function</b>	<b>Putative Tks5 Binding Partner</b>	<b>Protein Class<sup>b</sup></b>	<b>Specific Function<sup>b</sup></b>	<b>Association with Cancer</b>	<b>Association with Invadopodia</b>	<b>Target sequence or motif<sup>c</sup></b>	<b>Ref</b>
Actin-Related	SH3P7 (DBNL) <sup>d</sup>	Adaptor	Actin binding; antigen reception; JNK1 signaling; Rac activation; interacts with hematopoietic progenitor kinase 1a	Upregulated in lung cancer; increased MELK expression in brain, breast, melanoma, colorectal cancers (DBNL is a MELK substrate)	Localizes to podosomes and necessary for rosette formation; enhances membrane ruffling and invasiveness	PxxP (2) Class III (1)	1, 2, 3
	Tropomyosin 1 alpha-1 chain splice isoforms 2 and 3	Cytoskeletal	Stabilizing cytoskeletal actin filaments	Cell transformation suppressor; downregulated in cancer	Isoform 2 is found in and around invadopodia	Class III (2)	4, 5
	WIP-related protein (WIRE)	Adaptor	Relocalizes N-WASp to actin; plays an active role in formation of cell surface protrusions downstream of activated PDGFB receptors. Cooperates with WASp and WASL.	No strong evidence, possibly involved	Localizes to invadopodia of MTLn3 and MDA-MB-321 cells; localizes to podosomes of DCs, endothelial cells, and osteoclasts.	PxxP (47) Class I (10) Class II (7)	6
Actin Polymerization	Arp2/3 complex	Cytoskeletal	Serve as nucleation sites for new actin	Found in invasive cancer cells; overexpression in invasive breast, colorectal, lung cancers	Necessary for formation	PxxP (2) Class II (2) Class III (7)	7, 8
	Cortactin*	Cytoskeletal	Recruits Arp; stabilizes actin nucleation sites for actin branching	Association with poor prognosis, overexpressed in numerous cancers	Prominent component of invadopodia	PxxP (2) Class I (1) Class III (5)	9
	Drebrin	Cytoskeletal	Required for actin polymerization at immunological synapses	Involved in tumorigenesis; overexpression in prostate cancer cells	Necessary for podosome formation	PxxP (15) Class I (2) Class III (1)	10, 11, 12
	Cofilin-1	Cytoskeletal	Severs actin to generate new barbed ends for further actin growth	Involved in metastasis; upregulated in prostate cancer	Localizes at invadopodia, required for stability and ECM degradation		7, 13, 14
Actin Regulation	F-actin capping proteins alpha and beta	Actin binding	Binds ends of actin to block exchange of subunits	Upregulation and downregulation has been shown in prostate cancers	Localized at invadopodia	Class III (1)	15, 16, 17
	Tropomodulin-3	Cytoskeletal	Blocks elongation and depolymerization; regulates actin length			PxxP (1)	
Cytoskeleton component/related	Beta-actin	Cytoskeletal	Nonmuscle cytoskeletal actin	Mutations are associated with tumorigenesis; upregulated in	Found in invadopodia	PxxP (1) Class III (2)	18, 19, 20

				prostate cancer in hypoxic conditions				
	Gamma-actin	Cytoskeletal	Globular actin; cytoplasmic; polymerization leads to F-actin strands	Mutations associated with tumorigenesis		PxxP (1) Class III (2)	18	
	Kinesin-related motor protein Eg5	Cytoskeletal Motor	Required for establishing a bipolar spindle; involved in centrosome migration	Increased expression in actively proliferating cells; Cancer therapeutic target		PxxP (1) Class I (1) Class II (1) Class III (1)	21, 22	
	Myosin II Myosin light polypeptide 6 Myosin regulatory light chain 2	Motor	Motor proteins that move along actin filaments; required for cytoskeleton organization; Regulatory myosins regulate contractile activity	Role in metastasis	Present in ring-like structures and around a subset of invadopodia	PxxP (1) Class II (1) Class III (9)	23, 24	
	Tubulin	Cytoskeletal	Makes up microtubules	Cancer therapeutic target	Required for elongation of invadopodia	Class III (4)	25, 26, 27	
	Vimentin	Cytoskeletal	Intermediate filament specific to mesenchymal tissue	Associated with EMT and loss of adhesions; overexpression associated with invasiveness	Required for elongation of invadopodia	Class III (1)	26, 28	
Nucleotide synthesis	C1-tetrahydrofolate synthase	Enzyme	De novo synthesis of purines and thymidylate; regeneration of methionine	Upregulated in colon cancer; potential cancer therapeutic target		PxxP (7) Class I (4) Class II (3) Class III (2)	29, 12	
	Inosine-5'-monophosphate dehydrogenase 2	Enzyme	Catalyzes first rate-limiting step in guanine nucleotides	Attractive target for cancer; upregulated in cancers		Class III (3)	30, 31	
Translation machinery	Ribosomal subunits:	Ribosomal	Creates ribosomes which catalyze protein synthesis	Some ribosomal subunits have been shown to be overexpressed in cancer; S16 upregulated in prostate cancer		S3: PxxP (5) Class I (1)	32, 33	
	40S S3							
	40S S11							S11: Class III (2)
	40S S13							S13: PxxP (1) Class III (4)
	40S S16							S16: Class III (1)
	40S S18							S18: Class III (2)
	60S L11							L11: Class III (5)
	60S L12							L12: Class III (1)

						L23: Class III (1)  L26: Class III (1)	
	Elongation factor 1-alpha 1	Translation	Recruits tRNA to A site	Overexpressed in cancer; oncogene; has potential as a prostate cancer marker		PxxP (2) Class III (1)	32, 34, 35
	Elongation factor 2	Translation	Ribosomal translocation of mRNA from A site to P site	Expression and activity increased in cancer cells	Found in invadopodia	PxxP (2) Class III (4)	36, 37, 20
	Eukaryotic initiation factor 4A-1	Translation; Helicase	Responsible for RNA helicase activity of translation initiation complex; involved in cap recognition and required for mRNA binding to ribosome	Well established oncogene		Class III (1)	38, 39
	Eukaryotic translation initiation factor 3 subunit 2	Translation	Cap independent translation initiation; associates with ribosomal 40S subunit and promotes binding of methionyl-tRNA <sub>i</sub> and mRNA	Overexpressed in colon cancer		Class III (1)	40, 41
	Methionyl-tRNA synthetase	Enzyme	Covalently links methionine with cognate tRNA	Overexpression of substrate tRNA; met can cause transformation; overexpressed in cancer		PxxP (5) Class I (1) Class III (3)	42, 43
RNA binding proteins	Dead box protein 3	Enzyme	RNA Helicase involved in RNA metabolism and gene expression	Overexpressed in breast cancer; tumor suppressor in hepatocellular carcinoma		PxxP (1) Class III (2)	44, 45
	hnRNP K	RNA splicing/binding	Complexes with heterogeneous nuclear RNA (Pre-mRNAs)	Increased expression and nuclear shift in cancer	Localizes to macrophage podosomes and invadopodia	PxxP (9) Class I (5) Class II (3)	46, 47, 20, 48
Transcription machinery	Methylosome protein 50	Adaptor	Interaction with spliceosome proteins inhibits spliceosome assembly	Involved in tumorigenesis		PxxP (3) Class III (1)	49
	Methylosome subunit p1 Cln	Channel	Regulates spliceosome assembly	Involved in tumorigenesis		PxxP (1)	49
	Ras-GTPase-activating protein binding protein 1	Enzyme; Adaptor	DNA unwinding enzyme; involved in MAPK signaling; member of hnRNA binding proteins	Highly overexpressed in various cancers and closely associated with invasion and metastasis		PxxP (2) Class I (1) Class II (1)	50
	Small nuclear ribonucleoprotein associated	RNA binding	Component of spliceosome	Alternative splicing can lead to cancer; increased splicing rates in cancer (possible therapeutic		PxxP (10) Class I (5) Class III (4)	51

	proteins B and B'			target)			
	Protein arginine N-methyltransferase 5  SKB1 protein arginine N-methyltransferase	Enzyme	Methylates histones H2A and H4 (histones involved in transcriptional repression) Components of methylosome	Oncogene; overexpressed in cancer		PxxP (2) Class III (6)	49, 52, 53, 54
	RuvB-like 1 (Pontin)  RuvB-like 2 (Reptin)	Enzyme	Helicase activity, activation of acetylation of H2A and H4	Increased expression in cancer; promotes increased proliferation		Pontin: PxxP (1) Class I (1)  Reptin: PxxP (1) Class III (2)	55
Chaperone proteins	GRP 78 glucose-regulated protein precursor	Chaperone	Precursor to Hsp	Helps with adaptation to stress in tumor microenvironment; increased expression in cancers		PxxP (1) Class III (1)	56
	Hsp60	Chaperone	Prevents protein aggregation; helps protein folding	Enhanced expression in breast carcinoma, prostate cancer, and myeloid leukemia		Class III (2)	57, 58
	Hsp70.1; 70.8	Chaperone	Resistance to cell death, prevents protein aggregation, helps protein folding	Expression enhanced after transformation; increased expression in LNCaPs	Hsp 70 protein 8 isoforma 1 variant found in invadopodia	PxxP (2) Class III (9)	57, 58, 20
	Hsp90-alpha4; beta	Chaperone	Forms stable complexes with actin to protect filaments; prevents protein aggregation; helps protein stabilization and trafficking; facilitates protein activation	Potential cancer target	Hsp90-Beta found in invadopodia	PxxP (1) Class III (11)	57, 59, 20
	Stress-70 protein	Chaperone	Implicated in control of cell proliferation and aging; may act as chaperone	Up-regulated in cancers			60, 61
	T-complex protein 1: beta, delta, theta, and zeta subunits	Chaperone	Molecular chaperone; folds polypeptides including actin and tubulin		T-complex protein 1 isoform a found in invadopodia	PxxP (2) Class III (8)	20
Mitosis related	NDR1 protein kinase	Enzyme	Regulates proper cell function related to development, growth and mitosis; required for centriole duplication	Downregulated in tubular carcinoma and some prostate cancers; appears to be a tumor suppressor but some upregulation in cancer suggests proto-oncogenic activity		PxxP (1) Class III (2)	62, 63
	Protein phosphatase 2C beta	Enzyme	Kinase inhibitor including oncogenic signaling proteins	Associated with cancer related biological processes; increased expression		PxxP (3) Class III (1)	64

Ras activation	14-3-3 beta 14-3-3 gamma 14-3-3 theta 14-3-3 zeta	Adaptor	Mediates signal transduction by binding phosphoserine-containing proteins; regulates Ras effectors	in cancers; oncogene Cancer therapy target; regulates important cancer processes	(14-3-3 epsilon is involved with invadopodia and cofilin)	Beta: PxxP (1) Class II (1) Class III (1)  Gamma: PxxP (1) Class II (1)  Theta: PxxP (1) Class II (1)  Zeta: PxxP (1) Class II (1)	65
	CrkL <sup>d</sup>	Adaptor	Activates Ras and JUN; cytoskeleton regulator; substrate of Bcr-Abl	Oncogene; increased expression found in some cancers	Abl kinases required for invadopodia formation	PxxP (4) Class I (1) Class III (1)	66, 67, 68
	Nck1 Nck2	Adaptor	Transducing signals from RTKs to downstreams like RAS; coordinates actin cytoskeleton remodeling	Overexpression in cancer; Nck1 overexpression transforms fibroblasts	Nck1 localizes to invadopodia, important for formation and function; Nck2 links Tks5 to invadopodia regulation	Nck1: PxxP (2) Class I (2)	69, 70, 71
	Grb2	Adaptor	Signal transduction and cell communication; links EGFR to activation of Ras, Erk1/2	Over expression in cancers	Does not localize to invadopodia, does localize to degradative structures formed by transformed fibroblasts	PxxP (1)	69, 72, 73
Remaining	5'-AMP activated protein kinase  (catalytic alpha-1 chain; gamma-1 subunit)	Enzyme	Cellular energy homeostasis; regulator of cellular polarity through actin cytoskeleton remodeling; activated by environmental stress	Activated to treat cancer; some enzymes overexpressed in cancer are inhibited by AMPK	Activation leads to decrease in fatty acid synthesis, leading to a decrease in invadopodia	PxxP (2) Class III (6)	74, 75, 76
	Creatine kinase B-type	Enzyme	Catalyzes conversion of creatine to phosphocreatine	Levels increased in some cancers; downregulated in LNCaP and PC3 cell lines		PxxP (2) Class III (1)	77, 78, 12
	D-3-phosphoglycerate dehydrogenase	Enzyme	Catalyzes 3-phosphoglycerate into 3-phosphohydroxypyruvate	Increased activity in cancer		PxxP (3) Class II (1)	79
	Mouse Tks5	Adaptor	Scaffold protein involved in invadopodia and podosome formation	Increased expression in cancers	Necessary for invadopodia structure and function	PxxP (16) Class I (5) Class II (6) Class III (3)	80, 81, 82
	Peroxiredoxin 1	Enzyme	Antioxidant	Increased expression in cancer; expression	Possibly needs to be		83, 84,

				correlated with cancer progression and growth	inactivated for invadopodia formation		85
--	--	--	--	---	---------------------------------------	--	----

<sup>a</sup>List of binding partners based on proteins identified as associating with FLAG-Tks5 constructs (Stylli et al., 2009; Table S1).

<sup>b</sup>Information found using PhosphoSite (<http://www.phosphosite.org/>) and UniProt Knowledgebase (<http://www.uniprot.org/>).

<sup>c</sup>Target sequences and motifs are based on those previously described as being general consensus for SH3 binding specificity.

(Carducci, et al., 2012). Quantity of each motif found is displayed in parentheses next to motif type. Motif searches were carried out using ScanProsite (<http://www.prosite.expasy.org/scanprosite/>). Class I: (R/K)xxPxxP or (R/K)xPxxP; Class II: PxxPx(R/K); Class III: RxxK

<sup>d</sup>Could not confirm stable interaction with Tks5

- Li, Z., Park, H.R., Shi, Z., Li, Z., Pham, C.D., Du, Y., Khuri, F.R., Zhang, Y., Han, Q., and Fu, H. (2014). Pro-oncogenic function of HIP-55/Drebrin-like (DBNL) through Ser269/Thr291-phospho-sensor motifs. *Oncotarget* 5, 3197-3209.
- Boateng, L.R., Cortesio, C.L., and Huttenlocher, A. (2012). Src-mediated phosphorylation of mammalian Abp1 (DBNL) regulates podosome formation in transformed fibroblasts. *J. Cell Sci.* 125, 1329-1341.
- Chung, S., Suzuki, H., Miyamoto, T., Takamatsu, N., Tatsuguchi, A., Ueda, K., Kijima, K., Nakamura, Y., and Matsuo, Y. (2012). Development of an orally-administrative MELK targeting inhibitor that suppresses the growth of various types of human cancer. *Oncotarget* 3, 1629-1640.
- Bharadwaj, S. and Prasad, G.L. (2002). Tropomyosin-1, a novel suppressor of cellular transformation is downregulated by promoter methylation in cancer cells. *Cancer Lett.* 183, 205-213.
- Gimona, M., Buccione, R., Courtneidge, S.A., and Linder, S. (2008). Assembly and biological role of podosomes and invadopodia. *Curr. Opin. Cell Biol.* 20, 235-241.
- García, E., Jones, G.E., Machesky, L.M., and Antón, I.M. (2012). WIP: WASP-interacting proteins at invadopodia and podosomes. *Eur. J. Cell Biol.* 91, 869-877.
- Yamaguchi, H., Lorenz, M., Kempiak, S., Sarmiento, C., Coniglio, S., Symons, M., Segall, J., Eddy, R., Miki, H., Takenawa, T., and Condeelis, J. (2005). Molecular mechanisms of invadopodium formation: the role of the N-WASP-Arp2/3 complex pathway and cofilin. *J. Cell Biol.* 168, 441-452.
- Yamaguchi, H. and Condeelis, J. (2007). Regulation of the actin cytoskeleton in cancer cell migration and invasion. *Biochim. Biophys. Acta.* 1773, 642-652.
- Clark, E.S., Whigham, A.S., Yarbrough, W.G., and Weaver, A.M. (2007). Cortactin is an essential regulator of matrix metalloproteinase secretion and extracellular matrix degradation in invadopodia. *Cancer Res.* 67, 4227-4235.
- Peitsch, W.K., Hofmann, I., Bulkescher, J., Hergt, M., Spring, H., Bleyl, U., Goerd, S., and Franke, W.W. (2005). Drebrin, an actin-binding, cell-type characteristic protein: induction and localization in epithelial skin tumors and cultured keratinocytes. *J. Invest. Dermatol.* 125, 761-774.
- Gimona, M., Grashoff, C., and Kopp, P. (2005). Oktoberfest for adhesion structures. *EMBO reports* 6, 922-926.
- Glen, A., Evans, C.A., Gan, C.S., and Cross, S.S., Hamdy, F.C., Gibbins, J., Lippitt, J., Eaton, C.L., Noirel, J., Wright, P.C., Rehman, I. (2010). Eight-plex iTRAQ analysis of variant metastatic human prostate cancer cells identifies candidate biomarkers of progression: an exploratory study. *Prostate* 70, 1313-1332.
- Wang, W., Eddy, R., and Condeelis, J. (2007). The cofilin pathway in breast cancer invasion and metastasis. *Nat. Rev. Cancer* 7, 429-440.
- Lee, E., Cho, H., and Kim, C. (2011). Proteomic analysis of cancer stem cells in human prostate cancer cells. *Biochem. Biophys. Res. Commun.* 412, 279-285.
- Artym, V.V., Zhang, Y., Seillier-Moiseiwitsch, F., Yamada, K.M., and Mueller, S.C. (2006). Dynamic interactions of cortactin and membrane type 1 matrix metalloproteinase at invadopodia: defining the stages of invadopodia formation and function. *Cancer Res.* 66, 3034-3043.
- Ummanni, R., Junker, H., Zimmermann, U., Venz, S., Teller, S., Giebel, J., Scharf, C., Woenckhaus, C., Dombrowski, F., and Walther, R. (2008). Prohibitin identified by proteomic analysis of prostate biopsies distinguishes hyperplasia and cancer. *Cancer Lett.* 266, 171-185.
- Chêne, L., Ciroud, C., Desgrandchamps, F., Boccon-Gibod, L., Cussenot, O., Berthon, P., and Latil, A. (2004). Extensive analysis of the 7q31 region in human prostate tumors supports *TES* as the best candidate tumor suppressor gene. *Int. J. Cancer* 111, 798-804.
- Chou, C.C., Davis, R.C., Fuller, M.L., Slovin, J.P., Wong, A., Wright, J., Kania, S., Shaked, R., Gatti, R.A., and Salser, W.A. (1987). Gamma-actin: unusual mRNA 3'-untranslated sequence conservation and amino acid substitutions that may be cancer related. *PNAS* 84, 2575-2579.
- Ohl, F., Jung, M., Xu, C., Stephan, C., Rabien, A., Burkhardt, M., Nitsche, A., Kristiansen, G., Loening, S.A., Radonić, A., and Jung, K. (2005). Gene expression studies in prostate cancer tissue: which reference gene should be selected for normalization? *J. Mol. Med.* 83, 1014-1024.
- Attanasio, F., Caldieri, G., Giacchetti, G., van Horssen, R., Wieringa, B., and Buccione, R. (2011). Novel invadopodia components revealed by differential proteomic analysis. *Eur. J. Cell Biol.* 90, 115-127.
- Naki, R., Iida, S., Takahashi, T., Tsujita, T., Okamoto, S., Takada, C., Akasaka, K., Ichikawa, S., Ishida, H., Kusaka, H., et al. (2015). K858, a novel inhibitor of mitotic kinesin Eg5 and antitumor agent, induces cell death in cancer cells. *Cancer Res.* 69, 3901-3909.
- Hayashi, N., Koller, E., Fazli, L., and Gleave, M.E. (2008). Effects of Eg5 knockdown on human prostate cancer xenograft growth and chemosensitivity. *Prostate* 68, 1283-1295.
- Betapudi, V., Licate, L.S., and Egelhoff, T.T. (2006). Distinct roles of nonmuscle myosin II isoforms in the regulation of MDA-MB-231 breast cancer cell spreading and migration. *Cancer Res.* 66, 4725-4733.
- Jerrell, R.J. and Parekh, A. (2014). Cellular traction stresses mediate extracellular matrix degradation by invadopodia. *Acta Biomater.* 10, 1886-1896.

25. Jordan, A., Hadfield, J.A., Lawrence, J.J., and McGown, A.T. (1998). Tubulin as a target for anticancer drugs: agents which interact with the mitotic spindle. *Med. Res. Rev.* *18*, 259-296.
26. Schoumacher, M., Goldman, R.D., Louvard, D., and Vignjevic, D.M. (2010). Actin, microtubules, and vimentin intermediate filaments cooperate for elongation of invadopodia. *J. Cell Biol.* *189*, 541-556.
27. Zhu, M., Horbinski, C.M., Garzotto, M., Qian, D.Z., Beer, T.M., and Kyprianou, N. (2010). Tubulin-targeting chemotherapy impairs androgen receptor activity in prostate cancer. *Cancer Res.* *70*, 7992-8002.
28. Wei, J., Xu, G., Wu, M., Zhang, Y., Li, Q., Liu, P., Song, A., Zhao, L., Han, Z., Chen, G., et al. (2008). Overexpression of vimentin contributes to prostate cancer invasion and metastasis *via* Src regulation. *Anticancer Res.* *28*, 327-334.
29. Sugiura, T., Nagano, Y., Inoue, T., and Hirotsu, K. (2004). A novel mitochondrial C1-tetrahydrofolate synthetase is 144ignificanc in human colon adenocarcinoma. *Biochem. Biophys. Res. Commun.* *315*, 204-211.
30. Hedstrom, L. and Gan, L. (2006). IMP dehydrogenase: structural schizophrenia and an unusual base. *Curr. Opin. Chem. Biol.* *10*, 520-525.
31. Zhou, L., Xia, D., Zhu, J., Chen, Y., Chen, G., Mo, R., Zeng, Y., Dai, Q., He, H., Liang, Y., Jiang, F., and Zhong, W. (2014). Enhanced expression of IMPDH2 promotes metastasis and advanced tumor progression in patients with prostate cancer. *Clin. Transl. Oncol.* *16*, 906-913.
32. Thornton, S., Anand, N., Purcell, D., and Lee, J. (2003). Not just for housekeeping: protein initiation and elongation factors in cell growth and tumorigenesis. *J. Mol. Med.* *81*, 536-548.
33. Karan, D., Kelly, D.L., Rizzino, A., Lin, M., and Batra, S. (2002). Expression profile of differentially-regulated genes during progression of androgen-independent growth in human prostate cancer cells. *Carcinogenesis* *23*, 967-976.
34. Scaggiante, B., Dapas, B., Bonin, S., Grassi, M., Zennaro, C., Farra, R., Cristiano, L., Siracusano, S., Zanconati, F., Giansante, C., and Grassi, G. (2012). Dissecting the expression of *EEF1A1/2* genes in human prostate cancer cells: the potential of *EEF1A2* as a hallmark for prostate transformation and progression. *Br. J. Cancer* *106*, 166-173.
35. Rehman, I., Evans, C.A., Glen, A., Cross, S.S., Eaton, C.L., Down, J., Pesce, G., Phillips, J.T., Yen, O.S., Thalmann, G.N., Wright, P.C., and Hamdy, F.C. (2012). iTRAQ identification of candidate serum biomarkers associated with metastatic progression of human prostate cancer. *PLoS ONE* *7*, e30885.
36. Arora, S., Yang, J., Kinzy, T.G., Utsumi, R., Okamoto, T., Kitayama, T., Ortiz, P.A., and Hait, W.N. (2003). Identification and characterization of an inhibitor of eukaryotic elongation factor 2 kinase against human cancer cell lines. *Cancer Res.* *63*, 6894-6899.
37. Oji, Y., Tatsumi, N., Fukuda, M., Nakatsuka, S., Aoyagi, S., Hirata, E., Nanchi, I., Fujiki, F., Nakajima, H., Yamamoto, Y., et al. (2014). The translation elongation factor eEF2 is a novel tumor-associated antigen overexpressed in various types of cancers. *Int. J. Oncol.* *44*, 1461-1469.
38. Patil, A.H., Deshmukh, M., Singh, N.K., Srivastava, R., Swati, K.S., Verma, M., Gupta, S., Veeresh, S., Srivastan, R., and Srinivasan, S. (2012). From data repositories to potential biomarkers: application to prostate cancer. *Curr. Sci.* *102*, 1111-1116.
39. Modelska, A., Turro, E., Russell, R., Beaton, J., Sbarato, T., Spriggs, K., Miller, J., Gräf, S., Provenzano, E., Blows, F., Pharoah, P., Caldas, C., and Quesne, J.L. (2015). The malignant 144ignifica in breast cancer is driven by eIF4A1-mediated changes in the translational landscape. *Cell Death Dis.* *6*, e1603.
40. Dong, Z. and Zhang, J. (2006). Initiation factor eIF3 and regulation of mRNA translation, cell growth, and cancer. *Crit. Rev. Onc.* *59*, 169-180.
41. Wang, Z., Chen, J., Sun, J., Cui, Z., and Wu, H. (2012). RNA interference-mediated silencing of eukaryotic translation initiation factor 3, subunit B (EIF3B) gene expression inhibits proliferation of colon cancer cells. *World J. Surg. Oncol.* *10*, 119.
42. Kwon, N.H., Kang, T., Lee, J.Y., Kim, H.H., Kim, H.R., Hong, J., Oh, Y.S., Han, J.M., Ku, M.J., Lee, S.Y., and Kim, S. (2011). Dual role of methionyl-tRNA synthetase in the regulation of translation and tumor suppressor activity of aminoacyl-tRNA synthetase-interacting multifunctional protein-3. *PNAS* *108*, 19635-19640.
43. Poliakov, E., Managadze, D., and Rogozin, I.B. (2014). Generalized portrait of cancer metabolic pathways inferred from a list of genes overexpressed in cancer. *Genet. Res. Int.* *2014*, 1-8.
44. Botlagunta, M., Vesuna, F., Mironchik, Y., Raman, A., Lisok, A., Winndard Jr., P., Mukadam, S., Van Diest, P., Chen, J.H., Farabaugh, P., et al. (2008). Oncogenic role of DDX3 in breast cancer biogenesis. *Oncogene* *27*, 3912-3922.
45. Chang, P.C., Chi, C.W., Chau, G.Y., Li, F.Y., Tsai, Y.H., Wu, J.C., and Wu Lee, Y.H. (2006). DDX3, a DEAD box RNA helicase, is deregulated in hepatitis virus-associated hepatocellular carcinoma and is involved in cell growth control. *Oncogene* *25*, 1991-2003.
46. Ostrowky, J. and Bomsztyk, K. (2003). Nuclear shift of hnRNP K protein in neoplasms and other states of enhanced cell proliferation. *Br. J. Cancer* *89*, 1493-1501.
47. Cervero, P., Himmel, M., Krüger, M., and Linder, S. (2012). Proteomic analysis of podosome fractions from macrophages reveals similarities to spreading initiation centres. *Eur. J. Cell Biol.* *91*, 908-922.
48. Benelli, R., Monteghirfo, S., Balbi, C., Barboro, P., and Ferrari, N. (2009). Novel antivasular efficacy of metronomic docetaxel therapy in prostate cancer: hnRNP K as a player. *Int. J. Cancer* *124*, 2989-2996.
49. Wei, T.W., Hsia, J., Chiu, S., Su, L., Juan, C., Lee, Y.G., Chen, J.M., Chou, H., Huang, J., Huang, H., and Yu, C.R. (2014). Methylosome protein 50 promotes androgen- and estrogen-independent tumorigenesis. *Cell. Signal.* *26*, 2940-2950.
50. Deng, W., Yan, M., Yu, T., Ge, H., Lin, H., Li, J., Liu, Y., Geng, Q., Zhu, M., Liu, L., He, X., and Yao, M. (2015). Quantitative proteomic analysis of the metastasis-inhibitory mechanism of the miR-193a-3p in non-small cell lung cancer. *Cell Physiol. Biochem.* *35*, 1677-1688.
51. Van Alphen, R.J., Wiemer, E.A.C., Burger, H., and Eskens, F.A.L.M. (2009). The spliceosome as a target for anticancer treatment. *Br. J. Cancer* *100*, 228-232.
52. Jiang, W., Roemer, M.E., and Newsham, I.F. (2005). The tumor suppressor DAL-1/4.1B modulates protein arginine *N*-methyltransferase 5 activity in a substrate-specific manner. *Biochem. Biophys. Res. Commun.* *329*, 522-530.
53. Stopa, N., Krebs, J.E., and Shechter, D. (2015) The PRMT5 arginine methyltransferase: many roles in development, cancer and beyond. *Cell. Mol. Life Sci.* *72*, 2041-2059.
54. Gu, Z., Li, Y., Lee, P., Liu, T., Wan, C., and Wang, Z. (2012). Protein arginine methyltransferase 5 functions in opposite ways in the cytoplasm and nucleus of prostate cancer cells. *PLoS ONE* *7*, e44033.

55. Huber, O., Ménard, Haurie, V., Nicou, A., Taras, D., and Rosenbaum, J. (2008). Pontin and Reptin, two related ATPases with multiple roles in cancer. *Cancer Res.* *68*, 6873-6876.
56. Lee, A.S. (2007). GRP78 induction in cancer: therapeutic and prognostic implications. *Cancer Res.* *67*, 3496-3499.
57. Sarto, C., Binz, P., and Mocarrelli, P. (2000). Heat shock proteins in human cancer. *Electrophoresis* *21*, 1218-1226.
58. Cornford, P.A., Dodson, A.R., Parsons, K.F., Desmond, A.D., Woolfenden, A., Fordham, M., Neoptolemos, J.P., Ke, Y., and Foster, C.S. (2000). Heat shock protein expression independently predicts clinical outcome in prostate cancer. *Cancer Res.* *60*, 7099-7105.
59. Goetz, M.P., Toft, D.O., Ames, M.M., and Erlichman, C. (2003). The Hsp90 chaperone complex as a novel target for cancer therapy. *Ann. Oncol.* *14*, 1169-1176.
60. Lin, J., Xu, J., Tian, H., Gao, X., Chen, Q., Gu, Q., Xu, G., Song, J., and Zhao, F. (2007). Identification of candidate prostate cancer biomarkers in prostate needle biopsy specimens using proteomic analysis. *Int. J. Cancer* *121*, 2596-2605.
61. Kuramitsu, Y. and Nakamura, K. (2006). Proteomic analysis of cancer tissues: shedding light on carcinogenesis and possible biomarkers. *Proteomics* *6*, 5650-5661.
62. Lopez-Garcia, M.A., Geyer, F., Natrajan, R., Kreike, B., Mackay, A., Grigoriadis, A., Reis-Filho, J.S., and Weigelt, B. (2010). Transcriptomic analysis of tubular carcinomas of the breast reveals similarities and differences with molecular subtype-matched ductal and lobular carcinomas. *J. Pathol.* *222*, 64-75.
63. Hergovich, A., Cornils, H., and Hemmings, B.A. (2007). Mammalian NDR protein kinases: from regulation to a role in centrosome duplication. *BBA Proteins Proteom.* *1784*, 3-15.
64. Sugiura, T. and Noguchi, Y. (2009). Substrate-dependent metal preference of PPM1H, a cancer-associated protein phosphatase 2C: comparison with other family members. *Biometals* *22*, 469-477.
65. Hermeking, H. (2003). The 14-3-3 cancer connection. *Nat. Rev. Cancer* *3*, 931-943.
66. Kim, Y.H., Kwei, K.A., Girard, L., Salari, K., Kao, J., Pacyna-Gengelbach, M., Wang, P., Hernandez-Boussard, T., Gazdar, A.F., Petersen, I., et al. (2010). Genomic and functional analysis identifies *CRKL* as an oncogene amplified in lung cancer. *Oncogene* *29*, 1421-1430.
67. Singer, C.F., Hudelist, G., Lamm, W., Mueller, R., Handl, C., Kubista, E., and Czerwenka, K. (2006). Active (p)CrkL is overexpressed in human malignancies: potential role as a surrogate parameter for therapeutic tyrosine kinase inhibition. *Oncol. Rep.* *15*, 353-359.
68. Smith-Pearson, P.S., Greuber, E.K., Yogalingam, G., and Pendergast, A.M. (2010). Abl kinases are required for invadopodia formation and chemokine-induced invasion. *J. Biol. Chem.* *285*, 40201-40211.
69. Oser, M., Dovas, A., Cox, D., and Condeelis, J. (2011). Nck1 and Grb2 localization patterns can distinguish invadopodia from podosomes. *Eur. J. Cell Biol.* *90*, 181-188.
70. Labelle-Côté, M., Dusseault, J., Ismaï, S., Picard-Cloutier, A., Siegel, P.M., and Larose, L. (2011). Nck2 promotes human melanoma cell proliferation, migration and invasion *in vitro* and primary melanoma-derived tumor growth *in vivo*. *BMC Cancer* *11*, 443.
71. Stylli, S.S., T.I. S.T., Verhagen, A.M., Xu, S.S., Pass, I., Courtneidge, S.A., and Lock, P. (2009). Nck adaptor proteins link Tks5 to invadopodia actin regulation and ECM degradation. *J. Cell Sci.* *122*, 2727-2740.
72. Daly, R.J., Binder, M.D., and Sutherland, R.L. (1994). Overexpression of the Grb2 gene in human breast cancer cell lines. *Oncogene* *9*, 2723-2727.
73. Russo, A.L., Jedlicka, K., Wernick, M., McNally, D., Kirk, M., Sproull, M., Smith, S., Shankavaram, U., Kaushal, A., Figg, W.D., Dahut, W., Citrin, D., Bottaro, D.P., Albert, P.S., Tofilon, P.J., and Camphausen, K. (2009). Urine analysis and protein networking identify met as a marker of metastatic prostate cancer. *Clin. Cancer Res.* *15*, 4292-4298.
74. Luo, Z., Saha, A.K., Xiang, X., and Ruderman, N.B. (2005). AMPK, the metabolic syndrome and cancer. *Trends Pharmacol. Sci.* *26*, 69-76.
75. Scott, K.E.N. (2012). Novel metabolic regulation of invadopodia and invasion by Acetyl-CoA Carboxylase and lipogenesis. Doctoral Dissertation, Wake Forest University. (Publication No. T09:35:36Z).
76. Zhou, J., Huang, W., Rao, R., Ibaragi, S., Lan, F., Ido, Y., Wu, X., Alekseyev, Y.O., Lenburg, M.E., Hu, G-f., and Luo, Z. (2009). Inactivation of AMPK alters gene expression and promotes growth of prostate cancer cells. *Oncogene* *28*, 1993-2002.
77. Balasubramani, M., Day, B.W., Schoen, R.E., and Getzenberg, R.H. (2006). Altered expression and localization of Creatine Kinase B, Heterogeneous Nuclear Ribonucleoprotein F, and High Mobility Group Box 1 Protein in the nuclear matrix associated with colon cancer. *Cancer Res.* *66*, 763-769.
78. Glen, A., Gan, C.S., Hamdy, F.C., Eaton, C.L., Cross, S.S., Catto, J.W.F., Wright, P.C., and Rehman, I. (2008). iTRAQ-facilitated proteomic analysis of human prostate cancer cells identifies proteins associated with progression. *J. Proteome Res.* *7*, 897-907.
79. Cho, H.M., Jun, D.Y., Bae, M.A., Ahn, J.D., and Kim, Y.H. (2000). Nucleotide sequence and differential expression of the human 3-phosphoglycerate dehydrogenase gene. *Gene* *245*, 193-201.
80. Stylli, S.S., T.I., S.T., Kaye, A.H., and Lock, P. (2012). Prognostic significance of Tks5 expression in gliomas. *J. Clin. Neurosci.* *19*, 436-442.
81. Seals, D.F., Azucena Jr., E.F., Pass, I., Tesfay, L., Gordon, R., Woodrow, M., Resau, J.H., and Courtneidge, S.A. (2005). The adaptor protein Tks5/Fish is required for podosome formation and function, and for the protease-driven invasion of cancer cells. *Cancer Cell* *7*, 155-165.
82. Burger, K.L., Learman, B.S., Boucherle, A.K., Sirintrapun, S.J., Isom, S., Diaz, B., Courtneidge, S.A., and Seals, D.F. (2014). Src-dependent Tks5 phosphorylation regulates invadopodia-associated invasion in prostate cancer cells. *Prostate* *74*, 134-148.
83. Kim, J., Bogner, P.N., Baek, S., Ramnath, N., Liang, P., Kim, H., Andrews, C., and Park, Y. (2008). Up-regulation of Peroxiredoxin 1 in lung cancer and its implication as a prognostic and therapeutic target. *Clin. Cancer Res.* *14*, 2326-2333.
84. Diaz, B. and Courtneidge, S.A. (2011). Redox signaling at invasive microdomains in cancer cells. *Free Radic. Biol. Med.* *52*, 247-256.
85. Riddell, J.R., Bshara, W., Moser, M.T., Spornyak, J.A., Foster, B.A., and Gollnick, S.O. (2011). Peroxiredoxin 1 controls prostate cancer growth through toll-like receptor 4-dependent regulation of tumor vasculature. *Cancer Res.* *71*, 1637-1646.

### **Biographical Sketch**

Christina Adele Daly was born in Boone, NC, to Joseph and Mary Daly. She graduated from the North Carolina School of Science and Mathematics in May 2009. The following August, she entered Appalachian State University to study biology. She started biological research in the laboratories of Drs. Ted Zerucha and Ece Karatan in February 2011 where she completed her Honors Thesis work titled, “Zebrafish as a Model Organism for *Vibrio cholerae* Infection.” She completed her Bachelor of Science in Biology in May of 2013 and began the Master of Science in Biology program at Appalachian State University in August of 2014 in the laboratory of Dr. Darren Seals. Upon completion of her Master of Science in Biology in August of 2016, she will begin work in a cancer immunology lab at Wake Forest University in the laboratory of Dr. Karen Haas before ultimately applying to a Doctor of Philosophy program in cancer biology.